From perception to function, characterization of karrikin-like signaling in *Lotus japonicus*

Samy Carbonnel

Dissertation zur Erlangung des Doktorgrades Dr. rer. nat.
an der Fakultät für Biologie der
Ludwig-Maximilians-Universität München

München, 2019

Diese Dissertation wurde angefertigt
unter der Leitung von Prof. Dr. Caroline Gutjahr
im Bereich von Institute of Genetics
an der Ludwig-Maximillians-Universität München

Erstgutachterin: Prof. Dr. Caroline Gutjahr
Zweitgutachter: Prof. Dr. Martin Parniske

Dissertation eingereicht am: 15 August 2019
Tag der mündlichen Prüfung: 12 November 2019

ERKLÄRUNG

Ich versichere hiermit an Eides statt, dass meine Dissertation selbständig und ohne unerlaubte Hilfsmittel angefertigt worden ist.
Die vorliegende Dissertation wurde weder ganz, noch teilweise bei einer anderen Prüfungskommission vorgelegt.
Ich habe noch zu keinem früheren Zeitpunkt versucht, eine Dissertation einzureichen oder an einer Doktorprüfung teilzunehmen.

München, den 14.11.2019

Samy Carbonnel

Table of contents

I. Abbreviation index

ACC	1-Aminocyclopropane-1-carboxylic acid
ACO	ACC OXIDASE
ACS	ACC SYNTHASE
AM	Arbuscular Mycorrhiza
ANOVA	Analysis of Variance
At	*Arabidopsis thaliana*
AVG	Aminoethoxyvinylglycine
BRC1	BRANCHED 1
Col-0	Columbia-0
D14	DWARF 14
D14L	DWARF 14 Like
D53	DWARF 53
DEG	Differentially Expressed Gene
DLK2	DWARF 14 Like 2
DSF	Differential Scanning Fluorimetry
EAR	Ethylene-responsive element binding factor-associated amphiphilic repression
EIN2	ETHYLENE INSENSITIVE 2
EMS	Ethyl Methanesulfonate
ERF	ETHYLENE RESPONSE FACTOR
ETR1	ETHYLENE RECEPTOR 1
IAA	Indole-3-acetic acid
IAMT1	IAA carboxylmethyltransferase 1
LogFC	Logarithm Fold Change
FDR	False Discovery Rate
GA	Gibberellic Acid
GFP	GREEN FLUORESCENT PROTEIN
GID1	GIBBERELLIN INSENSITIVE DWARF 1
HTL	HYPOSENSITIVE TO LIGHT
IAA	Indole-3-acetic acid
KAI	KARRIKIN INSENSITIVE

KAR	Karrikins
KL	Karrikin Like
Ler	Landsberg erecta
Lj	*Lotus japonicus*
LORE1	LOTUS RETROTRANSPOSON 1
MAX	MORE AXILLARY GROWTH
Mt	*Medicago truncatula*
N.S.	Non-Significant
Os	*Oryza sativa*
PCA	Principal Component Analysis
PER	Post Embryonic Root
PIN	PIN-FORMED
PRL	Primary Root Length
QC	Quiescent Center
qPCR	quantitative Polymerase Chain Reaction
RH	Root-hair
RMS	RAMOSUS
RNS	Root nodule symbiosis
SCF	SKP-CULLIN-FBOX complex
SL	Strigolactone
SMAX	SUPPRESSOR of MAX2
SMXL	SUPPRESSOR of MAX2 Like
TILLING	Targeting Induced Local Lesions in Genomes
TPL	TOPLESS
TPR	TOPLESS RELATED

II. List of Publications

Villaécija Aguilar J. P., Hamon-Josse M., **Carbonnel S.**, Kretschmar A., Schmidt C., Dawid C., Bennett T., Gutjahr C. SMAX1/SMXL2 regulate root and root hair development downstream of KAI2-mediated signaling in Arabidopsis. **PLoS Genetics** *in pr*ess (2019).

Pimprikar P, **Carbonnel S**, Paries M, Katzer K, Klingl V, Bohmer MJ, Karl L, Floss DS, Harrison MJ, Parniske M, Gutjahr C. A CCaMK-CYCLOPS-DELLA complex activates transcription of RAM1 to regulate arbuscule branching. **Current Biology** 26: 987-998 (2016).

Gutjahr C, Gobbato E, Choi J, Riemann M, Johnston MG, Summers W, **Carbonnel S**, Mansfield C, Yang SY, Nadal M, Acosta IF, Takano M, Jiao WB, Schneeberger K, Kelly KA, Paszkowski U. Rice perception of arbuscular mycorrhizal fungi requires the karrikin receptor complex. **Science** 350: 1521-1524 (2015).

Carbonnel S., Gutjahr C. Control of arbuscular mycorrhiza development by nutrient signals. **Frontiers in Plant Science** 5:462 (2014). (review)

<u>These manuscripts are submitted or in preparation:</u>

Carbonnel S, Das D, Kolodziej M, Varshney K, Gutjahr C. SMAX1 promotes *Lotus japonicus* root system development by suppressing ethylene biosynthesis. ***In preparation for*** **PNAS**

⇨ Corresponding to results chapter 3).

Carbonnel S, Torabi S, Griesmann M, Bleek E, Tang Y, Buchka S, Basso V, Shindo M, Wang TL, Udvardi M, Waters M, Gutjahr C. Sub-functionalization of *Lotus japonicus* KAI2 receptors in development and ligand binding specificity. ***In preparation for*** **PLoS Genetics**

⇨ Corresponding to results chapter 1).

Carbonnel S, Griesmann M, Gutjahr C. MAX2-independent transcriptional responses to *rac*-GR24. ***In preparation for*** **Frontiers in Plant Science**

⇨ From a microarray analysis on *Lotus japonicus* roots treated with *rac*-GR24 and KAR1, we observed a common transcriptional response, which was unexpectedly observed as well in the *max2-4* mutant background. This transcriptional regulation independently of the canonical receptor complex has never been reported before and will be crucial for the understanding of previous transcriptomic reports and planning of future experiments in the field.

Altmann M, Altmann S, Palme J, Marín-de la Rosa N, Rodriguez PA, Wenig M, Villaécija-Aguilar JA, Sales J, **Carbonnel S**, Kugler K, Hecker M, Bassel GW, Grill E, Falter C, Mayer KFX, Gutjahr C, Vlot AC, Falter-Braun P. Extensive signal integration revealed by a phytohormone protein interactome map. ***In preparation for resubmission***

III. Declaration of contribution

Most of this work has been done by myself, with the help of Prof. Dr. **Caroline Gutjahr** for the experimental design. In addition, the following people contributed to this work:

- **Dr. Debatosh Das** did the RNAseq analysis in results chapter 3). He also amplified the seeds of the *ein2a-2 ein2b-1* mutant.
- **Dr. Mark Waters** from the University of Western Australia, carried out the protein expression, purification and Differential Scanning Fluorimetry assay in results chapter 1).

In addition, the following people contributed to this work under my direct supervision:

- **Veronica Basso**, as an MSc thesis student did preliminary experiments to set up hypocotyl elongation assays in *L. japonicus*, for chapter 1).
- **Karl-Heinz Braun**, as a technical assistant helped in the cloning of Golden Gate Level1 Esp3I constructs, for all chapters.
- **Stefan Buchka**, as a BSc thesis student measured the branch numbers in *L. japonicus* mutants, for chapter 1).
- **Cornelia Gschwilm**, as a research course MSc student helped in the gene expression analysis in *L. japonicus* hypocotyls in response to KARs and SL treatments, for chapter 1).
- **Verena Klingl**, as a technical assistant helped for several hairy-root transformations, RNA extraction, and cDNA synthesis, for chapters 1) and 2).
- **Markus Kolodziej**, as an MSc thesis student did most of the very difficult cloning for the SMXL degradation assay in *N. benthamiana*, for chapter 3).
- **Kartikye Varshney**, as a Ph.D. student helped in the gene expression analysis of the *smax1-2* mutant grown with ethylene biosynthesis and perception inhibitors, for chapter 3).

IV. Summary

Phytohormones are small molecules and key regulators for plant development. They translate and integrate perceived environmental cues into physiological responses. Recently, karrikins (KAR), smoke-derived compounds, were shown to trigger plant developmental responses by mimicking an unknown phytohormone called karrikin-like (KL). KAR and KL are perceived by the αβ-hydrolase KAI2 which interacts with the F-box protein MAX2. Upon KL perception, a protein complex is formed with the repressor SMAX1, which is marked by ubiquitination for proteasomal degradation. At the beginning of this thesis, knowledge of KL function in plants was limited. Few reports in Arabidopsis showed its importance in seed germination and hypocotyl development. In rice, the discovery that the KL receptor complex is required for arbuscular mycorrhiza symbiosis (AMS) led to the question: Is KL signaling function in AMS conserved among other plant species, and particularly dicotyledons? Arabidopsis being unable to establish AMS, a new model plant was required. Thus, the goal of this thesis was to establish *Lotus japonicus* as a new model plant to study the role of KL signaling in plant development and AMS.

To this end, *L. japonicus* homozygous mutant of each known KL signaling components, *KAI2, MAX2,* and *SMAX1,* were generated. In contrast to single-copy genes *MAX2* and *SMAX1*, the KL receptor is duplicated in legumes. These two copies are functional as both rescued the elongated hypocotyl phenotype of the *Arabidopsis thaliana kai2-2* mutant. However, genetic analysis of the KL perception mutants revealed that KL signaling is not required for inhibition of hypocotyl elongation in *L. japonicus*. However, transcriptional and developmental hypocotyl responses to the presence of KAR were dependent on only one *LjKAI2* copy. Functional analysis in complemented *A. thaliana kai2-2* and *in-vitro* binding assay demonstrated that the two LjKAI2 versions showed different affinities to ligands. Three amino-acids located in the ligand-binding cavities were shown to be determinant for ligand binding specificity. In conclusion, these results potentially indicate the presence of several KL molecules *in planta* to control different physiological responses through the divergent receptors.

I also investigated the role of KL signaling in AMS using the *L. japonicus* KL receptor mutants. The level of colonization in the *L. japonicus* KL perception mutants was

reduced to 50% compared to the wild-type level, where the two KL receptors have a redundant function. In rice, *kai2* and *max2* do not support colonization, whereas, in Pea, *max2* mutant was less colonized than the wild-type. Recently in petunia, a *kai2* mutant was shown to be impaired in AMS. Thus, the relative importance of KL signaling during AMS emerges as specific to phylogenetic-groups. Plant hormones can act in a local as well as in a systemic manner. Complementation by hairy-root transformation of *max2* expressing the wild-type *MAX2* showed that root colonization was only rescued only in transformed roots indicating that KL signaling is required locally for the optimum colonization.

Due to the importance of KL signaling in roots for AMS, additional functions in *L. japonicus* root development were explored. Roots specifically responded, transcriptionally and developmentally, to KAR_1 treatment in a KL perception component dependent manner. The root growth regulatory potential of KL signaling was confirmed by aberrant root phenotypes of two independent *smax1* mutants. An RNAseq experiment of *smax1* mutant roots revealed an increased transcript accumulation of ethylene biosynthesis genes. This increased ethylene production was shown to be causative for the root phenotypes in *smax1* mutants. However, several differentially-expressed-genes were shown to be ethylene-signaling-independently-regulated and appeared as likely directly regulated by KL signaling. Thus, a member of the *Ethylene Response Factor* family was discovered as an early marker gene of KL signaling. Encoding a transcription factor, *ERF* could potentially act as a regulator for secondary KAR/KL responses. Altogether, our results illustrated that KL signaling influences root architecture development through SMAX1 removal, which acts as an inhibitor of ethylene biosynthesis.

Collectively, results of this thesis open new frontiers of research on KL receptor evolution and the presence of multiple KL ligands, but also on the interaction of KL and ethylene signaling and the transcriptional cascade responding to KL/KAR. This work provides genetic tools and research axis for exciting future research using *L. japonicus* as a model plant to study KL signaling.

V. Introduction

1) The discovery of karrikins

The forests of Australia, South Africa or North America, are challenged by wildfires each year during the dry season. Some plant species have evolved to take advantage of this perturbation. Their seeds germinate just after the fire to increase the fitness of the offspring on a ground depleted of competitors. “How these fire-following species perceive the fire” was a fascinating question. In 1990, Delange and Boucher were the first to report that a smoke, from burning plant-derived material, is sufficient to trigger the germination of the South-African fire-following species *Audouinia capitata*, and speculated that some compounds in the smoke would be perceived by their seeds, while the increase of sub-soil temperature during fire is unlikely to stimulate the germination (De Lange and Boucher 1990). Remarkably, cellulose-derived smoke from burned Whatmann paper is sufficient to induce germination of fire-following species. This less complex smoke allowed Australian researchers to find by fractionation a butenolide (3-methyl-2Hfuro[2,3-c]pyran-2-one) triggering seed germination of fire-following plants at very low concentrations (10^{-9} M) (Flematti et al. 2004). In addition, five similar molecules with methyl substitutions were identified in the smoke of burning plant-derived material (Fig. 1) (Flematti et al. 2009). These butenolides were called karrikins (KAR) in reference to the word “karrik” meaning “smoke” in the Nyungar aboriginal language (Dixon et al. 2009). The different KAR trigger the germination of numerous plant species, including species which do not experience fires in their environment such as the model plant *Arabidopsis thaliana* (Chiwocha et al. 2009; Nelson et al. 2009). This breakthrough discovery enabled the screening for the perception mechanism of KAR, thanks to the genetic resources and mutants associated with this model plant.

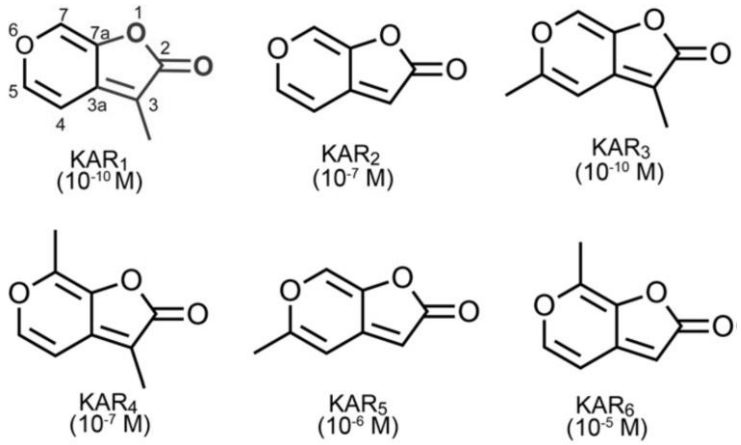

Figure 1: Chemical structures of karrikins. Half-maximal effective concentration (EC50) values on the fire-following species *Solanum orbiculatum* germination are indicated in parentheses (Guo et al. 2013).

2) Identification of karrikin receptor components

KAR induces *A. thaliana* germination (Nelson et al. 2009), but also enhance de-etiolation in a light-dependent manner (Nelson et al. 2010). Upon KAR treatment, seedlings have shorter hypocotyls and bigger cotyledons (Nelson et al. 2010). The strong and consistent responses to KAR of *A. thaliana* allowed a forward genetic screen to find *karrikin-insensitive* (*kai*) mutants. The first identified mutant *kai1* is defective in a gene encoding an F-box protein already known as MAX2 (MORE AXILLARY GROWTH 2) (Nelson et al. 2011). *MAX2* was described as required for strigolactone (SL) responses, the most recently discovered class of phytohormones (Umehara et al. 2008; Gomez-Roldan et al. 2008). SLs are perceived by the αβ-hydrolase D14 (DWARF 14) (Arite et al. 2009; Waters et al. 2012; Yao et al. 2016). Due to the insensitivity of *max2* mutant to SL and KAR, and the insensitivity of *d14* mutant only to SL, it was hypothesized that another αβ-hydrolase, homologous of D14 could be involved in KAR perception (Waters et al. 2012). In *A. thaliana*, two close homologs of *D14* are present: *D14-Like* and *D14-Like2* (*DLK2*) conserved in all land plants (Bythell-Douglas et al. 2017). Mutation in the *D14-like* gene led to KAR insensitivity (Waters et al. 2012). Thereby, the αβ-hydrolase D14-like was renamed KAI2 (Waters et al. 2012), and later identified as KAR receptor due to *in-vitro* binding KAR_1 (Guo et al. 2013). Thus, D14 and KAI2 provide the molecular basis for differential perception to SL and KAR respectively.

Prominently, due to the conservation of KAI2 in all land plants including non-fire following plants, and developmental responses to KAR in Arabidopsis (Nelson et al. 2010), KAR were quickly regarded as mimics of a putative endogenous hormone karrikin-like (KL) (Conn and Nelson 2016).

3) The SL signaling pathway, derived from the ancestral KL signaling pathway

SL are carotenoid-derived molecules. Their biosynthesis requires key enzymes like the isomerase DWARF27 and the CAROTENOID CLEAVAGE DIOXYGENASEs 7 and 8 (CCD7, CCD8), which together convert sequentially all-*trans*-β-carotene into carlactone, a common precursor used by several enzymes to synthesize actives SL (reviewed in (Jia et al. 2017)). Homologs of *D27*, *CCD7,* and *CCD8*, as well as SL themselves, are found down to the Liverworts, whereas the known receptor *D14* is found only in Angiosperms and Gymnosperms (Delaux et al. 2012). *KAI2* and *MAX2* are also present in basal plants, which led to the hypothesis that in these organisms KAI2 could act as SL receptor (Waters et al. 2017). Besides, phylogenetic analyses in extant land plants revealed that the SL receptor *D14* evolved from its paralogue, *KAI2* through duplication (Bythell-Douglas et al. 2017; Delaux et al. 2012). Convergent evolution has been observed in parasitic plants, in which KAI2 has been duplicated multiple times, diversified and evolved to perceive SLs in the root-exudate of their hosts (Conn et al. 2015). These KAI2 versions present a bigger ligand cavity and respond specifically to SLs and not to KAR_2 (Conn et al. 2015; Conn and Nelson 2016). Interestingly, a KAI2 from the basal plant *Selaginella moellendorfii* can partially rescue the Arabidopsis *kai2-2* mutant, but could not respond to exogenous KAR indicating an ancestral role and structure of KL (Waters et al. 2015b). In Arabidopsis, D14 and KAI2 are two functionally distinct receptors since promoter swap could not rescue any of the known *d14* and *kai2* phenotype in Arabidopsis (Waters et al. 2015b). Characterization of multiple KL receptor will allow to decipher the determinant amino-acids to exogenous and endogenous ligands specificity and shed some lights on the evolutionary processes on receptor diversifications.

Probably due to their common origin, there are strong similarities in perception and signal transduction between the SL and KL signaling pathway (Fig 2). Upon docking of SL inside the cavity of D14, the receptor hydrolyzes the enol-ether bond of the ligand. SL hydrolysis generates an intermediate product originated from the D-ring which triggers a change in the protein conformation and closes the lid on the cavity (Yao et al. 2016). This transient state stabilizes its interaction with MAX2 for subsequent signaling, which includes the degradation of D14 by the proteasome, in a putative feedback loop (Chevalier et al. 2014). Similarly, the hydrolysis activity of KAI2 towards GR24 (Toh et al. 2014), as well as the requirement of its catalytic triad for signaling were demonstrated (Waters et al. 2015b). In addition, *in vivo* KAI2 is degraded in the presence of KARs (Waters et al. 2015a). These results strongly suggest that KAI2 and D14 function similarly. However, some specificities are observed as they diverge in their triggered degradation, which is MAX2 and proteasome-independent in the case of KAI2 (Waters et al. 2015a).

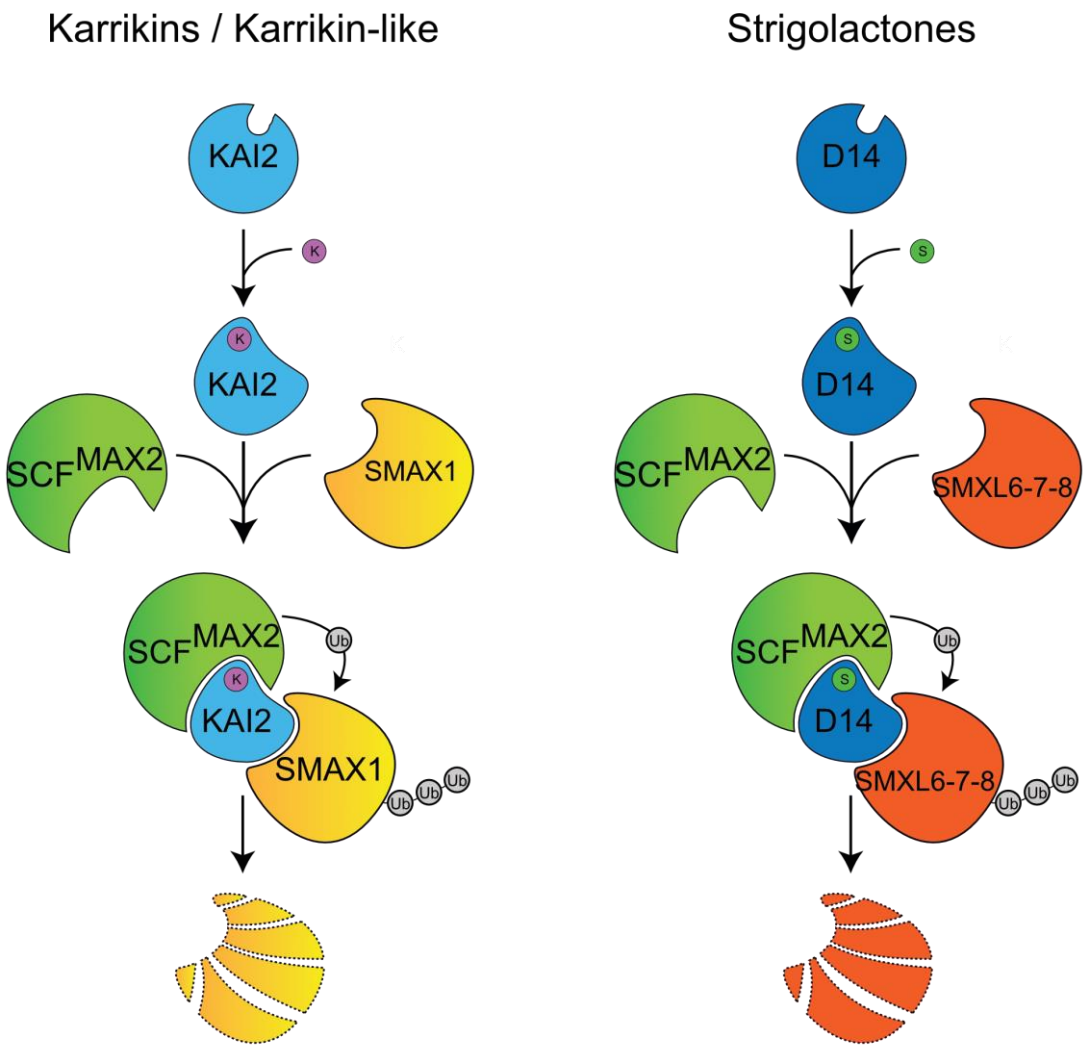

Figure 2: Models of the KL (left) and SL (right) signaling pathways. In their apo-structures, the cavity of the receptors is open. Upon ligand binding, a conformational change occurs with the closure of the lid. Thus, stabilizing the interaction with MAX2, which leads to the poly-ubiquitination of pathway-specific repressors, called SMAX1 and SMXL6-7-8, respectively, marked for proteasomal degradation.

4) The repressors of KL and SL signaling

To identify the repressors downstream of the perception components, several suppressor screens have been attempted on the shoot branching phenotype or delayed senescence of the *max2* mutant (Stirnberg et al. 2012a; Stirnberg et al. 2012b; Hur et al. 2012). However, these suppressor screens, directed towards SL related phenotypes, were unsuccessful, likely due to redundancy at the repressor level in Arabidopsis (see below). Another *max2* suppressor screen was executed, focusing on the rescue of KL related phenotypes: germination, hypocotyl elongation and cotyledon

morphology (Stanga et al. 2013). From this screen, a mutation found in a gene related to Class-I Clp ATPases, called *SMAX1* (*SUPPRESSOR OF MAX2 1*), suppressed several *max2* phenotypes, all related to KL signaling, including hypocotyl elongation, cotyledon expansion, and seed germination. and root skewing (Stanga et al. 2013). Later on, *smax1* was also shown to rescue root skewing and defects in root-hair development of *max2* and *kai2* mutants (Swarbreck et al. 2019; Villaecija Aguilar et al. 2019). However, a mutation in *SMAX1* does not suppress the leaf senescence and highly branched phenotypes of *max2*, suggesting independent or redundant factors are involved in these SL phenotypes (Stanga et al. 2013; Soundappan et al. 2015). Due to the similarities between the two pathways, close homologs of *SMAX1*, called *SMXL* (*SUPPRESSOR OF MAX2 LIKE*) were hypothesized to be able to suppress the highly branched phenotype of *max2* (Stanga et al. 2013). In the same year, two independent teams working on a rice SL insensitive highly-branched dominant mutant called *d53* (*dwarf 53*), determined that the causative mutation was a deletion of 15 bp leading to a small deletion of 5 amino-acid (Jiang et al. 2013; Zhou et al. 2013). Translational fusion of D53 with GFP showed the rapid degradation of D53 upon GR24 treatment in a MAX2 and D14 dependent fashion, whereas *d53* was resistant to degradation. In addition, D53 is ubiquitinated prior to degradation, and interacts directly with D14 and MAX2, indicating that D53 is the repressor of SL signaling (Zhou et al. 2013; Jiang et al. 2013). *OsD53* is the ortholog of the triplicated *SMXL6, 7* and *8* in Arabidopsis (Walker and Bennett 2017), showing why previous *max2* suppressor screens targeted at SL-related phenotypes were unsuccessful and lending strong support to the idea of SMAX1 being the repressor of KL signaling.

Further work in Arabidopsis, could confirm the specific degradation of SMXL6, 7 and 8 in response to GR24 treatment, in a D14 and MAX2 dependent fashion for the tested SMXL6 and 7 (Wang et al. 2015; Soundappan et al. 2015). The *Atsmxl6-7-8* triple mutant was not reported to have strong abnormal development phenotypes, however, when crossed with a *max2* mutant, it suppressed several phenotypes including the high number of rosette branches and the dwarfism of the SL perception mutant (Soundappan et al. 2015). The mutation of one of these SL repressors was not sufficient to rescue the high branching phenotype of *max2*, confirming functional redundancy among the three SMXL6, 7 and 8. Nevertheless, the quadruple mutant *smxl678 max2* had still a long hypocotyl. Comparative analysis of the different suppression effect in *max2* by either *smax1* or *smxl678* mutations, allowed to

distinguish their functions, with SMAX1 and SMXL6, 7 and 8 repressing KL and SL signaling respectively (Fig 3) (Soundappan et al. 2015; Stanga et al. 2013; Swarbreck et al. 2019; Villaecija Aguilar et al. 2019).

In addition to the SMXL proteins involved in SL signaling repression, another clade was described, containing in Arabidopsis SMXL3, 4 and 5, which are redundant central regulators of phloem formation (Wallner et al. 2017). Their regulation is independent of KL or SL signaling (Wallner et al. 2017; Wu et al. 2017).

5) SMAX1 and SMXLs could be mediators of transcriptional repression

In the KL and SL repressor mutants, transcripts of known KAR and *rac*-GR24 induced-genes, such as *DLK2* (*D14-LIKE 2*) in *smax1*, and *BRC1* (*BRANCHED1*) in *smxl678* accumulate at high levels (Soundappan et al. 2015; Stanga et al. 2013). Transcriptional de-repression is a common mechanism in most plant hormonal pathways. In the case of auxin, jasmonic acid, and brassinosteroids, it works through the degradation of specific targets involved in the recruitment of active transcriptional repressors, the TOPLESS (TPL) and TOPLESS RELATED (TPR) proteins (Pauwels et al. 2010; Shyu et al. 2012; Tiwari et al. 2004; Oh et al. 2014). TOPLESS proteins recruit HISTONE DEACETYLASEs which leads to a compaction of the chromatin, which physically blocks the transcription (reviewed in (Liu et al. 2014)). The recruitment of the key transcriptional repressors TPL/TPR is dependent on an EAR motif (Ethylene-responsive element binding factor-associated amphiphilic repression) (reviewed in (Kagale and Rozwadowski 2014)). A similar EAR motif is conserved in all SMAX1 and SMXL proteins and is important for the interaction between AtSMAX1 and AtSMXL7 to different TPL and TPRs (Soundappan et al. 2015; Wang et al. 2015; Ma et al. 2017). Further, deletion of the EAR motif in SMXL6, 7 and 8 inhibited their transcriptional repression activity in vivo (Wang et al. 2015). However, deletion or mutation of the EAR motif of AtSMXL7 has shown to be partially functional in a *smxl678-max2* quadruple mutant (Liang et al. 2016).

6) KL and SL functions in plant development

Besides their insensitivity to KAR, *max2* and *kai2* mutants show multiple common developmental phenotypes (Fig 3). As expected from the induction of seed germination by KARs, they have delayed germination in Arabidopsis (Nelson et al. 2011; Waters et al. 2012). At the seedling stage, KL perception mutants are perturbed in photomorphogenesis. In Arabidopsis and rice, *kai2* and *max2* mutants have long hypocotyl and mesocotyl, respectively, whereas KAR treatment leads to their reduction in the corresponding wild-types (Nelson et al. 2011; Waters et al. 2012; Gutjahr et al. 2015). Cotyledon morphology is also affected by KAR, with increased expansion upon treatment (Nelson et al. 2010), and small hooked cotyledons in the KL perception mutants (Waters et al. 2012). During the vegetative development of Arabidopsis, the *kai2* mutants show elongated leaves and curled margins (Waters et al. 2012). Also, disruption of KL signaling leads to decreased resistance to drought stress, due to higher stomatal aperture and a more permeable cuticle in Arabidopsis (Bu et al. 2014; Li et al. 2017). The involvement of KL signaling in the root was unknown for a long time, whereas SL were thought to play major roles in controlling primary root length, lateral root density, root-hair density and length (Kapulnik et al. 2011; Ruyter-Spira et al. 2011; Mayzlish-Gati et al. 2012; Jiang et al. 2016). Those conclusions were drawn based on the combined use of *max2* mutants and the synthetic SL *rac*-GR24, which affect both KL and SL signaling (Nelson et al. 2011; Scaffidi et al. 2014). Recently, in-depth phenotypic characterization of several KL and SL Arabidopsis mutants could separate the functions of each pathway in the early stage of root development (Swarbreck et al. 2019; Villaecija Aguilar et al. 2019), with a common conclusion that KL signaling reduces root skewing in Arabidopsis. In addition, root-hair length and density are positively regulated by KL signaling (Villaecija Aguilar et al. 2019).

Specific phenotypes of the *max2* mutant, absent in *kai2*, are observed in the SL receptor mutant *d14* (Fig 3). These phenotypes, displayed as well by SL biosynthesis mutants, unambiguously indicate a function of the hormone in the regulation of these processes. This is the case for the inhibition of shoot branching by SL, as highly-branched shoots are observed in *d14*, *max2* and SL biosynthesis mutants in multiple species (e.g. rice, Arabidopsis, pea, petunia and barley) (Arite et al. 2009; Hamiaux et al. 2012; Waters et al. 2012; Guo et al. 2013; Marzec et al. 2016). SL mutants also display wider leaves in Arabidopsis with decreased senescence (Waters et al. 2012;

Ueda and Kusaba 2015; Bennett et al. 2016). The function of SL in root development is more ambiguous, as in addition to the phenotypes described above several publications report an inhibition of adventitious and lateral root formation by SL (reviewed in (Al-Babili and Bouwmeester 2015; Kapulnik and Koltai 2014)). However, these results were obtained using *max2* and the synthetic SL *rac*-GR24, which affect both KL and SL signaling (Nelson et al. 2011; Scaffidi et al. 2014), with the notable exception of a report using as well SL biosynthesis mutants (Rasmussen et al. 2012). A recent manuscript indicates a combined effect of both signalings in regulating lateral root density in Arabidopsis (Villaecija Aguilar et al. 2019). Furthermore, the positive role of SL in root elongation was postulated with the use of SL biosynthesis mutant in rice and maize (Guan et al. 2012; Arite et al. 2012).

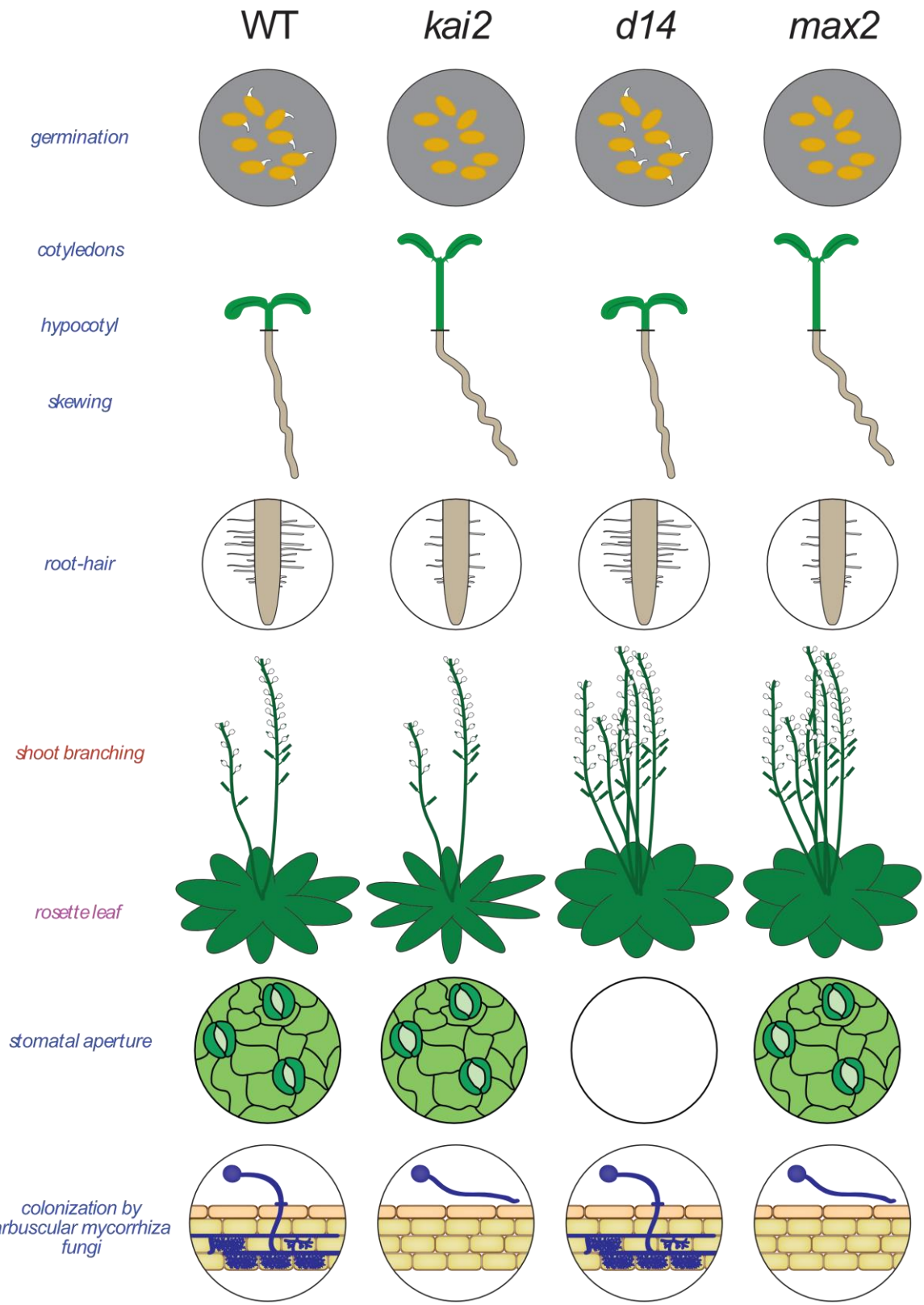

Figure 3: Developmental phenotypes of KL and SL perception mutants. Schematic summary of developmental phenotypes of *kai2*, *d14* and *max2* mutants in rice and/or Arabidopsis, related to KL (blue), SL (red) or both signaling (purple).

7) Interactions with other phytohormones

Interactions between phytohormone signalings is a common mechanism for fine-tuning growth or responses to biotic and abiotic stresses. Early in the discovery of the SL mutant phenotypes, which include dwarfism and increased shoot-branching, two other phytohormones involved in apical dominance were suspected to be involved in this phenomenon: auxin and cytokinin. Few pieces of evidence were found to link cytokinin to SL (Li et al. 2019; Dun et al. 2012; Kyozuka et al. 2013; Koren et al. 2013), but more connections were discovered with auxin. Levels of the auxin IAA (indole-3-acetic acid) were slightly increased in the Pea *rms3/d14* mutant and all rice SL biosynthesis and perception mutants (Beveridge et al. 1996; Arite et al. 2007). In Arabidopsis, equivalent mutants displayed a strong increase in auxin transport (Bennett et al. 2006). The auxin efflux transporter PIN1 (PIN-FORMED 1), with basal localization at the plasma-membrane, accumulates at higher levels in Arabidopsis *max* mutants (Bennett et al. 2006; Shinohara et al. 2013). Further, inhibition of bud growth was achieved by inhibition of auxin transport in the SL mutants, placing auxin downstream of SL signaling (Bennett et al. 2006; Lin et al. 2009). Treatment with the synthetic SL *rac*-GR24 quickly removes plasma-membrane localized PIN1 in a *MAX2* dependent fashion, unveiling one mechanism of action of SL on influencing auxin transport (Shinohara et al. 2013). Finally, the *pin347* triple mutant partially suppressed the *max2* branching phenotype (Van Rongen et al. 2019). These results support the “canalization” hypothesis in which high auxin flux from the bud (source) to the main stem (sink) allow bud growth (reviewed in (Bennett et al. 2014)). Thereby, through PIN polarization, SL signaling can affect auxin transport and indirectly growth of axillary buds.

Involvement of auxin in connection to root development controlled by SLs was also investigated. Levels of PIN proteins in the root meristem were reduced by long exposure to rac-GR24 (Ruyter-Spira et al. 2011), whereas it promoted PIN2 endocytosis in relation to root-hair development (Pandya-Kumar et al. 2014). However, the use of *max2* and rac-GR24 in these studies is problematic and does not allow to conclude whether SL or KL signaling affect the PINs.

Ethylene is a key hormone for root-hair formation and elongation (Vandenbussche and Van Der Straeten 2012). The induction of root-hair elongation by rac-GR24 in a MAX2 dependent fashion suggested the involvement of ethylene in this process. Indeed, the

response to *rac*-GR24 was strongly inhibited in ethylene-insensitive mutants or by ethylene biosynthesis inhibition (Kapulnik et al. 2011). This report concluded that ethylene is epistatic to SLs or KL signaling to regulate root-hair development.
Gibberellins (GA) are key hormones required for seed germination. Since treatment with KARs breaks primary dormancy, their epistasis was studied shortly after the discovery of KAR. In Arabidopsis, GA biosynthesis and perception, are partially required for the induction of seed germination by KARs (Nelson et al. 2009). In addition, treatment with KARs induces GA biosynthesis genes, placing part of the KL signaling upstream of GA signaling for seed germination (Nelson et al. 2009). In rice, surprisingly the SL receptor D14 was shown to interact with SLR1/DELLA, the GA repressor (Nakamura et al. 2013). Further, a small additive effect was observed at the transcriptional level between SL and GA (Lantzouni et al. 2017). In addition, a prolonged GA treatment repressed SL exudation by rice roots (Ito et al. 2017). However, no further strong evidence has been discovered so far to confirm crosstalk between GA and KL or SL signaling.

In summary, apart from the very well characterized connection between SL signaling on auxin distribution in controlling shoot branching, no other interactions with other phytohormones are strongly supported and/or characterized.

8) Arbuscular mycorrhiza symbiosis, regulated by SL and KL signaling

Before to be defined as plant hormone with functions in plant development, SL were discovered to be released in the rhizosphere in response to phosphate deficiency (Lopez-Raez et al. 2008; Umehara et al. 2008). In the root exudates, SL act as stimulants of symbiotic arbuscular mycorrhiza (AM) fungi by triggering spore germination and hyphal branching (Akiyama et al. 2005; Besserer et al. 2006; Besserer et al. 2008). AM is an ancient symbiosis, established between 80% of land plants and fungi belonging to the glomeromycotina order (Parniske 2008; Spatafora et al. 2016). Through AM symbiosis (AMS) host plants receive mineral nutrients, phosphate in particular, in exchange for photo-synthetically fixed carbons in the form of sugar and lipids (Wang et al. 2017).

The development of the AMS occurs in several steps (reviewed in (Pimprikar and Gutjahr 2018) (Fig 4). During a pre-contact phase, a crucial molecular dialog takes place between the plant and the AM fungus. Host roots exude diffusible molecules, like SLs, and in return, the fungus releases a mixture of chitin-oligomers called Myc-Factors (MacLean et al. 2017). Once in contact with the root surface, the fungus forms an attachment structure called hyphopodium, from where it penetrates the epidermis and then successive cell layers. Subsequently, fungal hyphae grow until reaching the inner cortex of the host root. The fungal intraradical hyphae spread longitudinally in the apoplast space, and penetrate cortical cells to form tree-like structures, specialized for nutrient exchange, called arbuscules.

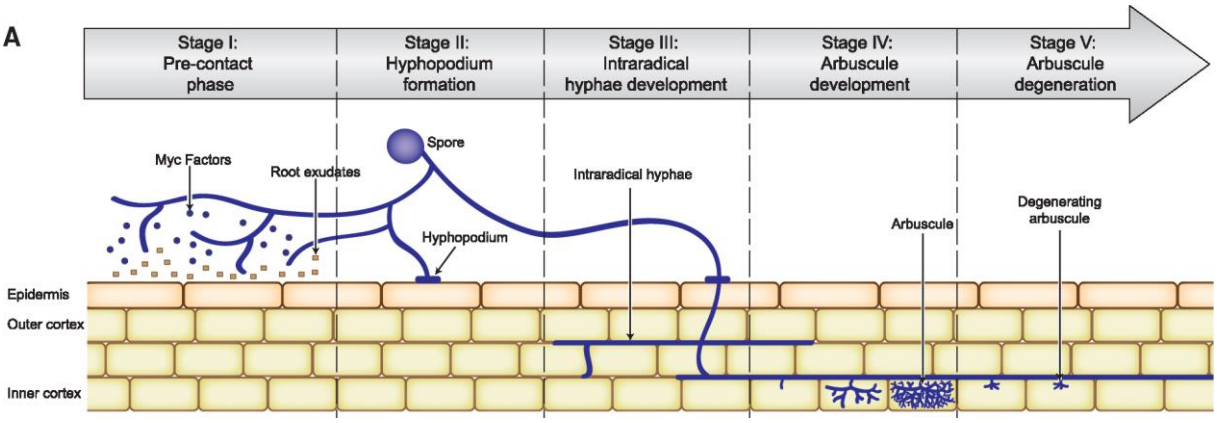

Figure 4: Schematic representation of AM development. (Pimprikar and Gutjahr 2018)

The plant controls the development of the symbiont in function of its nutrient status, and the synthesis and release in the rhizosphere of SLs is one mechanism involved in this regulation (Carbonnel and Gutjahr 2014). Accordingly, SL biosynthetic mutants in pea and rice have reduced AM colonization (Gomez-Roldan et al. 2008; Foo et al. 2013; Yoshida et al. 2012; Gutjahr et al. 2012). In contrast, mutation of the SL receptor *D14* enhances root colonization, likely due to a feedback loop mechanism which leads to a higher synthesis and release of SLs, strongly promoting the symbiosis (Yoshida et al. 2012; Gutjahr et al. 2015). However, in rice, *d3/max2* mutants display extremely low levels of AM colonization (Yoshida et al. 2012; Gutjahr et al. 2015). Supporting this result, a reduction of root colonization was observed in the pea *rms4*/*max2* mutant (Foo et al. 2013). The divergence of AM colonization between the two SLs perception mutants *d14* and *max2* is explained by the function of KL signaling in the process. Indeed, in rice and petunia *kai2/d14like* mutant, the AM colonization is blocked at an

early stage, and the fungal hyphae do not enter the host root (Gutjahr et al. 2015; Liu et al. 2019).

Both SLs and KL signaling have important functions in AMS. In contrast to SLs which have been extensively studied, the mechanism of action of KL signaling in influencing the AMS is still unknown.

VI. Aim of thesis

Since the recent discovery of KAR responses in *A. thaliana* (Nelson et al. 2009), the knowledge on KL signaling and functions has increased extensively. Those discoveries were made in only two species: *A. thaliana* and *Oryza sativa*. The use of these two model plants was undoubtedly beneficial for the research field, to confirm developmental functions and skirt species-specific gene redundancy. The recent discovery that the KL receptor complex is required for arbuscular mycorrhiza symbiosis (AMS) in rice (Gutjahr et al. 2015) led to an open question: **Is the importance of KL signaling in AMS conserved among plant species and particularly in dicotyledons?** *A. thaliana* is unable to establish AMS; therefore, a new model plant was required to answer this question. In general, the use of a distant plant species will allow **challenging previous findings related to SL and KL function in plant development**. Further, the requirement of KL signaling in AMS, made us wonder whether **KL signaling has additional and previously unknown roles in root development.** Legumes, dicotyledonous and of agronomical importance, can perform AMS to enhance nutrients uptake in nutrient-deficient soil. Two model legumes commonly used in research are *Medicago truncatula* and *Lotus japonicus*, with the latest already established in the laboratory. Large non-transgenic genetic resources have been generated in *L. japonicus* with more than 120000 LORE1 transposon insertion lines (Mun et al. 2016) and close to 5000 ethyl-methanesulfonate (EMS) lines (Perry et al. 2003), which constitutes an advantage to rapidly obtain the mutants involved in the KL and SL pathways. Thus, my thesis aimed to initiate the research on the **function of KL signaling in development and its requirement for AMS in *L. japonicus***.

VII. Results

1) *L. japonicus*, a new model plant to gain insight into ligand perception in KL and SL signaling

a) KAI2 underwent duplication prior to diversification in legumes

To characterize the KL as well as the SL perception machinery in *L. japonicus* we retrieved KAI2, D14, and MAX2 by Protein BLAST using Arabidopsis KAI2, D14, and MAX2 as templates. Construction of a phylogenetic tree revealed that *L. japonicus D14* (*Lj5g3v0310140.4*) is a single copy gene whereas, in contrast to Arabidopsis and rice, *KAI2* is duplicated in the genome of *L. japonicus* (Fig 1.1). We called the two paralogs *KAI2a* (*Lj2g3v1931930.1*) and *KAI2b* (*Lj0g3v0117039.1*). The *KAI2* duplication event must have taken place prior to the diversification of the legumes or at least before the separation of the Millettioids and Robinioids (Wojciechowski et al. 2004) as it is also detected in Soybean and *M. truncatula*.

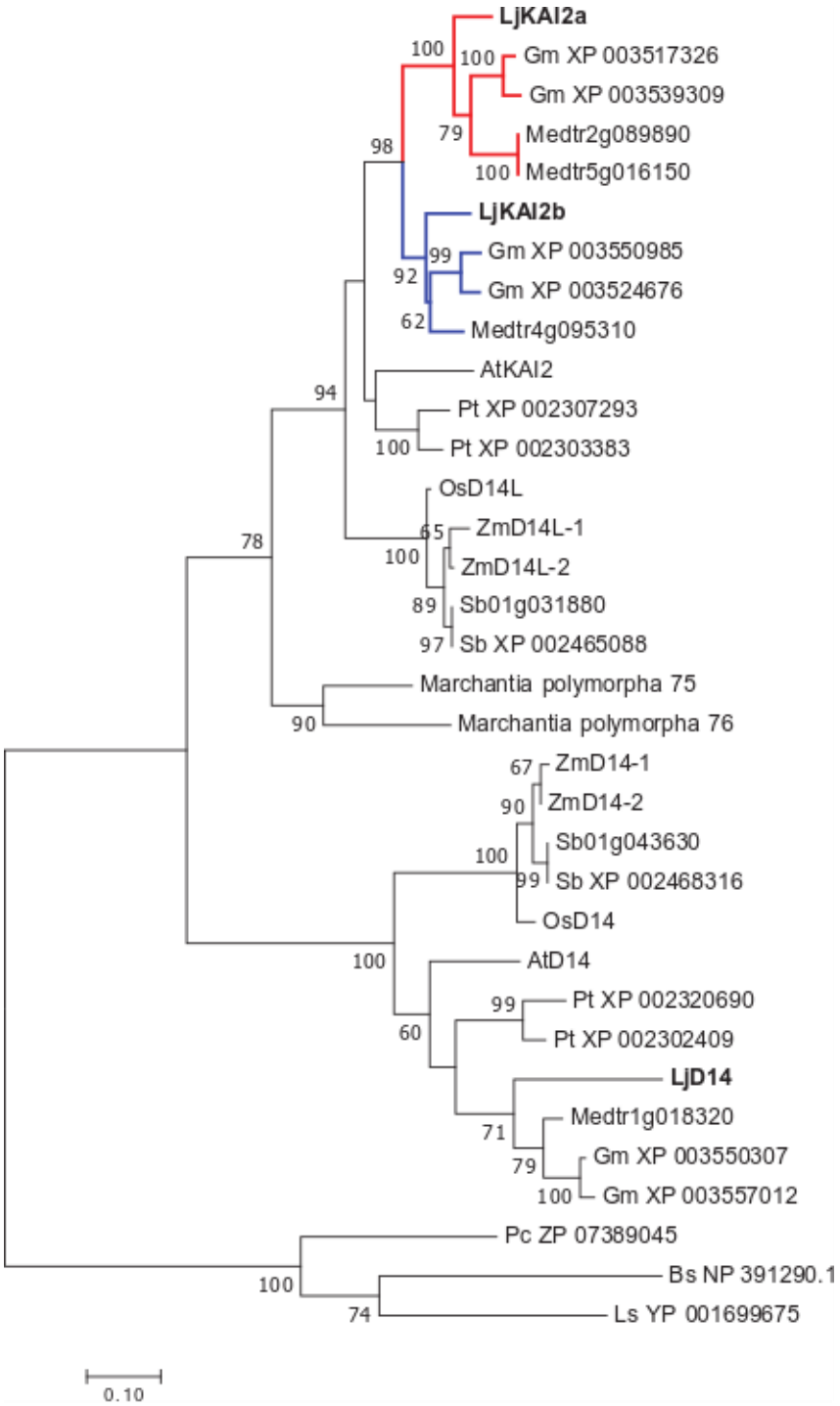

Figure 1.1: Phylogenetic tree of D14 and KAI2. The tree with the highest log likelihood (-6038.38) is shown. The percentage of trees in which the associated taxa clustered together is shown next to the branches, with a value below 50 ignored. *KAI2* duplication in the legumes is highlighted by red/blue branches.

Likely, the F-box protein-encoding gene *MAX2,* also underwent duplication as a result of whole-genome duplication, as the two *MAX2* copies are in syntenic regions of the genome (Fig 1.2.a). However, only one *MAX2* copy (*LjT31N04.80.r2.m*) is functional as the other copy *MAX2-like* (LjSGA_021646.2, LjSGA_145358.1) has an early stop codon, resulting in a putative protein of 216 instead of 710 amino acids (Fig 1.2.b). Presumably, an insertion event of a nucleotide occurred in *MAX2-like* creating a frameshift, as the deletion of T453 would allow the synthesis a full-length MAX2-like.

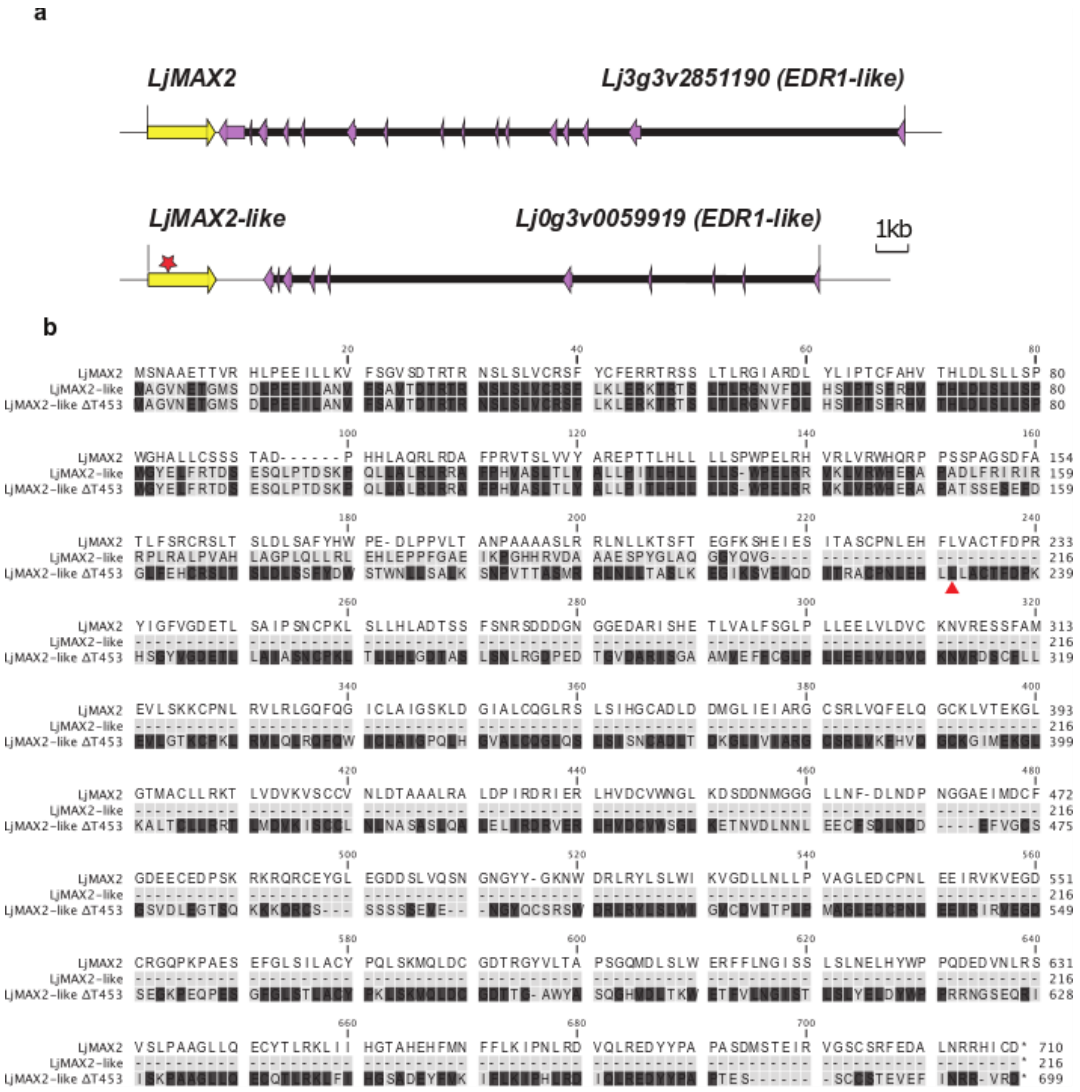

Figure 1.2: A single functional copy of *MAX2* in *L. japonicus*. (a) Schematic representation of the conserved synteny between *MAX2* and *MAX2-like* locus in *L. japonicus*. Colored arrows and black lines show respectively exon and intron structures. Red star indicated the position of an early stop codon in *MAX2-like*. **(b)** Protein alignment of MAX2, MAX2-like and an artificial MAX2-like with a deletion of the thymine at the position 453 in the coding sequence (MAX2-like ΔT453). Position of the nucleotide deletion is indicated in the translated sequence by a red triangle. Amino-acid conservation between MAX2-like to the MAX2 reference is indicated by a dark background.

Since *L. japonicus* seems to require only one copy of *MAX2*, we questioned why it retained two intact copies of *KAI2*. We hypothesized that their expression may have specialized to vary between different organs and analyzed their transcript accumulation in leaves, stems, flowers, and roots of *L. japonicus* (Fig 1.3.a). *KAI2a* transcripts accumulated predominantly in aerial organs, whereas *KAI2b* accumulated at higher levels in roots, which were grown in a sand-vermiculite mix. However, when *L. japonicus* was grown on water-agar in Petri dishes *KAI2a* transcripts accumulated more highly than *KAI2b* in both roots and hypocotyls, indicating differences in organ-specific as well as environment-responsive expression of *KAI2a* and *b* (Fig 1.3.b). Overall, the transcript accumulation of *KAI2a* and *KAI2b* was higher than *D14* and *MAX2*.

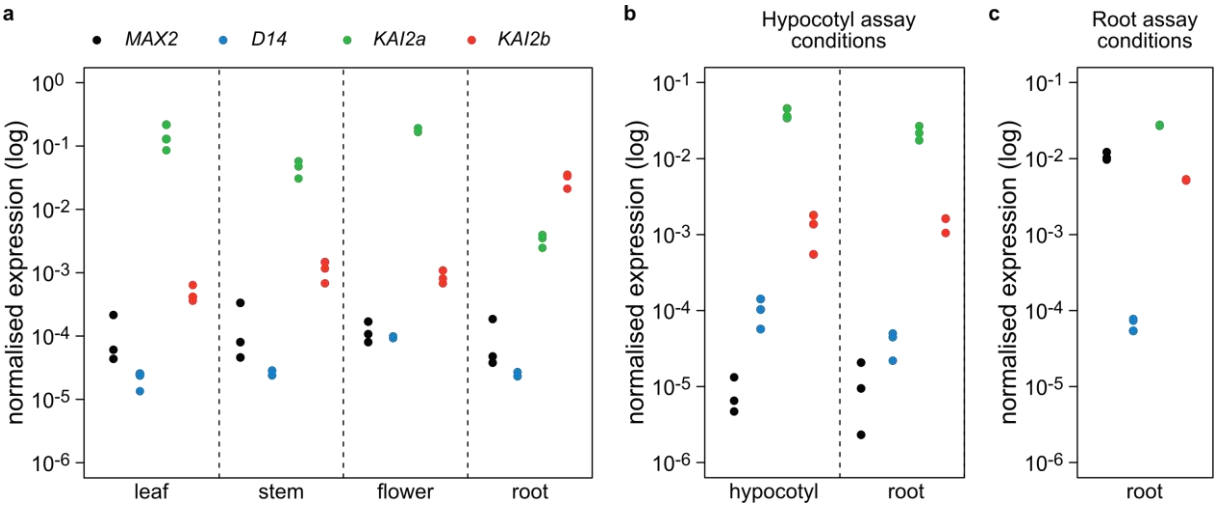

Figure 1.3: (a-b) Transcript accumulation in wild-type of *MAX2, D14, KAI2a* and *KAI2b* in **(a)** leaf, stem, flower and root of plants grown in pots; **(b)** in hypocotyl and roots of plants grown on plates in short-day conditions (8h light / 16h dark); **(c)** in roots of plants grown on plates in long-day conditions (16h light / 8h dark) (n=3).

b) *Lotus D14* and *KAI2*s can replace their orthologs in Arabidopsis

In addition to differences in expression pattern, the two KAI2 paralogs may have evolved ligand specificities and different functions. To examine whether the *L. japonicus KAI2a* and *KAI2b* gene products function as KL receptors, we transgenically complemented the well-described *A. thaliana kai2-2* mutant (Waters et al. 2012) with the two genes. The well-known elongated hypocotyl phenotype of the *Atkai2-2* mutant (Waters et al. 2012) was almost fully rescued by *KAI2a* and partially by *KAI2b* driven

by the Arabidopsis *KAI2* promoter and compared to the restoration efficiency of transgenic *AtKAI2* (Fig 1.4.a). As expected, *D14* under the control of the *AtKAI2* promoter did not restore the hypocotyl length in *Atkai2-2*. We, therefore, examined functional conservation of *L. japonicus D14* by complementing the Arabidopsis *d14-1* mutant, which displays enhanced shoot branching (Waters et al. 2012) with *D14* under the control of the Arabidopsis *D14* promoter. *L. japonicus D14* restored wild-type-like shoot branching of the *Atd14-1* mutant (Fig 1.4.b). However, *L. japonicus KAI2a* and *LjKAI2b,* driven by the *AtD14* promoter did not affect the number of rosette branches in *Atd14-1*. These results together with the phylogenetic analysis (Fig 1.1) indicate that *L. japonicus KAI2a*, *KAI2b,* and *D14* are, respectively functional orthologues of the *Arabidopsis* KL (*KAI2*) and SL (*D14*) receptor genes, and that they are not interchangeable, similar to the situation in Arabidopsis (Waters et al. 2015b). The different ability of *KAI2a* and the paralog *KAI2b* to rescue the *Atkai2-2* hypocotyl phenotype might be due to variation in affinity to endogenous KL ligand(s) or to interacting *Arabidopsis* proteins caused by variations in amino acids exposed at the protein surface.

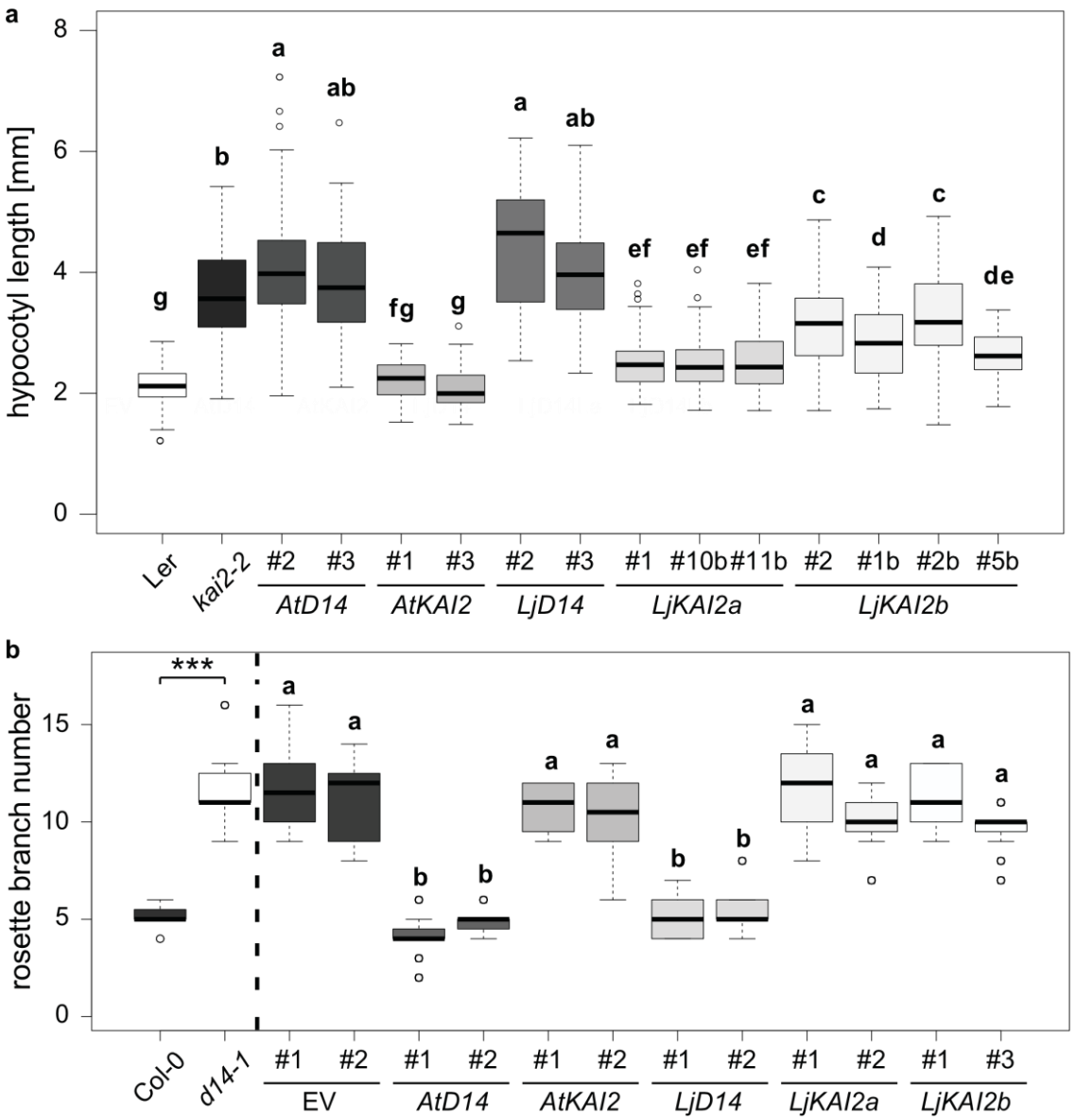

Figure 1.4: *L. japonicus D14*, *KAI2a* and *KAI2b* can respectively replace *D14* and *KAI2* in Arabidopsis. (a) Hypocotyl length of *A. thaliana* wild-type (*Ler*), *kai2-2* and *kai2-2* lines complemented by *AtD14, AtKAI2, LjD14, LjKAI2a,* and *LjKAI2b*, driven by the *AtKAI2* promoter. Plants were grown 6-day post-germination in short-day conditions (8h light / 16h dark) (n ≤ 37). **(b)** Rosette branch number at 26 day-post germination of *A. thaliana* wild-type (*Col-0*), *d14-1* and *d14-1* lines carrying an empty vector (EV) or expressing *AtD14, AtKAI2, LjD14, LjKAI2a,* and *LjKAI2b*, driven by the *AtD14* promoter (n = 24). Letters indicate significant differences (ANOVA, post-hoc Tukey test).

c) Identification of KL and SL perception mutants in *L. japonicus*

To investigate whether *KAI2a* and *KAI2b* have specific functions in *L. japonicus*, we obtained and characterized mutants perturbed in these genes in addition to *D14* and

MAX2. We found *LORE1* retrotransposon insertions in *KAI2a*, *KAI2b* and *MAX2* (*max2-1, max2-2, max2-3, max2-4, kai2a-1, kai2b-3*) (Malolepszy et al. 2016; Fukai et al. 2012) and early stop codon mutations in *D14* and *KAI2b* (*d14-1, kai2b-1, kai2b-2*) by TILLING (Perry et al. 2003) (Fig 1.5.a, Table 1.1). Since some of the *max2* and *kai2b* mutants had problems with seed germination or seed production (Table 1.1), we continued working with *kai2b-1, kai2b-3, max2-3, max2-4.* Quantitative RT-PCR analysis revealed that these mutants displayed reduced transcript accumulation of the respective mutated genes in roots except for *d14-1* (Fig 1.5.b). We also examined, whether the mutation of *KAI2a* would lead to compensatory expression differences of *KAI2b* and *vice versa*. However, the transcript accumulation of *KAI2a* and *KAI2b* was not affected by mutation of the respective other paralogs.

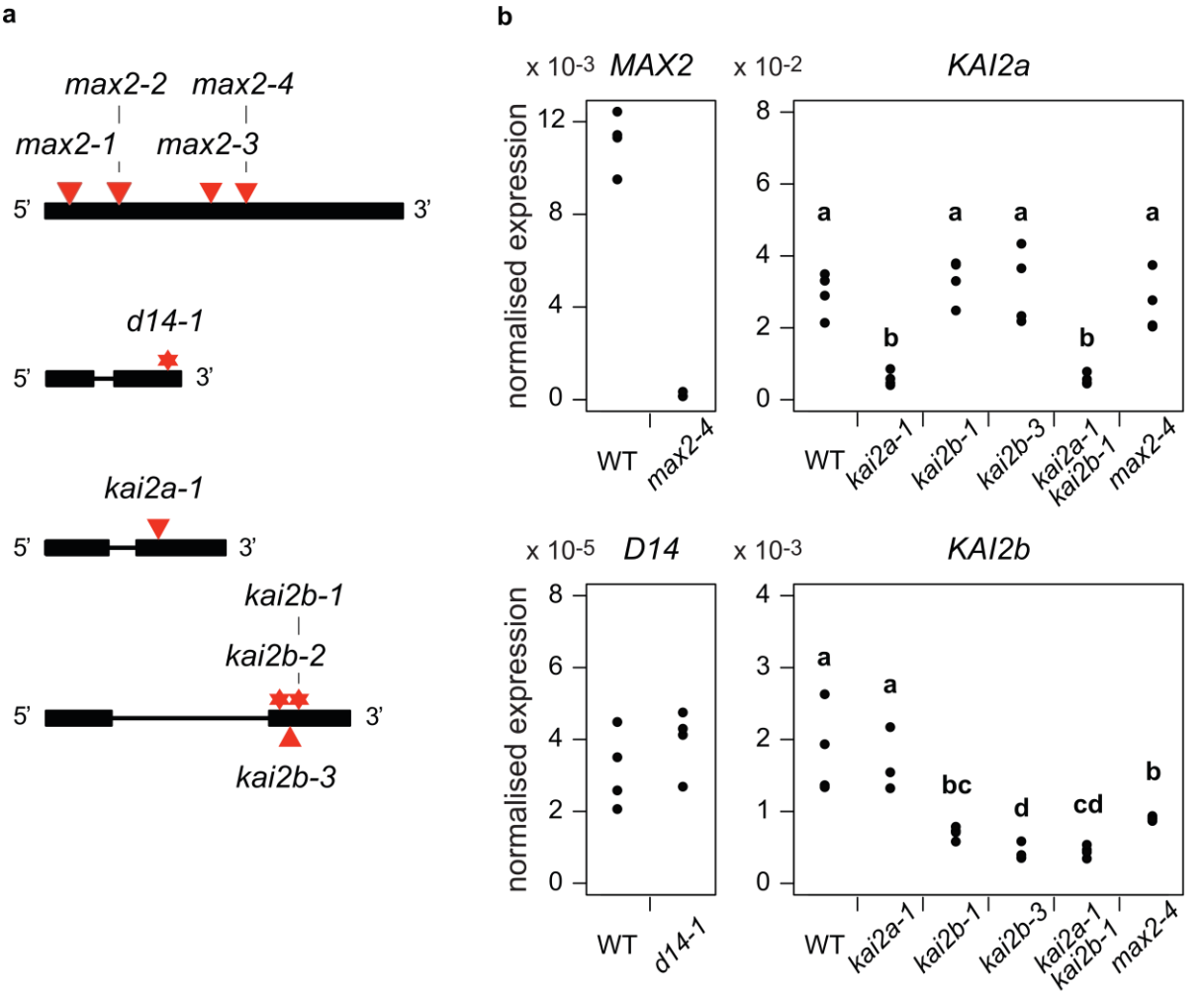

Figure 1.5: (a) Schematic representation of the *L. japonicus MAX2, D14, KAI2a*, and *KAI2b* genes. Black boxes and lines show respectively exon and intron structures. LORE1 insertion and EMS mutations are indicated by triangle and stars respectively, labeled with the number of the respective mutant allele. **(b)** Transcript accumulation in roots of *KAI2a*, *KAI2b*, MAX2, and *D14* in their respective mutant background (n = 4). Letters indicate significant differences (ANOVA, post-hoc Tukey test).

d) SL signaling represses shoot branching in *L. japonicus*

To confirm the conserved function of SL in shoot branching inhibition in *L. japonicus*, we looked at the shoot phenotype of these first-time described mutants in *L. japonicus*. Both *d14-1* and all allelic *max2* mutants of *L. japonicus* displayed increased shoot branching, indicating that similar to Arabidopsis, pea and rice (Beveridge et al. 1996; Stirnberg et al. 2007; Ishikawa et al. 2005; Waters et al. 2012), the *L. japonicus* SL receptor components D14 and MAX2 are involved in shoot branching inhibition (Fig 1.6). Since all allelic *max2* mutants had a similar shoot branching phenotype, we performed all other experiments with *max2-3* and *max2-4* because it was difficult to amplify seed from the *max2* mutants, and this problem was particularly severe for *max2-1* and *max2-2*.

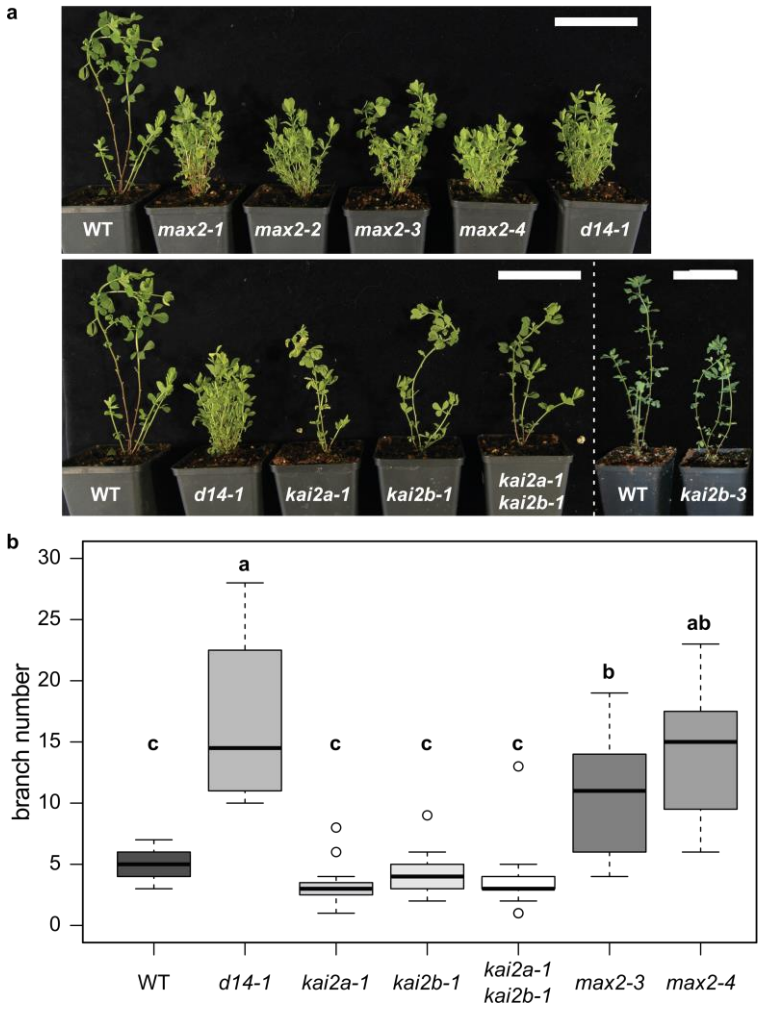

Figure 1.6: (a) Shoot phenotype of wild-type and several *L. japonicus* KL and SL perception mutants at 8 week-post germination. Scale bars: 7 cm. **(b)** Number of branches of 7 weeks old *L. japonicus* wild-type, *d14-1, kai2a-1, kai2b-1*, *kai2a-1/kai2b-1, max2-3 and max2-4* (n ≤ 12). Letters indicate significant differences (ANOVA, post-hoc Tukey test).

e) KL signaling is not required but sufficient for inhibition of hypocotyl elongation in *L. japonicus*

Previous research has shown that Arabidopsis and rice *KAI2* are required to suppress hypocotyl and mesocotyl elongation, respectively (Waters et al. 2012; Gutjahr et al. 2015). However, *L. japonicus kai2a* and *kai2b* single mutants did not display an increased hypocotyl length (Fig 1.7). To address functional redundancy between *KAI2a* and *KAI2b*, we created a *kai2a-1 kai2b-1* double mutant by crossing. Neither *kai2a-1 kai2b-1* double mutants nor two allelic *max2* mutants showed an increase in hypocotyl length, indicating that the requirement of KL signaling for suppression of hypocotyl elongation is not conserved in *L. japonicus*.

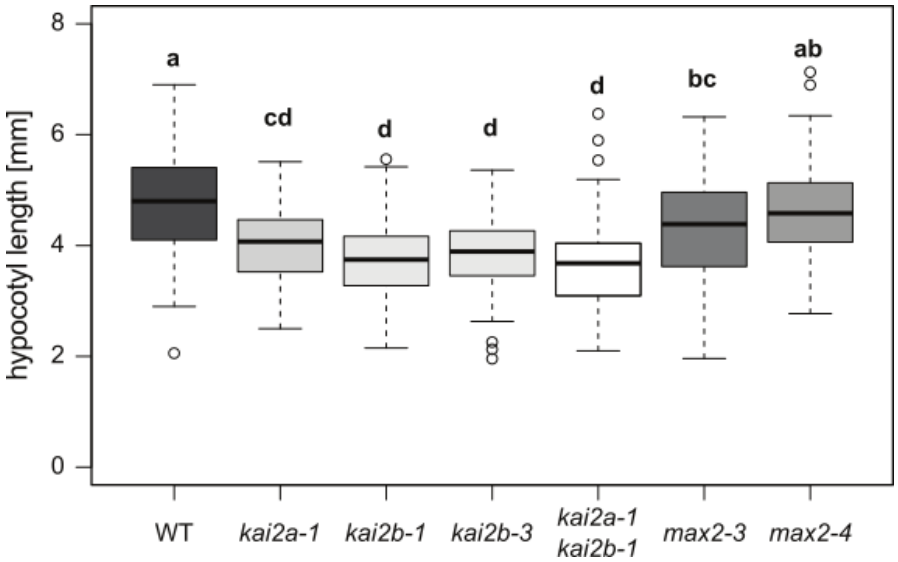

Figure 1.7: Hypocotyl length at 1 week-post germination of *L. japonicus* wild-type, *kai2a-1, kai2b-1, kai2-3, kai2a-1/kai2b-1, max2-3* and *max2-4* (n ≤ 72). Letters indicate significant differences (ANOVA, post-hoc Tukey test).

To examine whether *L. japonicus* hypocotyls are responsive to KAR treatment, we measured the dose-response to KAR_1, KAR_2 and also the *rac*-GR24 of hypocotyl elongation in wild-type. Hypocotyl elongation was progressively inhibited with increasing concentrations of all three compounds, but the response was most sensitive to KAR_2 (Fig 1.8).

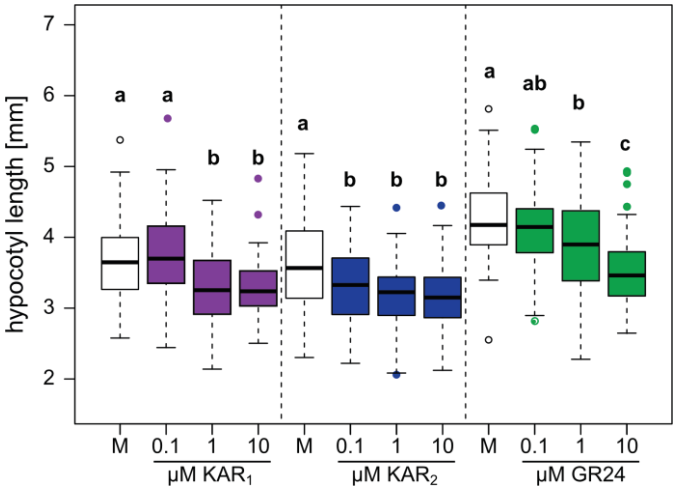

Figure 1.8: Hypocotyl length of *L. japonicus* seedlings one-week post-germination, after treatment with solvent (M) or three different concentration (0.1µM, 1µM and 10µM) of KAR_1, KAR_2 or *rac*-GR24 (n ≤ 95). Letters indicate significant differences (ANOVA, post-hoc Tukey test).

Then, we tested if this response was dependent on KL perception components. Hypocotyl growth of the *kai2a-1 kai2b-1* double mutant and the *max2-4* mutant did not respond to KAR_1 or KAR_2 treatment, while *d14-1* mutant hypocotyls responded to both compounds in a wild-type-like fashion (Fig 1.9). Further, we investigated whether *KAI2a* and *KAI2b* alone were sufficient for perception and response to these compounds. The *kai2a-1* mutant did not show a reduction in hypocotyl length after treatment with both KAR. In contrast, the hypocotyl length in the two allelic *kai2b* mutants was reduced in response to both KAR species.

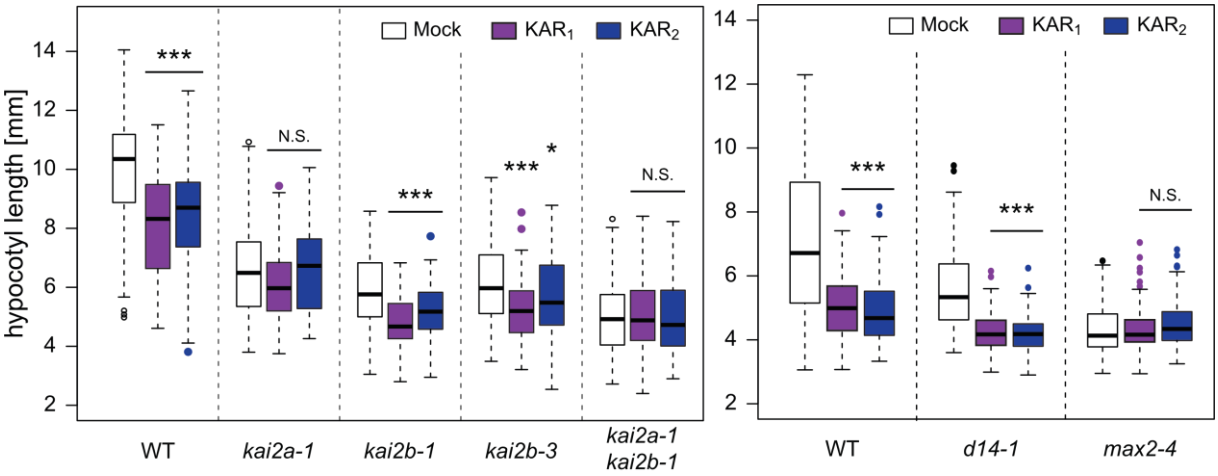

Figure 1.9: Hypocotyl length of *L. japonicus* wild-type and KL perception mutant seedlings after treatment with solvent (mock), 1µM KAR_1 or 1µM KAR_2 (n ≤ 66). Asterisks indicate significant differences between the compounds versus mock treatment (ANOVA, post-hoc Dunnett test, N.S.>0.05, *≤0.05, **≤0.01, ***≤0.001).

To confirm the divergence in response to KAR_1 and KAR_2 in *L. japonicus* KL perception mutants, we analyzed the induction of the KAR marker gene *DLK2*, which is well-established in Arabidopsis (Waters et al. 2012). *DLK2* transcript accumulated in large amounts in the WT and *kai2b-3* mutants, whereas its expression was strongly reduced in the *kai2a-1* mutant (Fig 1.10.a). This expression pattern may reflect the difference in transcript accumulation in hypocotyl between *KAI2a* and *KAI2b* (Fig 1.3.b). Also, *DLK2* is induced by KAR_1, KAR_2, and *rac*-GR24 treatment in the wild-type but also in the *kai2b-3* mutant (Fig 1.10.b). Whereas no differences in basal *DLK2* expression between *kai2a-1* and the *kai2a-1 kai2b-1* is observed, *max2-4* mutant has an even lower transcript accumulation (Fig 1.10.a). In addition, *rac*-GR24 treatment in the *kai2a-1 kai2b-1* double mutant induces *DLK2*, but not in the *max2-4* mutant (Fig 1.10.b). Therefore, it is likely that *D14*-mediated signaling is involved in the expression of *DLK2* in the hypocotyl. Mutation of the *KAI2a* gene is sufficient to abolish transcriptional response to KAR_1 and KAR_2, which indicates the absence of *KAI2b* function in this response. These results are in accordance with the non-requirement of *KAI2b* in repressing hypocotyl elongation by KAR_1 and KAR_2.

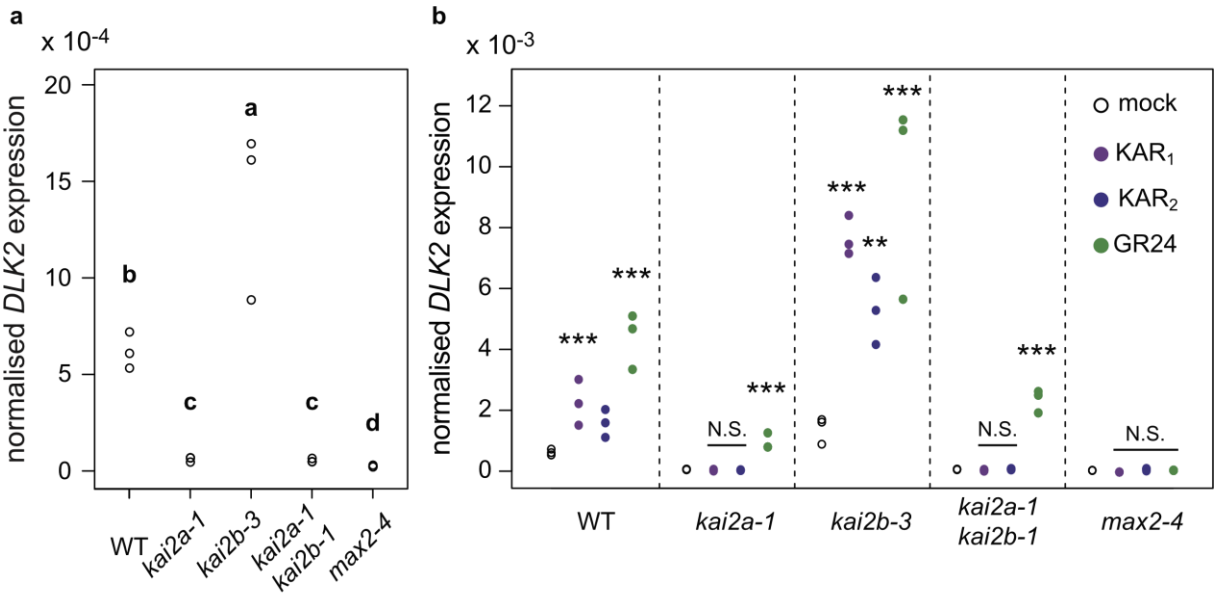

Figure 1.10: Transcript accumulation of *DLK2* in hypocotyls after 2h treatment with solvent (mock), 1µM KAR_1, 1µM KAR_2 and 1µM *rac*-GR24. **(a)** Mock treatment alone was used to generate basal expression level (n = 3). Letters indicate significant differences (ANOVA, post-hoc Tukey test). Asterisks indicate significant differences between the compounds versus mock treatment (ANOVA, post-hoc Dunnett test, N.S.>0.05, *≤0.05, **≤0.01, ***≤0.001).

Taken together these results indicate that the duplicated *KAI2* have unequal functions in *L. japonicus*, with *KAI2a* being the only paralog required to mediate hypocotyl responses to exogenously applied KAR.

f) KAI2a and KAI2b have different ligand affinities

Due to differential hypocotyl response by *KAI2a* and *KAI2b*, we examined whether *L. japonicus* KAI2a and KAI2b would have different ligand affinities. We quantified the hypocotyl growth response to KAR_1 and KAR_2 of the *Atkai2-2* lines complemented with *KAI2a* or *KAI2b* (Fig 1.11.a). Two independent lines complemented with *KAI2a* displayed the same reduction in hypocotyl growth in response to KAR_1 and KAR_2, similar to the line complemented with *AtKAI2*. However, the two lines expressing *KAI2b* responded more strongly to KAR_1 than to KAR_2, contrasting with the common observation, that Arabidopsis hypocotyl growth tends to be more responsive to KAR_2 (Waters et al. 2012; Nelson et al. 2010). We inspected if KAI2 from another species also displays a preference towards a specific KAR molecule. A cross of the *kai2* mutant *htl-2* with an Arabidopsis line transgenic for the cDNA of the rice *D14L*/*KAI2* (Gutjahr et al. 2015) was available, and we tested its response to the two KAR molecules. The *OsKAI2* expressing line was more responsive to KAR_2 than to KAR_1 (Fig 1.11.b), confirming that differential responsiveness to different KAR is due to the amino acid sequence of the receptor and unlikely to be caused by a general incompatibility of a heterologous KAI2 protein with the Arabidopsis background. Together, these results imply that KAI2a and KAI2b differ in their affinities to KAR_1 and KAR_2 or their possible breakdown products (Waters et al. 2015b).

It is known that in Arabidopsis, KAI2 and D14 mediate responses to the two stereoisomers contained in the synthetic SL *rac*-GR24 (Scaffidi et al. 2014). To test if the differences in ligand perception between KAI2a and KAI2b for KARs, can also be observed for GR24 stereoisomers, we complemented the *A. thaliana d14-1 kai2-2* double mutant with *KAI2a* and *KAI2b* and tested the hypocotyl response to $GR24^{5DS}$ and $GR24^{ent\text{-}5DS}$ (Fig 1.11.c). Lines expressing *KAI2a* responded to both stereoisomers, with a stronger response to $GR24^{ent\text{-}5DS}$, whereas the lines expressing *KAI2b* did not respond to any of the two stereoisomers.

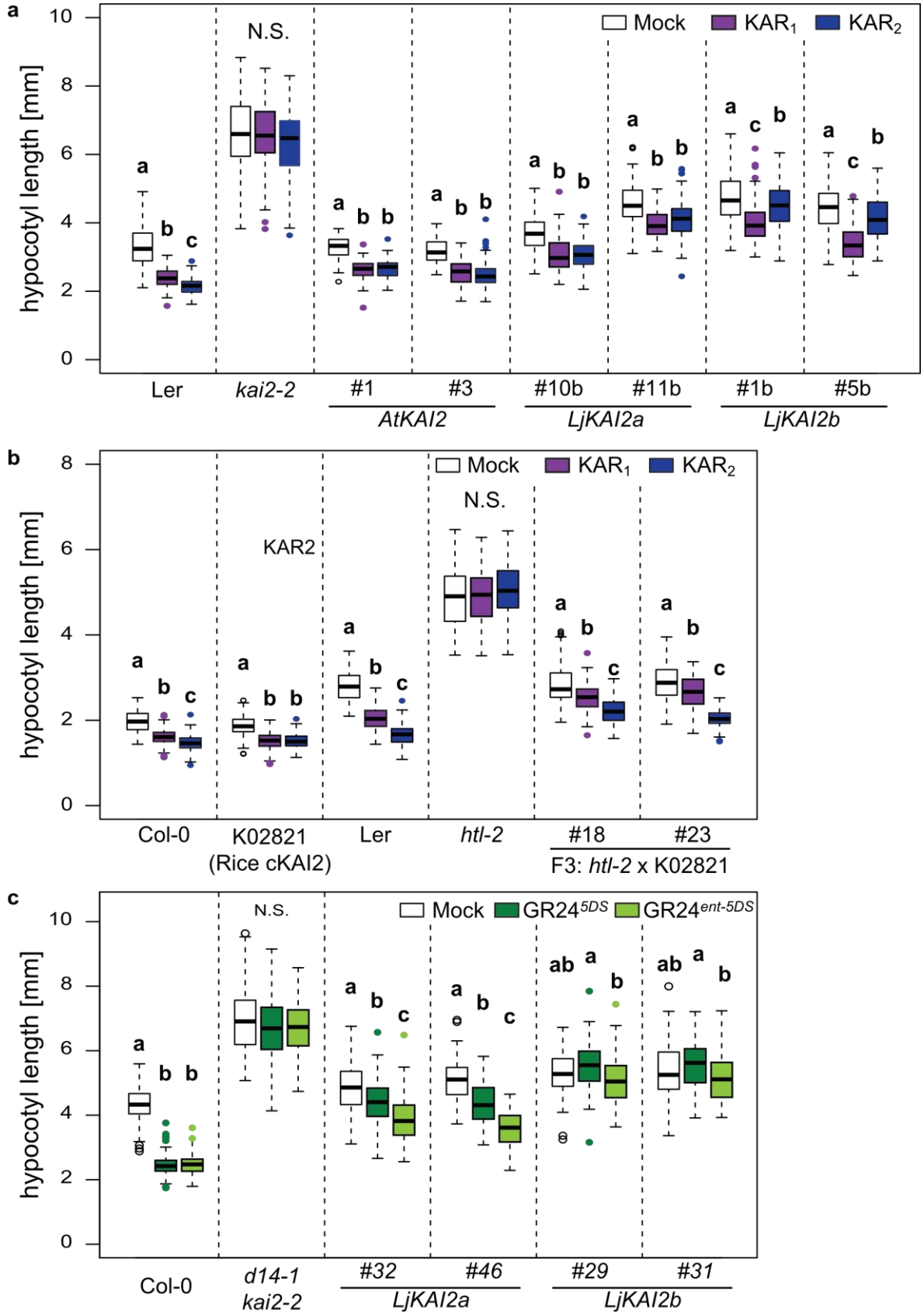

Figure 1.11: *L. japonicus* KAI2a, KAI2b, and Rice D14L have different affinities to ligands. (a-b) Hypocotyl length of *A. thaliana kai2* mutants complemented with *KAI2*s from Arabidopsis, Lotus, and rice, after treatment with solvent (mock), 1μM of KAR_1 or KAR_2. **(a)** Wild-type (Ler), *kai2-2* and *kai2-2* lines complemented by *AtKAI2, LjKAI2a,* and *LjKAI2b*, driven

by the *AtKAI2* promoter (n ≤ 33). **(b)** Wild-type (Ler and Col-0), *htl-2* (Ler), K02821-line transgenic for *p35s:OsD14L* (Col-0), and 2 lines from the *htl-2* x K02821 cross (n ≤ 80). **(c)** Hypocotyl length of *A. thaliana* wild-type (Col-0), *d14-1 kai2-2*, and *d14-1 kai2-2* lines complemented by *LjKAI2a* and *LjKAI2b*, driven by the *AtKAI2* promoter after treatment with solvent (mock), 1µM GR24^{5DS} or GR24$^{ent\text{-}5DS}$ (n ≤ 59) Letters indicate significant differences (ANOVA, post-hoc Tukey test).

To confirm that KAI2a and KAI2b have different ligand affinities, we analyzed their ligand interaction *in vitro* by differential scanning fluorimetry (DSF). This assay has been successfully used to characterize ligand binding to D14 and KAI2 proteins *in vitro* (Hamiaux et al. 2012; Waters et al. 2015b). However, it failed to show binding of KAI2 to KAR_1 and KAR_2, possibly because KAR are metabolized *in planta* and their metabolic products, not the molecules themselves, bind to the receptor (Waters et al. 2015b). GR24$^{ent\text{-}5DS}$ is known to bind to KAI2 proteins from Arabidopsis, *Selaginella moellendorfii,* and *Marchantia polymorpha* (Waters et al. 2015b). We, therefore, employed GR24$^{ent\text{-}5DS}$ and could confirm its specific binding to KAI2a but not to KAI2b (Fig 1.12). Together these results indicate that KAI2a and KAI2b have differences in their binding pocket, which determine ligand binding specificity.

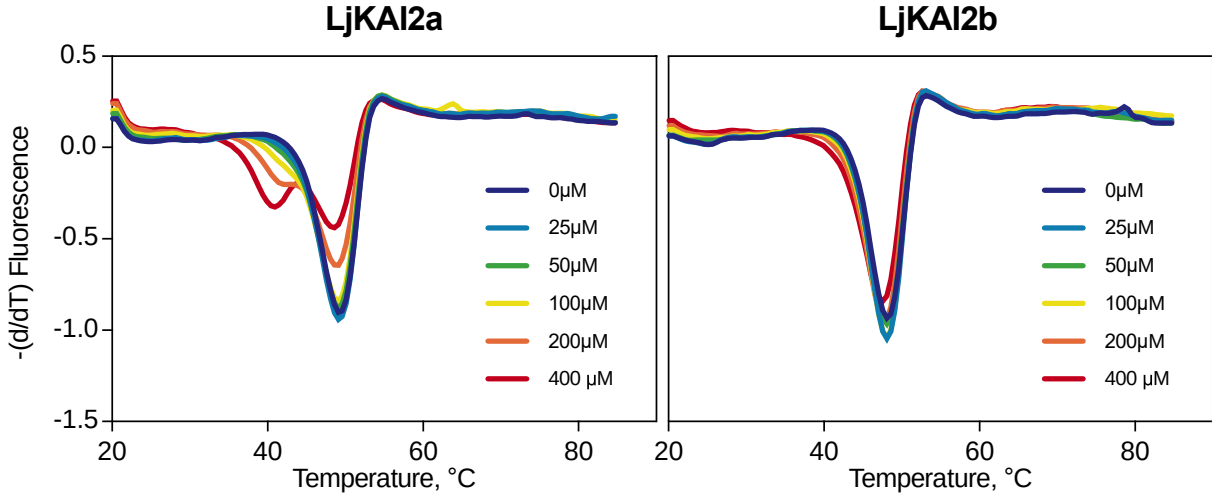

Figure 1.12: GR24$^{ent\text{-}5DS}$ binds to LjKAI2a but not to LjKAI2b in Differential Scanning Fluorimetry. Purified SUMO fusion KAI2a and KAI2b were incubated with a fluorescent dye and increasing concentration of GR24$^{ent\text{-}5DS}$. First derivative of the change of fluorescence was plotted against the temperature. Peaks indicate the protein melting temperature. The shift of the peak in LjKAI2a indicates protein-ligand interaction. The DSF assay was conducted by Mark Waters, University of Western Australia.

g) Three amino acid residues close to the cavity are decisive for ligand binding specificity

A comparison of the protein sequences of KAI2a and b in legumes revealed conserved differences between the two paralog clades for 16 amino acids (Fig 1.13.a). However, four of them (KAI2a: Y157L, I188T, M223V; and KAI2b: I119V) are not conserved in *L. japonicus*. We asked whether the remaining amino-acids can be responsible for the observed differential ligand affinities between LjKAI2a/AtKAI2 and LjKAI2b, and therefore, focused on the amino-acids (KAI2b: T103, M161, L191, A226), which are different between OsKAI2 and LjKAI2b. We modeled the two LjKAI2s on the KAR_1 bound AtKAI2 crystal structure (4JYM) (Guo et al. 2013), and checked, which of these residues are positioned in the binding pocket. Two of these residues appeared to be either at the entrance (L/M 160/161) or inside the cavity (S/L 190/191) (Fig 1.13.b). In addition, we found another residue inside the cavity (F/W 157/158), which is different between the Lotus KAI2a and KAI2b but is not conserved across the inspected legumes.

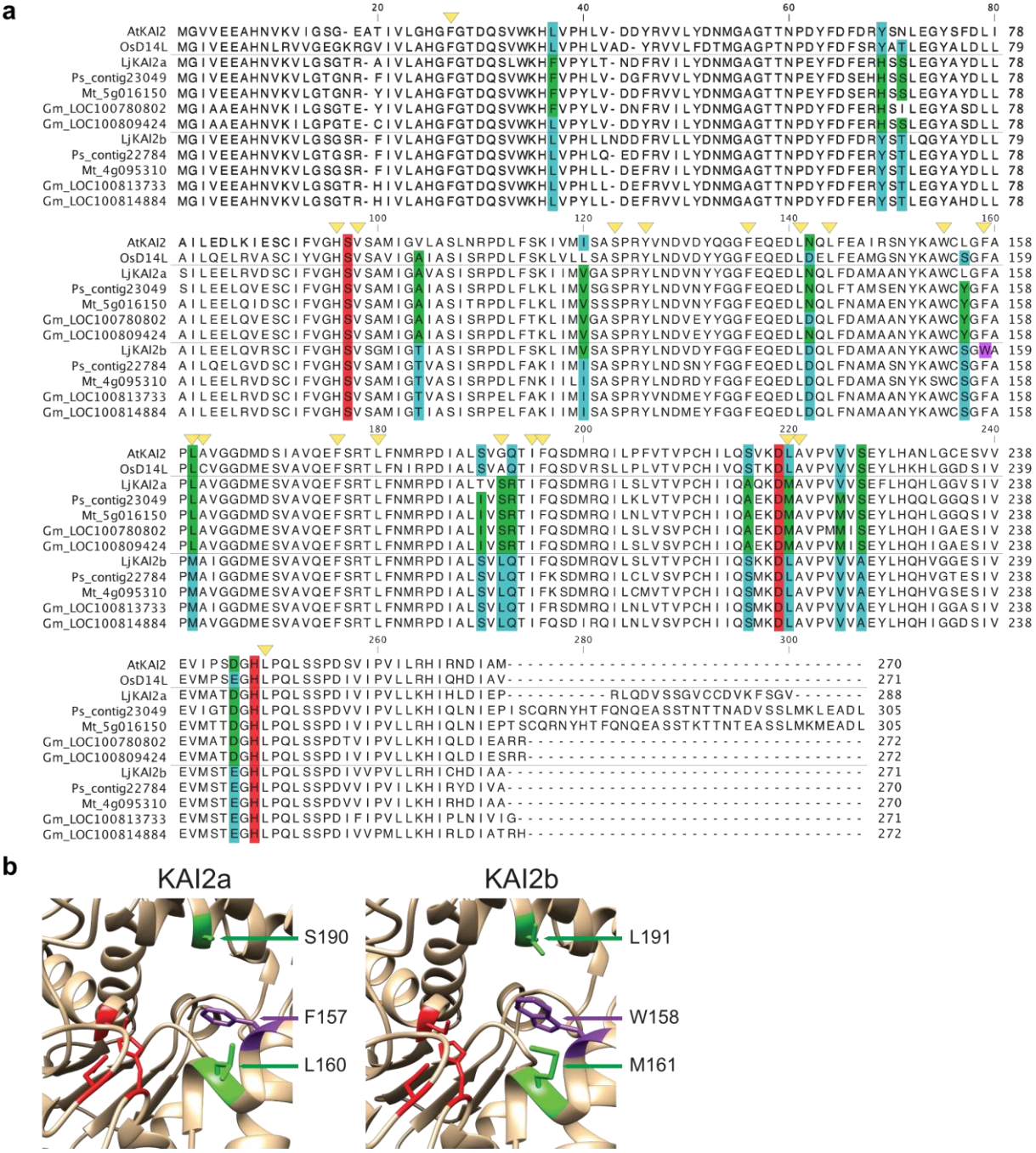

Figure 1.13: Specific conservation of residues in the legume KAI2a and KAI2b clades. **(a)** Protein alignment of KAI2a and KAI2b from the legumes *L. japonicus, Pisum sativum, M. truncatula,* and *Glycine max*, compared to the single Arabidopsis KAI2 and Rice D14L. Residues, which differ between the KAI2a and KAI2b clades but are conserved across the legumes are respectively colored in green and blue. Residues of the catalytic triad are colored in red. A non-conserved tryptophan in LjKAI2b located in the cavity is colored in violet. Yellow triangles indicate residues forming the cavity. **(b)** Zoom into the ligand cavity of LjKAI2a and LjKAI2b protein models. Conserved residues diverging between KAI2 clades are colored in green and the non-conserved residue in violet. Catalytic triad residues are in red.

To confirm the involvement of these three amino acid residues in determining the ligand binding specificity, we exchanged them between the two receptors. *In vitro*, mutated LjKAI2a(3b) (LjKAI2a: F157W, L160M, S190L) lost the capacity to bind GR24$^{ent\text{-}5DS}$ (Fig 1.14). In contrast, mutated LjKAI2b(3a) (LjKAI2b: W158F, M161L, L191S) gained the ability to bind GR24$^{ent\text{-}5DS}$. Together these results indicate that the residues at the KAI2a positions 157, 160, 190 determine the ligand preference between the two *L. japonicus* KL receptors.

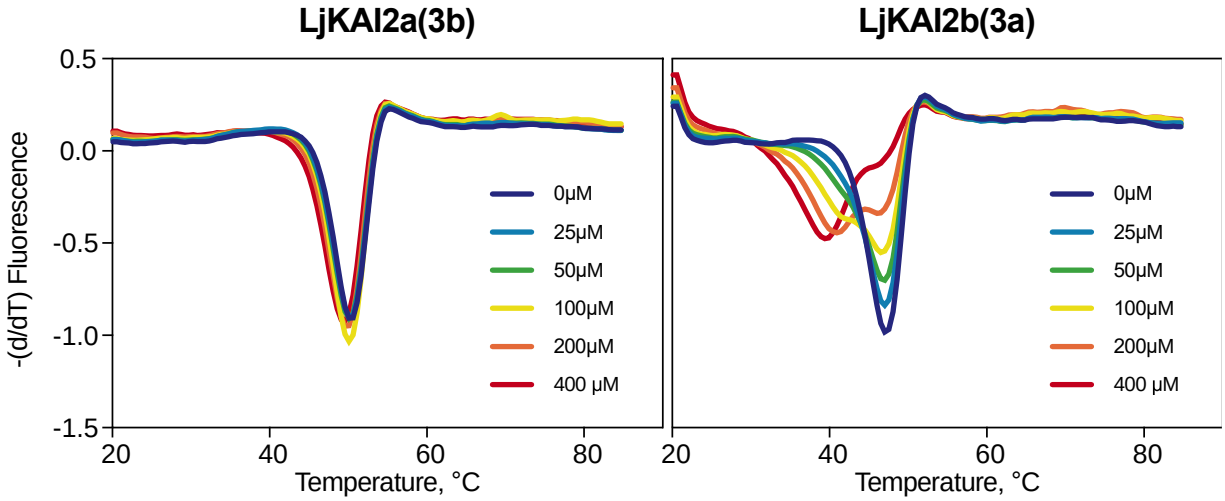

Figure 1.14: Three amino acid exchange in LjKAI2b(3a) lead to GR24$^{ent\text{-}5DS}$ binding. Purified SUMO fusion KAI2a(3b) and KAI2b(3a) were incubated with a fluorescent dye and increasing concentration of GR24$^{ent\text{-}5DS}$. First derivative of the change of fluorescence was plotted against the temperature. Peaks indicate the protein melting temperature. The shift of the peak in LjKAI2b(3a) indicates protein-ligand interaction. The DSF assay was conducted by Mark Waters, University of Western Australia.

2) KL perception has a quantitative effect on AM colonization of *L. japonicus*

a) A reduction of AM colonization in *L. japonicus* KL perception mutants

To test the requirement of the KL pathway in AMS in *L. japonicus*, we inoculated three *max2* alleles with *rhizophagus irregularis* DAOM 197198 spores. Since *d14l-kai2* and *max2* mutations in rice block early colonization events (Gutjahr et al. 2015), we particularly pay attention to hyphopodia formation. Surprisingly, *L. japonicus max2* mutants showed a similar amount of hyphopodia than the wild-type (Fig 2.2.a). Besides, all fungal structures were observed in the *max2* colonized roots, which includes vesicles (data not shown) and intact arbuscules (Fig 2.2.b). However, the total root-length colonization was reduced in these mutants to half the wild-type colonization (Fig 2.2), suggesting a minor function of KL or SL signaling in AMS.

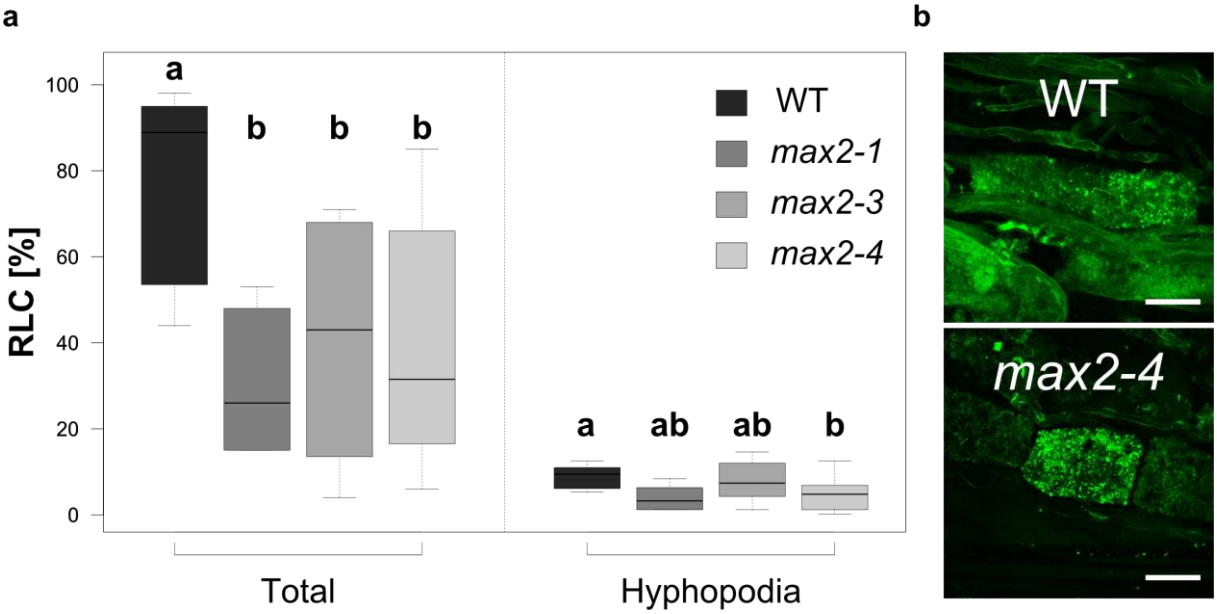

Figure 2.1: AM colonization in *L. japonicus max2* mutants. (a) Root length colonization (RLC) in wild-type, *max2-1*, *max2-3* and *max2-4* after 6 weeks post-inoculation (n ≤ 5). **(b)** Example of arbuscule in wild-type and *max2-4* stained with wheat-germ-agglutinin coupled with Alexa-Fluorophor488. Scale bar = 20µm. Letters indicate significant differences between genotypes (ANOVA, post-hoc Tukey test).

To differentiate the involvement of KL or SL signaling in AMS, we quantified the colonization in the respective receptor mutants (Fig 2.3). The *kai2a-1 kai2b-1* mutant had lower colonization than the wild-type, at a similar level than *max2-4*. Whereas, the

d14-1 mutant did not display a significant decrease in colonization. Thus, we tested if one of the KL receptors have gained a specialized function in AMS. However, root colonization of the single mutants of *kai2a* and *kai2b* was not significantly reduced in AM root length colonization (Fig 2.3). Altogether, these results indicate that KL signaling has a less substantial role than in rice in promoting AMS in *L. japonicus*, and it is mediated by both KAI2 receptors.

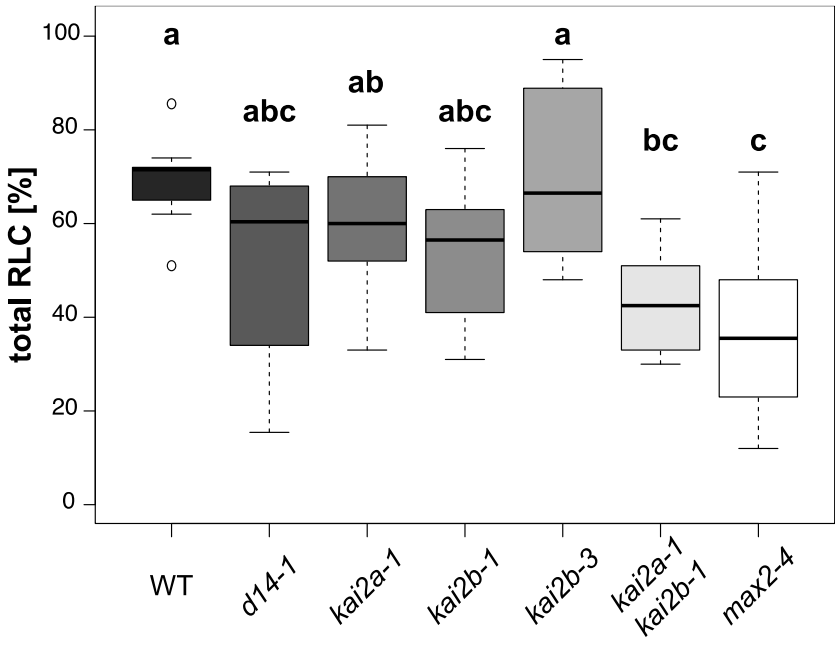

Figure 2.2: AM colonization in *L. japonicus* KAR and SL perception mutants. Root length colonization (RLC) after 6 weeks post-inoculation (n = 10). Letters indicate significant differences between genotypes (ANOVA, post-hoc Tukey test).

b) KAR signaling is required locally for AM colonization

Regulation of root symbiosis integrates control mechanism localized in the root but also in the shoot. In the case of the root-nodule symbiosis (RNS), to avoid decrease growth due to excess of nodulation, a cytokinin-mediated shoot signal inhibits further nodule development (Kawaguchi 2014). Similarly, there is evidence of a long distance signal traveling from shoot to the root regulating AMS depending on the phosphate status of the plant (discussed in (Carbonnel and Gutjahr 2014)).

To investigate if KL signaling is required in root or shoot, we used *Agrobacterium rhizogenes*-mediated root (hairy-root) transformation to complement the *max2-4* mutant by expressing *MAX2* under its own promoter. Complemented roots of the

max2-4 mutant showed higher colonization similar to wild-type level as compared to roots transformed with an empty vector as a control (Fig 2.4). The hairy-root transformation results in a plant root system composed of transformed and non-transformed roots. This allowed us to compare the colonization levels in complemented and non-complemented roots in the *max2-4* mutants. The level of colonization in the non-transformed roots was lower than the transformed roots, similar to the non-complemented *max2-4* mutant. These results indicate that *MAX2* mediated signaling, and therefore likely KL signaling, is required locally to promote root AM colonization.

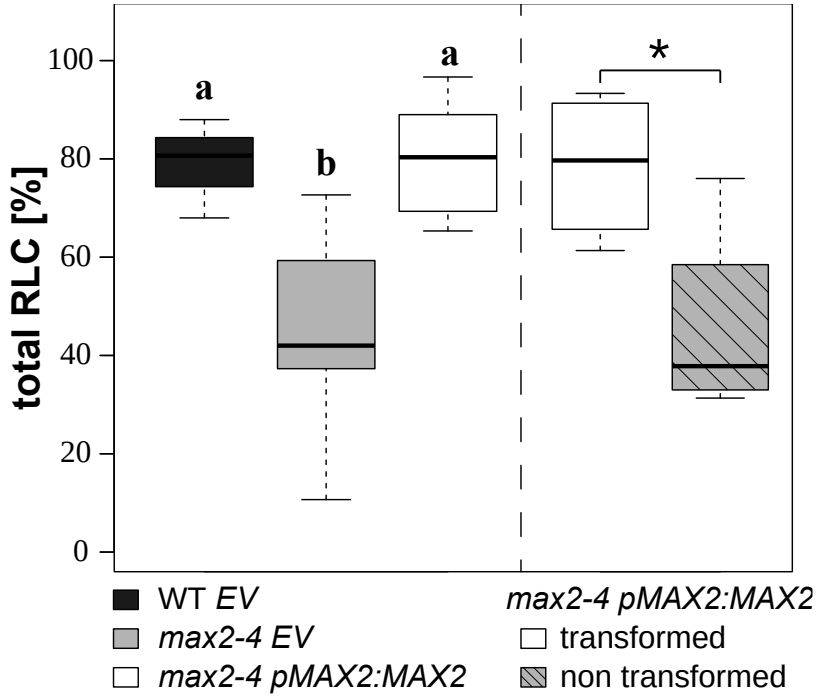

Figure 2.3: Rescue of full AM colonization by transgenic complementation of *max2-4*. Root length colonization (RLC) of wild-type and *max2-4* hairy-roots, expressing an empty vector (EV) or *pMAX2:MAX2*, after 6 weeks post-inoculation ($n \leq 3$). Letters indicate significant differences between genotypes (ANOVA, post-hoc Tukey test). The asterisk indicates a significant difference (paired Welch t.test, *≤0.05).

3) Ethylene-mediated, KL signaling shapes the root system

a) KAR_1 treatment affects the root system architecture

It was previously suggested, that SL signaling is involved in modulating root development of Arabidopsis and *M. truncatula* (Ruyter-Spira et al. 2011; Jiang et al. 2016; De Cuyper et al. 2015). We examined whether *L. japonicus* root systems would respond to *rac*-GR24 as well as KAR_1 and KAR_2 and applied different doses of all three compounds (Fig 3.1.a). Surprisingly, in contrast to Arabidopsis and *M. truncatula*, *L. japonicus* root systems did not respond to *rac*-GR24. They neither responded to KAR_2. Exclusively, KAR_1 treatment leads to a decrease in primary root length and an increase of post-embryonic root (PER) numbers, which includes lateral and adventitious roots that are difficult to distinguish in young *L. japonicus* seedlings and thus, to a higher PER density (Fig 3.1.a). The instability of *rac*-GR24 over time in the medium could potentially prevent a root developmental response in our experiments (Halouzka et al. 2018). However, refreshing the medium with new KAR or *rac*-GR24 at 5 days post-germination did not alter the outcome, PER density remained unaffected by *rac*-GR24 treatment (Fig 3.1.b). Together with the *L. japonicus* hypocotyl responses to KAR_1, KAR_2, and *rac*-GR24 (chapter I), this result indicates organ-specific sensitivity or responsiveness to the three compounds in *L. japonicus* and a more stringent perception or response in the root.

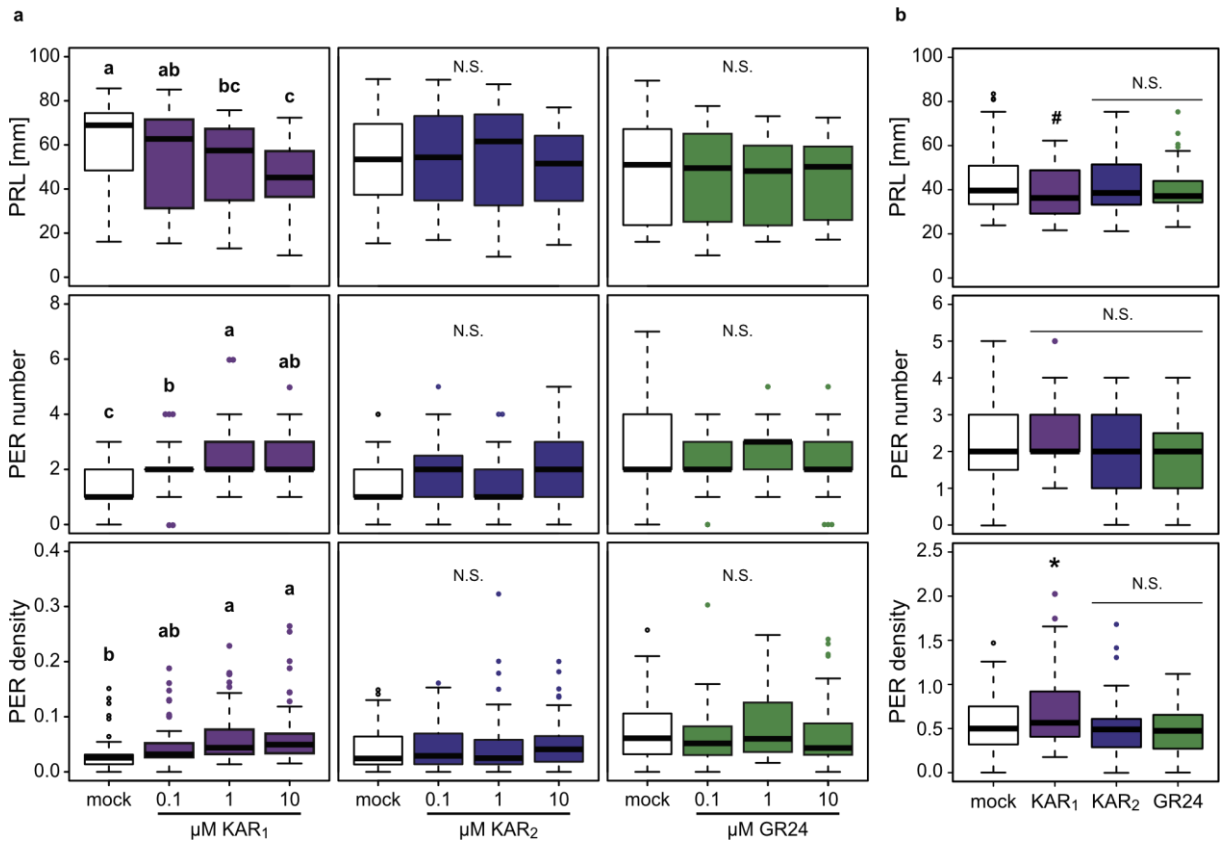

Figure 3.1: *L. japonicus* root system architecture is affected specifically by KAR_1 but not by KAR_2 treatment. (a-b) Primary root length (PRL), post-embryonic root (PER) number and PER density of wild-type plants, 2 week-post germination after treatment with solvent (mock) or **(a)** three different concentrations (0.1µM, 1µM and 10µM) of KAR_1, KAR_2 or *rac*-GR24 (n ≥ 32), or **(b)** 1µM KAR_1, 1µM KAR_2, or 1µM *rac*-GR24 (n ≥ 43). **(b)** Plants were transferred on fresh medium after 5 days. Letters indicate significant differences (ANOVA, post-hoc Tukey test). Asterisks indicate significant differences (ANOVA, Dunnett test, N.S.>0.1, #≤0.1, *≤0.05).

To inspect, whether changes in the *L. japonicus* root system architecture upon KAR_1 treatment are mediated by canonical KL perception, we examined PER density in response to KAR_1 in the KL and SL perception mutants. The *Ljkai2a-1 kai2b-1* double mutant and the *max2-4* mutant did not respond to KAR_1 treatment with changes in root system architecture (Fig 3.2.a-b). The *Ljd14-1* and *Ljkai2b-3* single mutants showed an increase in PER density upon 1µM KAR_1 treatment, but this was not the case for the *Ljkai2a-1* single mutant. It is possible that *Ljkai2a-1* is less sensitive to KAR_1; therefore, we increased the KAR_1 concentration to 3 µM (Fig 3.2.c). At this higher concentration, all *Ljkai2* single mutants but not the *Ljkai2a-1 kai2b-1* double mutant displayed an increased PER density. Taken together, these results indicate that

canonical KL perception, through KAI2a KAI2b and MAX2, influences *L. japonicus* root architecture specifically upon KAR_1 treatment.

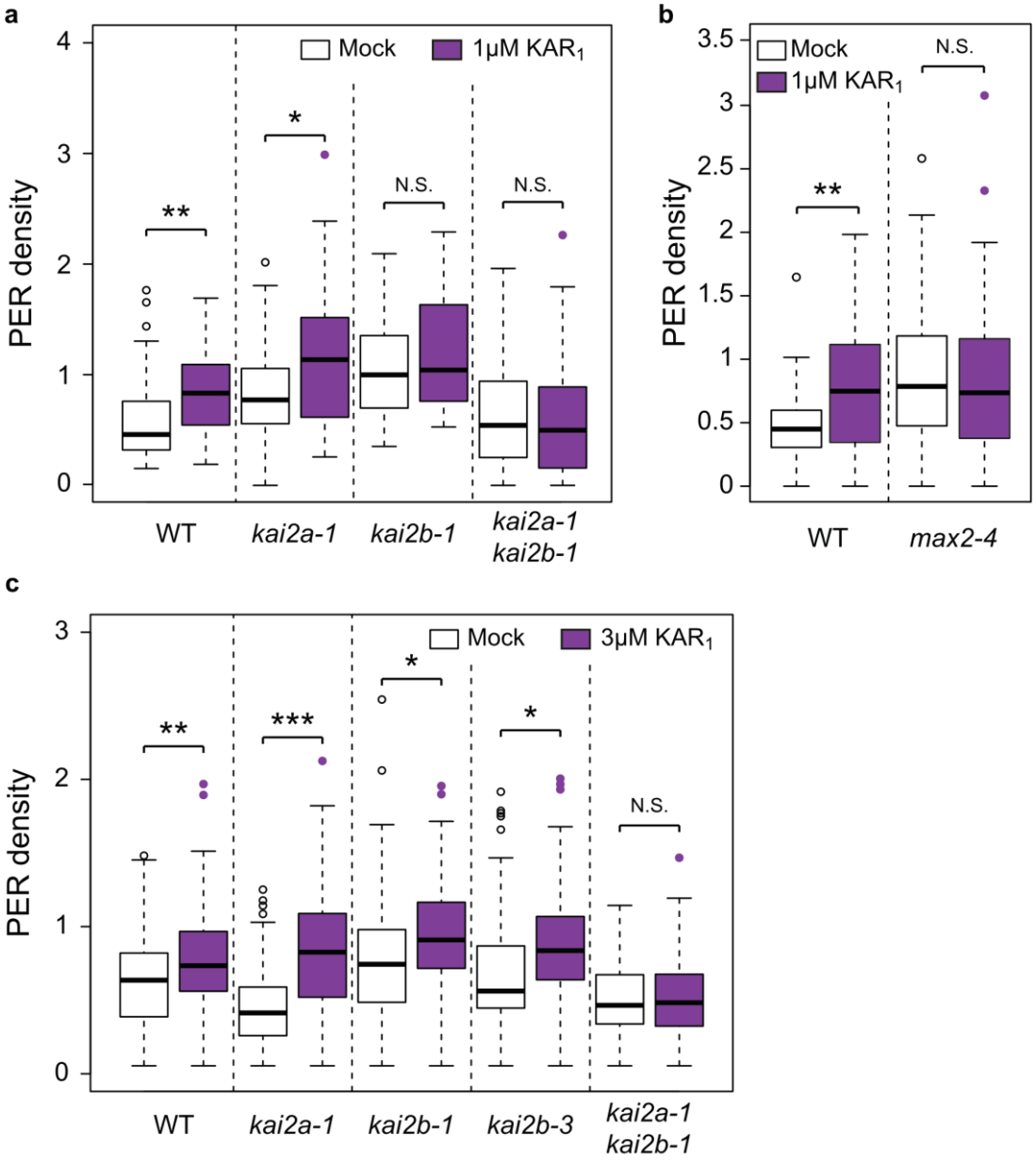

Figure 3.2: KAR_1 response in root system architecture requires *MAX2* and *KAI2a/KAI2b*. **(a-c)** Post-embryonic-root (PER) density of *L. japonicus* plants, 2 weeks post-germination after treatment with solvent (mock) and **(a-b)** 1µM or **(c)** 3µM KAR_1 (n ≥ 34). Asterisks indicate significant differences between the KAR_1 versus mock treatment (Welch t-test, N.S.>0.1, #≤0.1, *≤0.05, **≤0.01, ***≤0.001).

To confirm the divergence in the perception of KAR_1 and KAR_2 and *rac*-GR24 in *L. japonicus* roots, we analyzed the induction of the well-established in Arabidopsis KAR marker gene *DLK2* (Waters et al. 2012). *LjDLK2* (*Lj2g3v0765370.1*) is induced by KAR_1 treatment but not in the *Ljmax2-4* mutant, in which its transcript accumulates at

lower levels also without treatment (Fig 3.3.a). Notably, similarly to the absence of a developmental response (Fig 3.1), KAR_2 failed to induce *DLK2* in roots, confirming – together with the hypocotyl response to KAR_1 and KAR_2 (Chapter I) an organ-specific perception/response to different KAR. Considering the requirement of higher KAR_1 concentration for root developmental responses in the single *kai2* mutants (Fig 3.2.c), we analyzed the transcriptional response with 3 µM KAR_1 in these mutants (Fig 3.3.b). *DLK2* was induced in all *kai2* single mutants, but not in the *Ljmax2-4* and *Ljkai2a-1 kai2b*-1 double mutant. Surprisingly, 1 µM *rac*-GR24 also induced *DLK2* in a *KAI2s* and *MAX2*-dependent fashion. Taken together, these results indicate that developmental and transcriptional root responses to KAR_1 require *LjKAI2s* and *LjMAX2*, where *KAI2a* and *KAI2b* have redundant functions in this tissue.

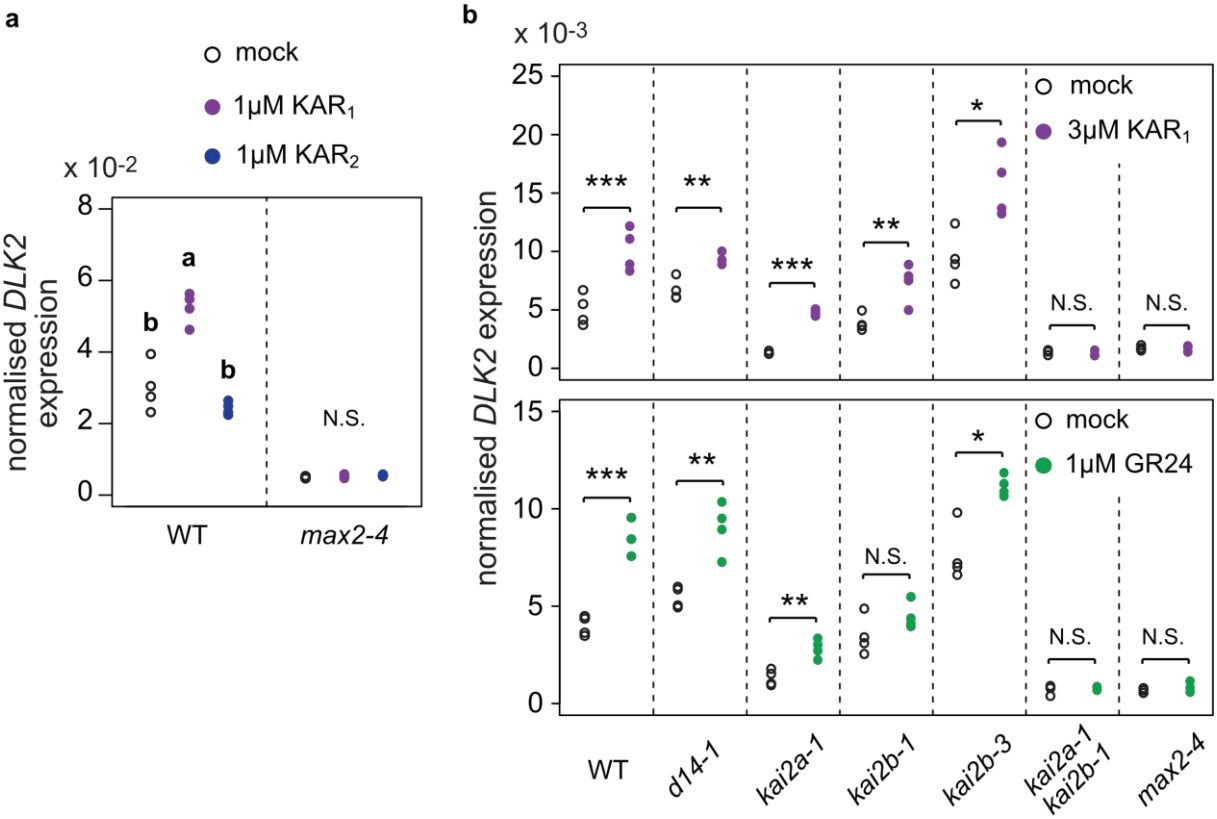

Figure 3.3: *DLK2* induction in roots depends on signaling molecules and *KAI2a/KAI2b*
(a-b) qPCR-based expression of *DLK2* in *L. japonicus* roots. **(a)** Analysis in wild-type and *max2-4* roots with solvent (mock), 1µM KAR_1 or 1µM KAR_2. **(b)** Analysis in wild-type, *d14-1, kai2a-1, kai2b-1, kai2b-3, kai2a-1/kai2b-1* and *max2-4* roots with solvent (mock), 3µM KAR_1 or 1µM *rac*-GR24 (n = 4). Letters indicate significant differences (ANOVA, post-hoc Tukey test). Asterisks indicate significant differences versus mock treatment (Welch t.test, *≤0.05, **≤0.01, ***≤0.001).

b) The KL signaling repressor SMAX1 is encoded by a single copy gene in *L. japonicus*

The effect on root architecture development of KAR_1 treatment in a *KAI2a/KAI2b* and *MAX2* dependent fashion is a good indication that KL signaling can modulate root growth. Upon KAR_1 perception, the KL signaling model predicts the degradation of a specific repressor of the pathway, known as SMAX1 and SMXL2 in Arabidopsis. We, therefore, hypothesized that a mutant of the KL repressor would mimic constitutive signaling and exhibit a root architecture phenotype.

To characterize the KL repressor in *L. japonicus* we retrieved SMAX1 and the closest homologs known as SMXLs by Protein BLAST using Arabidopsis SMAX1 as a query. Construction of a phylogenetic tree revealed that SMAX1 and the SMXLs form 4 separate clades, allowing us to name them according to the *A. thaliana* nomenclature (Stanga et al. 2013) (Fig 3.4). However, not each Arabidopsis SMXL has a close homolog in Lotus, but some recent gene duplication and gene loss occurred. In the case of SMAX1, only one copy is maintained in Lotus in contrast to the two in Arabidopsis. Similarly, SMXL5 is not found in Lotus, whereas SMXL3 is duplicated and renamed SMXL3a and SMXL3b. Concerning SMXL6 and 7, they seem to originate from a common ancestor gene which has been duplicated independently in Arabidopsis and Lotus. Few reports have assigned a regulatory function to the 4 SMXL clades. AtSMAX1/SMXL2 have been characterized as repressor of KL signaling (Stanga et al. 2013; Soundappan et al. 2015; Stanga et al. 2016), AtSMXL6/7/8 also known as D53 in rice have been shown to be the repressors of SL signaling (Jiang et al. 2013; Zhou et al. 2013; Soundappan et al. 2015; Wang et al. 2015), whereas AtSMXL3/4/5 have been shown to be central regulators of phloem formation in a KL and SL independent fashion (Wallner et al. 2017).

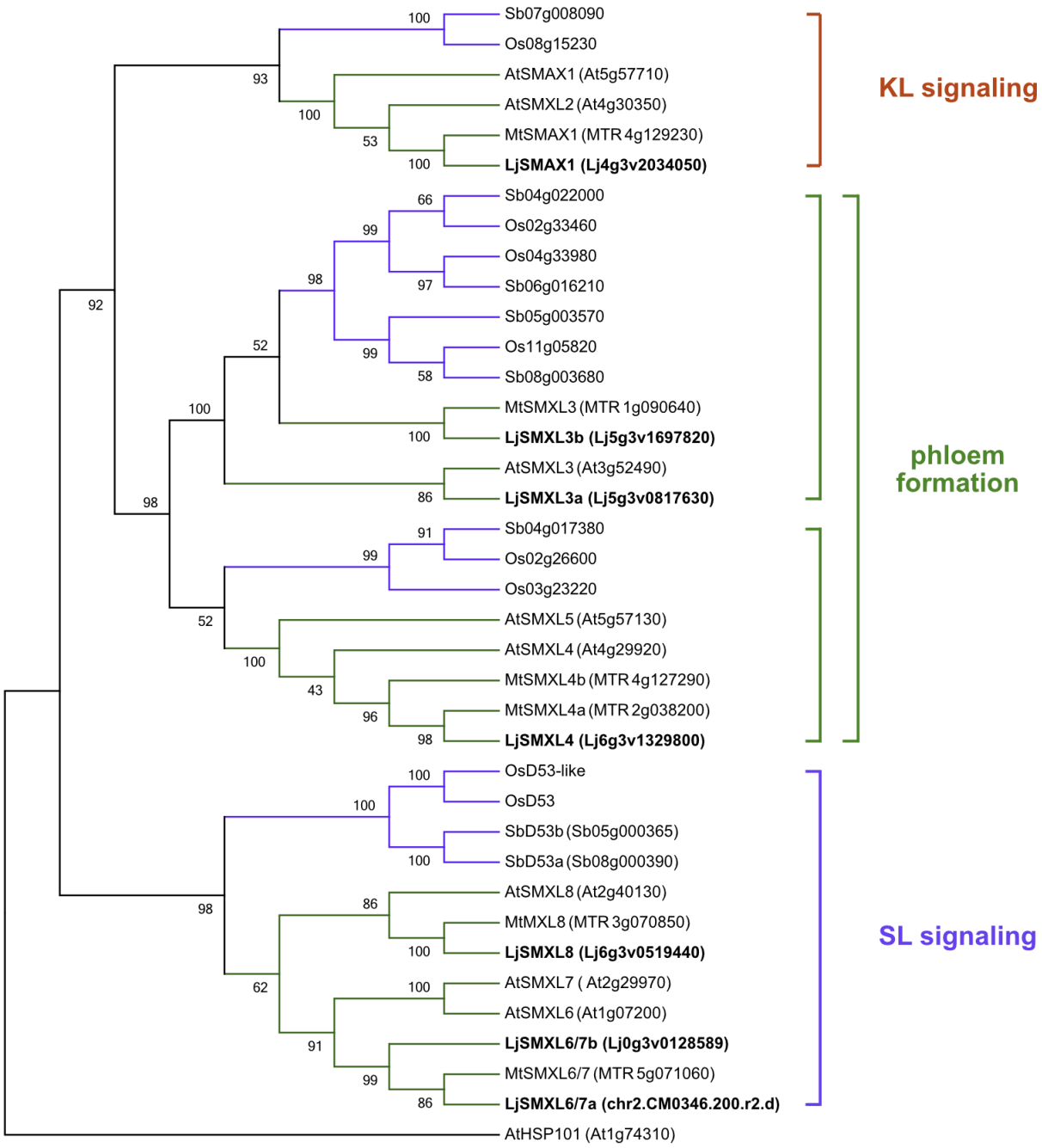

Figure 3.4: Phylogenetic tree of SMAX1 and SMXL from *L. japonicus, A. thaliana, M. truncatula, Sorghum bicolor* and *O. sativa*, rooted with AtHSP101. Branch colors indicate monocotyledons (blue) and dicotyledons (green). Bootstrap values of 1000 repetitions are indicated at each node. The four clades of SMXL are indicated by a colored bracket with their known function.

We investigated the transcript accumulation of the different *SMXL* genes in leaf, stem, flower, and root of *L. japonicus* (Fig 3.5). The genes putatively involved in phloem formation, *SMXL3a*, *SMXL3b,* and *SMXL4*, are weakly expressed in all tested organs. In contrast, transcripts of genes putatively involved in repression of KL (*SMAX1*) or SL

(*SMXL6/7a, SMXL6/7b, SMXL8*) signaling accumulated at higher levels. We also noted that *SMAX1* is ubiquitously expressed in all organs.

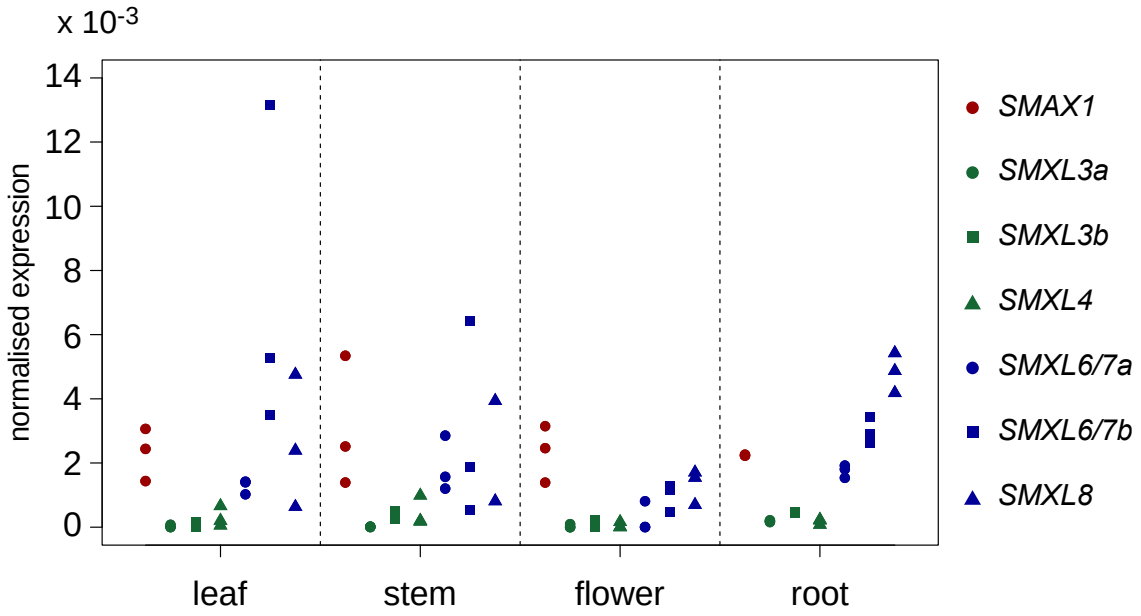

Figure 3.5: Quantitative RT-PCR-based transcript accumulation of *SMAX1* and *SMXLs*, in leaves, stem, flower, and roots of wild-type plants grown in pots (n = 3). Colors indicate putative involvement of the genes in known pathways: KL signaling repression (red), phloem formation (green) and SL signaling repression (blue).

To confirm that the *L. japonicus* SMAX1 is a repressor of KL signaling, we tested its stability *in vivo* in the presence of the KL perception complex: KAI2 and MAX2. We co-expressed from a single plasmid and driven by strong promoters the LjSMXL proteins C-terminally fused with a green fluorescent protein (GFP), with MAX2 and one of the KL (KAI2a/KAI2b) or the SL (D14) receptors, in *Nicotiana benthamiana* leaves. Furthermore, a cassette expressing a red fluorescence protein (mCherry) was added to the same expression vectors as a transformation marker. We then analyzed the presence or absence of GFP signal in transformed cells, as a read-out of SMXL stability (Fig 3.6). All translational SMXL-GFP fusions localized to the nucleus revealing no GFP cleavage. Thus, the green fluorescence is a good indicator of SMXL accumulation. Further, the presence of these heterologous proteins in *N. benthamiana* leaves indicates that the endogenous *N. benthamiana* receptors are insufficient to induce their full degradation.

Accumulation of SMXL3a-GFP, SMXL3b-GFP, and SMXL4-GFP was unchanged by the co-presence of the SL or KL receptors, D14 and KAI2s, respectively (Fig 3.6).

However, SMXL8-GFP was not observed in cells co-transformed with *LjD14*, while it accumulated when the cells were co-transformed with *LjKAI2a* or *LjKAI2b*. In contrast, SMAX1-GFP accumulated in the nucleus only when co-transformed with the SL receptor gene *LjD14*, whereas no green fluorescence was observed in the presence of either KAI2a or KAI2b. Described as a SL signaling repressor, SMXL8 is expected to be specifically degraded by SL signaling (Jiang et al. 2013; Zhou et al. 2013; Soundappan et al. 2015), whereas SMAX1 is predicted to be specifically degraded by KL signaling (Stanga et al. 2013; Soundappan et al. 2015). This specificity is determined by the corresponding receptors of these pathways, D14 and KAI2, respectively (Waters et al. 2012). Together, these results illustrate that the canonical relationship of SMAX1-KAI2 and SMXL8-D14 suggested in Arabidopsis works also with Lotus proteins. Further, it is the first time that SMAX1 destabilization by the KL receptor is shown.

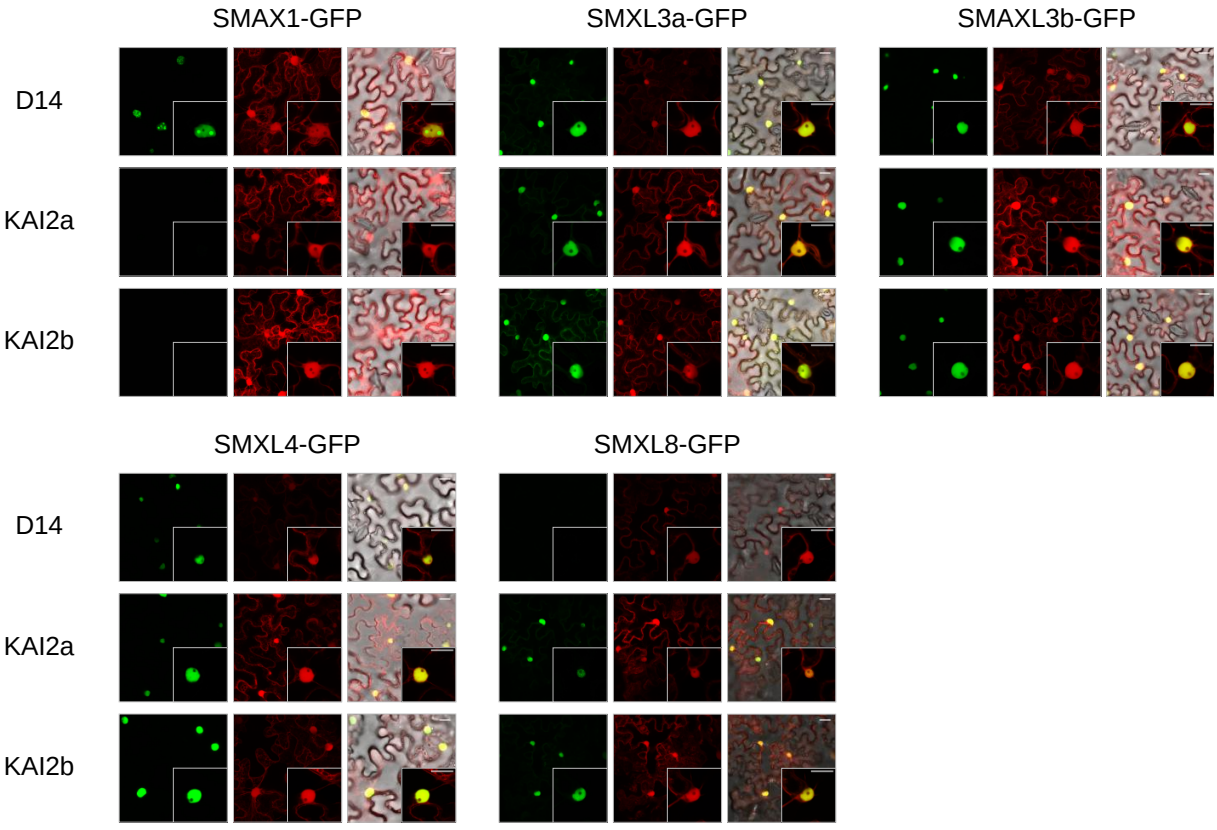

Figure 3.6: SMAX1-GFP stability is specifically affected by KAI2a and KAI2b. Confocal microscopy pictures of *N. benthamiana* co-expressing MAX2, in combination with different α/β-hydrolases and SMXLs, fused with GFP. Scale bars = 25µm.

Yet, the SMAX1 degradation mechanism is unknown, but it is suspected to be breakdown by the proteasome after MAX2-mediated ubiquitination. Since *LjMAX2* is expressed in all performed combinations, we wondered if this F-box protein was necessary for repressor destabilization (Fig 3.7). Absence of LjMAX2 led to the stabilization of SMAX1-GFP and SMXL8-GFP in the nucleus even in the presence of KAI2a or KAI2b, and D14 respectively. The requirement of MAX2, a member of the SCF complex, suggests a proteasomal degradation after ubiquitination of the repressors.

The outcome of these experiments implies specific interaction between perception components and repressors of the SL and KL pathways, with the following complex formations: D14-MAX2-SMXL8 and KAI2a/b-MAX2-SMAX1.

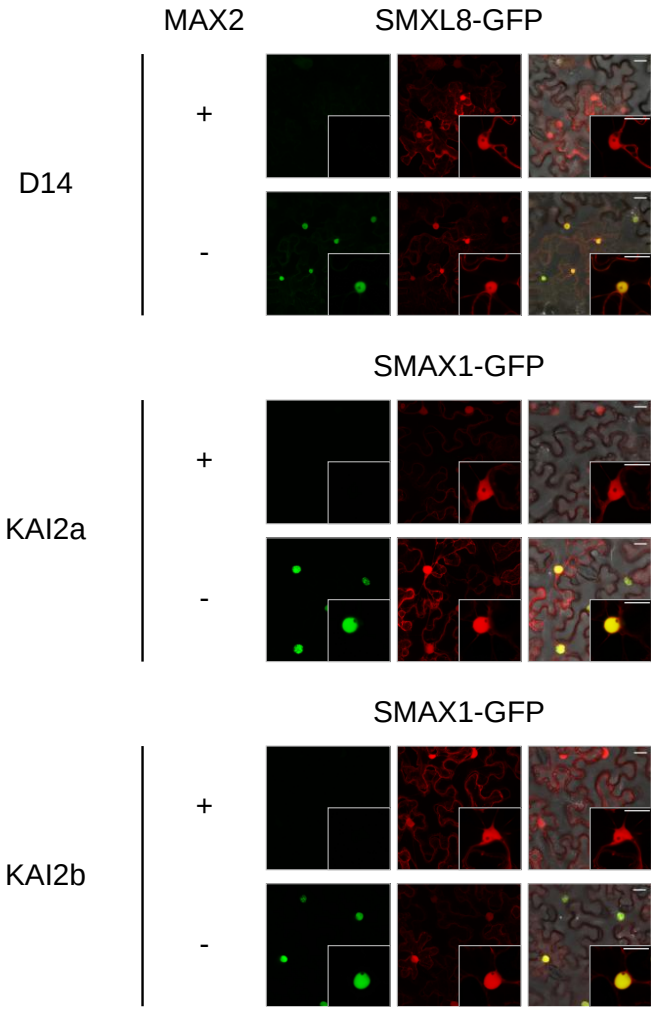

Figure 3.7: MAX2 is required for SMAX1 and SMXL8 degradation. Confocal microscopy pictures of *N. benthamiana* co-expressing SMAX1-GFP with KAI2a or KAI2b, and SMXL8-GFP with D14, in presence and absence of MAX2. Scale bars = 25µm.

It is generally assumed that the perception of SLs and KLs is required for repressor degradation. We wondered if endogenous SL and KL in *N. benthamiana* leaves were perceived respectively by LjD14 and LjKAI2a/b to mediate repressors ubiquitination. The conserved catalytic triad of D14 and KAI2 have been shown to be required for ligand perception and signaling, as a serine to alanine mutation in the catalytic site prevents GR24 hydrolysis and binding (Abe et al. 2014; Hamiaux et al. 2012), restricts GR24 mediated interaction with MAX2 and OsD53 (Jiang et al. 2013), but also fails to rescue the corresponding mutants (Waters et al. 2015b; Hamiaux et al. 2012). We, therefore, created the *L. japonicus* catalytic triad mutants $D14^{S95A}$, $KAI2a^{S95A}$ and $KAI2b^{S96A}$, and tested their ability to destabilize SMXL8 and SMAX1 in *N. benthamiana* (Fig 3.8). Unexpectedly, mutation of the Serine of the catalytic triad into Alanine did not affect SMAX1 and SMXL8 stability. These results indicate that catalytic activity of the receptors is not required for the signaling in this heterologous system. Likely, over-expression and crowding of the receptors in the nucleus lead to forced but still specific interactions and complex formation with ubiquitination of the repressors, and consequently, ligand perception was not required for signal transduction.

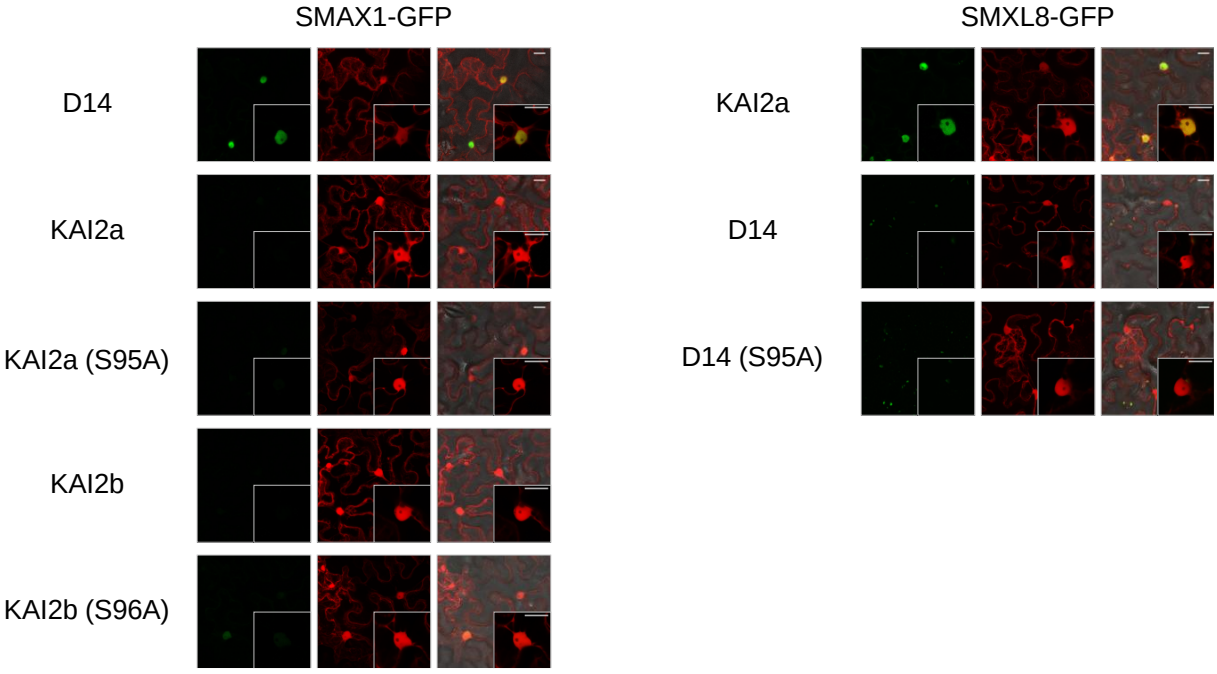

Figure 3.8: Catalytic triad of the receptor is not required for SMAX1 and SMXL8 degradation. Microscopy pictures of *N. benthamiana* co-expressing SMAX1-GFP and SMXL8-GFP with KAI2a, KAI2b, D14, or a modified version with the catalytic triad Serine mutated into Alanine. Scale bars = 25µm.

Repressor instability, even in a likely ligand perception independent fashion, is specifically determined by the receptor of the same pathway. These results confirm that SMAX1 is the KL signaling repressor, a target for degradation by KL signaling, mediated by KAI2a/b and MAX2.

c) The *smax1* mutant over-accumulates *DLK2* transcript

To confirm a function of KL signaling in plant development, and particularly in root architecture of *L. japonicus*, we searched for mutants in *SMAX1*. We found three *LORE1* retrotransposon insertions (*smax1-1, smax1-2, smax1-3*), all located in the first exon (Fig 3.9.a). Segregating seeds carrying the *smax1-1* insertion were of poor quality with extremely low germination rates. Therefore, we focused on the two other alleles, *smax1-2* and *smax1-3*. We investigated whether the mutation in *SMAX1* specifically affects KL signaling. For comparison, we retrieved mutants in *SMXL3a*, *SMXL3b* and *SMXL4* (*smx3a-1, smxl3b-1,* and *smxl4-1*) carrying as-well *LORE1* insertions (Fig 3.9.a). Quantitative RT-PCR analysis revealed that all mutations led to a reduced transcript accumulation of the respective mutated genes in roots (Fig 3.9.c). Interestingly, *SMAX1* and *SMXL3b* transcripts are also slightly affected by each other's mutations. To examine whether KL signaling is perturbed in the *smax1* mutant, we checked the transcript accumulation of the KAR marker gene *DLK2. DLK2* accumulates at a high level in *smax1-3* mutant roots, supporting that *SMAX1* is non-functional in this mutant, whereas it stays at very low levels in all the other *smxl* single mutants (Fig 3.9.b). Accumulation of *DLK2* in *smax1-3* mimics constitutive KL signaling, indicating a de-repression of the transcript in the mutant, which qualifies SMAX1 again as a specific transcriptional repressor in KL signaling.

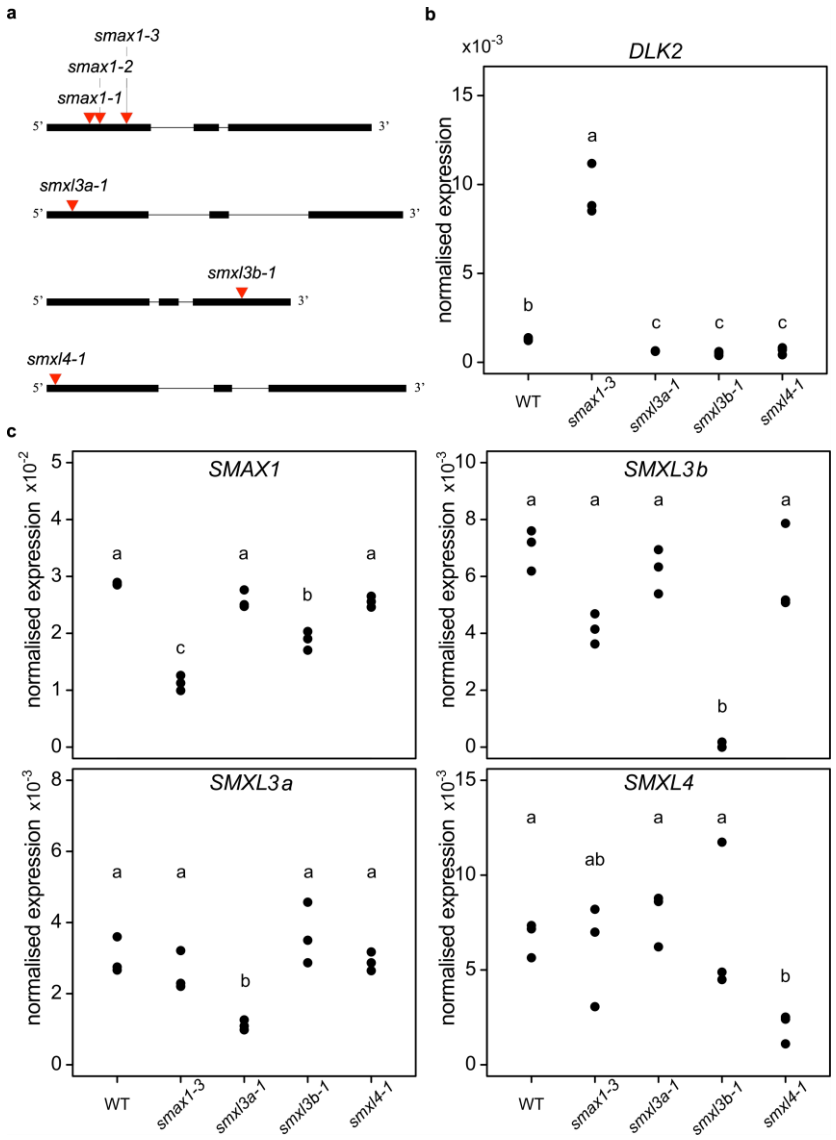

Figure 3.9: (a) Schematic representation of the *L. japonicus SMAX1, SMXL3a, SMXL3b*, and *SMXL4* genes. Black boxes and lines show respectively exon and intron structures. LORE1 insertions are indicated by red triangles, labeled with the number of the respective mutant allele. **(b-c)** Transcript accumulation as determined by qRT-PCR in roots of *DLK2, SMAX1*, *SMXL3a*, *SMXL3b* and *SMXL4 i*n the *smax1* and *smxl* mutants background (n = 3). Letters indicate significant differences (ANOVA, post-hoc Tukey test).

d) *smax1* mutation has pleiotropic effects

Since KAR_1 treatment, which should cause enhanced degradation of SMAX1, leads to decreased primary root length (PRL) and increased post-embryonic (PER) root number in a KAI2-dependent fashion (Fig 3.1 and 3.2), we hypothesized that *L. japonicus smax1* mutants should have similar phenotypes. Indeed, both allelic *smax1* mutants display a strong root phenotype when grown on plates (Fig 3.10.a). The

primary root length is heavily reduced in the *smax1* mutants, whereas the number of PER is similar to the wild-type, resulting in an increased PER density (Fig 3.10.b). To support that the homozygous *LORE1* insertion in *SMAX1* is responsible for the observed root phenotype, we carried out a co-segregation analysis with the *smax1-2* locus. From a population of 72 individuals, 13 seedlings were homozygous wild-type for the *SMAX1-2* locus, 44 were heterozygous and 15 were homozygous mutant, respecting a mendelian segregation (X^2= 3.67, p= 0.16). The root architecture of homozygous wild-type and heterozygous *SMAX1-2*$^{+/-}$ was similar, with longer primary root and lower PER density in comparison to the homozygous *smax1-2* mutant (Fig 3.10.c). The co-segregation analysis confirms that mutation in *SMAX1* is causative for the short root phenotype.

The decrease in PRL and increase in PER density observed in response to KAR_1 treatment and in the *smax1* mutants together demonstrate the capacity of KL signaling to modulate root growth and architecture.

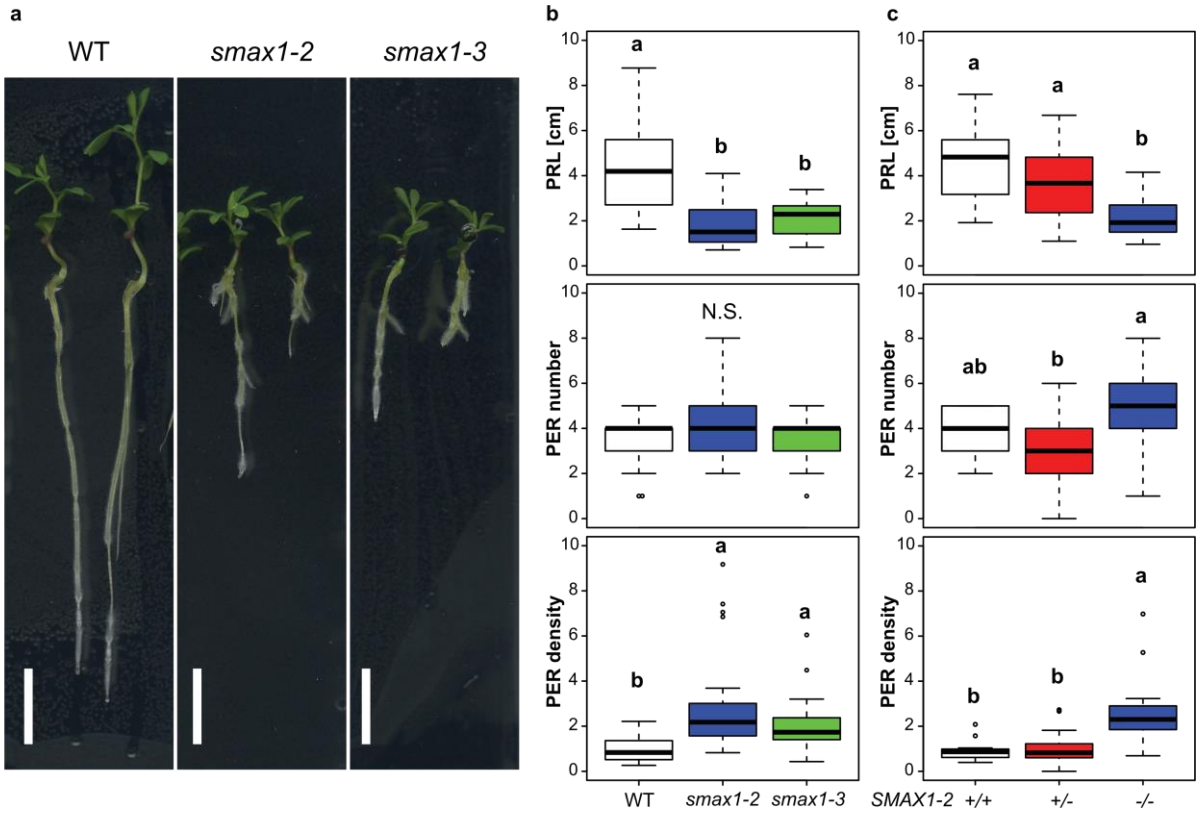

Figure 3.10: *L. japonicus smax1* mutants display short primary roots and increased post-embryonic root density. (a) Representative images of wild-type, *smax1-2,* and *smax1-3*, grown on Petri dishes at 10 days post-germination. Scale bar = 1cm. **(b-c)** Primary root length (PRL), post-embryonic root (PER) number and PER density of **(b)** wild-type, *smax1-2* and *smax1-3* (n ≥ 23), and **(c)** a segregating population of the *smax1-2* mutation (n ≥ 13). Letters indicate significant differences (ANOVA, post-hoc Tukey test).

A recent manuscript reported that the *smax1 smxl2* double mutant in *A. thaliana* has increased root-hair length and density (Villaecija Aguilar et al. 2019). In *L. japonicus*, the *smax1* mutants appeared to be altered as well in root-hair development (Fig 3.11.a). The first root-hairs emerged 400 µm closer to the quiescent-center in the root tip as compared to the wild-type (Fig 3.11.b) and in addition, the root-hairs appeared to be longer in the mutants. To confirm this observation, we measured the root-hair length between 1.5 mm to 2 mm from the apex. The root-hairs of the *smax1* mutants were on average 3 times longer. Together, these results are in line with observations in Arabidopsis and strongly suggest a function of KL signaling in root-hair development.

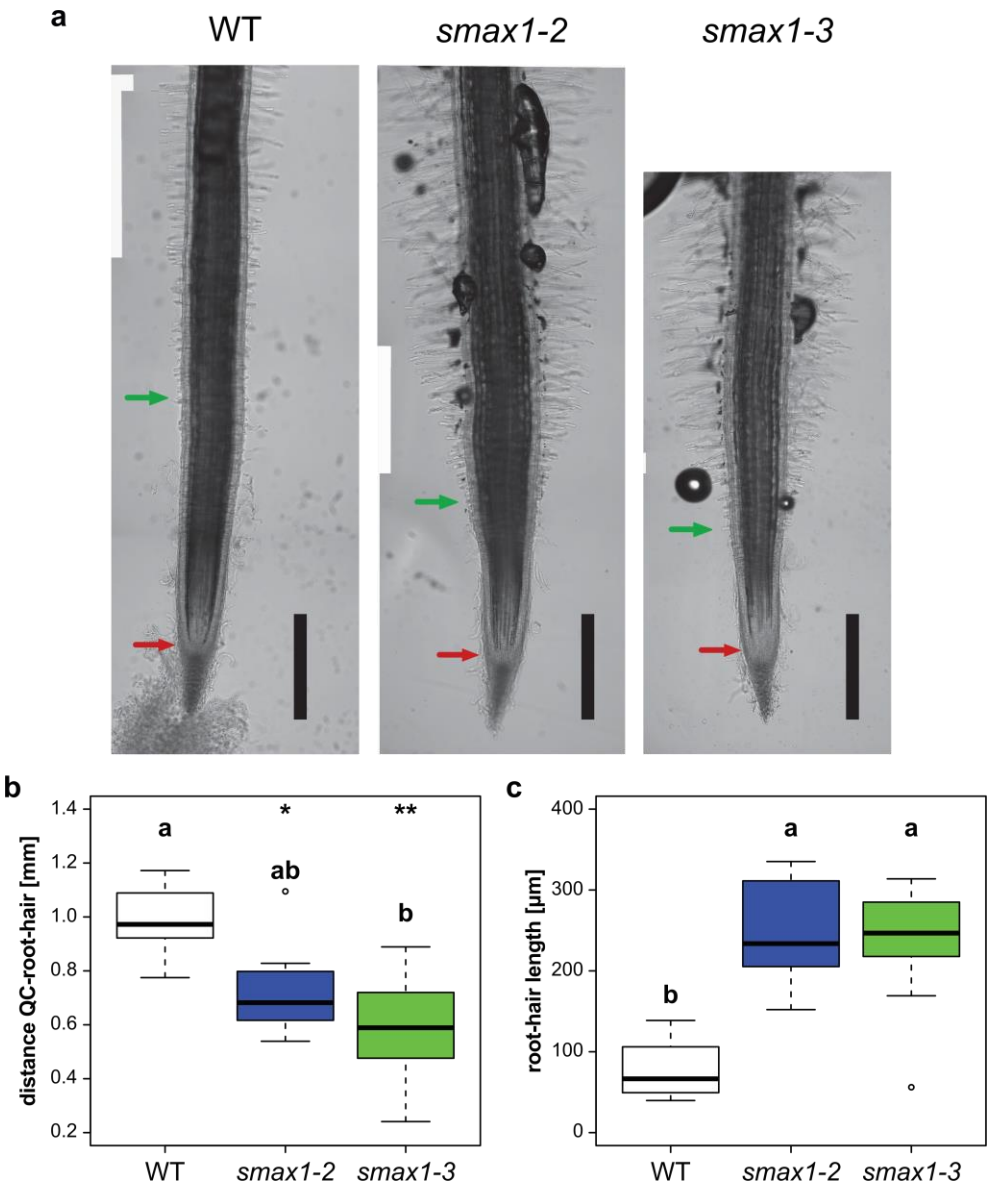

Figure 3.11: *L. japonicus smax1* mutants display longer root-hairs and closer to the root tip. (a) Representative images of wild-type, *smax1-2* and *smax1-3* root apex, grown on plates at 10 days post-germination. Red arrows indicate position of the Quiescent Center (QC), Green arrows indicate closest root-hair from the apex. Scale bar = 500µm. **(b)** Distance of the first root-hair from the quiescent-center (QC) and **(c)** root-hair length at 1.5 to 2 mm from the apex, in the wild-type, *smax1-2,* and *smax1-3* (n ≥ 6). Letters indicate significant differences (ANOVA, post-hoc Tukey test). Asterisks indicate significant differences compared to the wild-type (ANOVA, post-hoc Dunnett test, N.S.>0.05, *≤0.05, **≤0.01, ***≤0.001).

Due to the short primary root of the *smax1* mutants, we hypothesized either a defect in cell division or in cell elongation. Longitudinal sections showed a swollen root tip in the transition zone, with compact cells in the two *smax1* alleles (Fig 3.12.a). To quantify this phenotype, we focused on the most continuously observable cells, which are the cortical cells, and we determined their cumulative length for the 25 first observable cortical cells situated below the epidermis starting from the meristematic zone (Fig 3.12.b). In wild-type, after 5 to 6 cells, the following cells quickly elongated and matured, whereas, in the two *smax1* mutants, the cell elongation seemed to be slow and delayed, starting only after 14-15 cells. The root width was also significantly larger in *smax1-2*, and a similar tendency was observed in *smax1-3* (Fig 3.12.c). Likewise, and despite having a shorter length, cortical cells were significantly wider in the *smax1-3*, and a comparable phenotype was observed in *smax1-2* (Fig 3.12.d). In conclusion, *smax1* mutants have a defect in cortical cell elongation, which presumably leads to lateral expansion of those cells resulting in a swollen root tip.

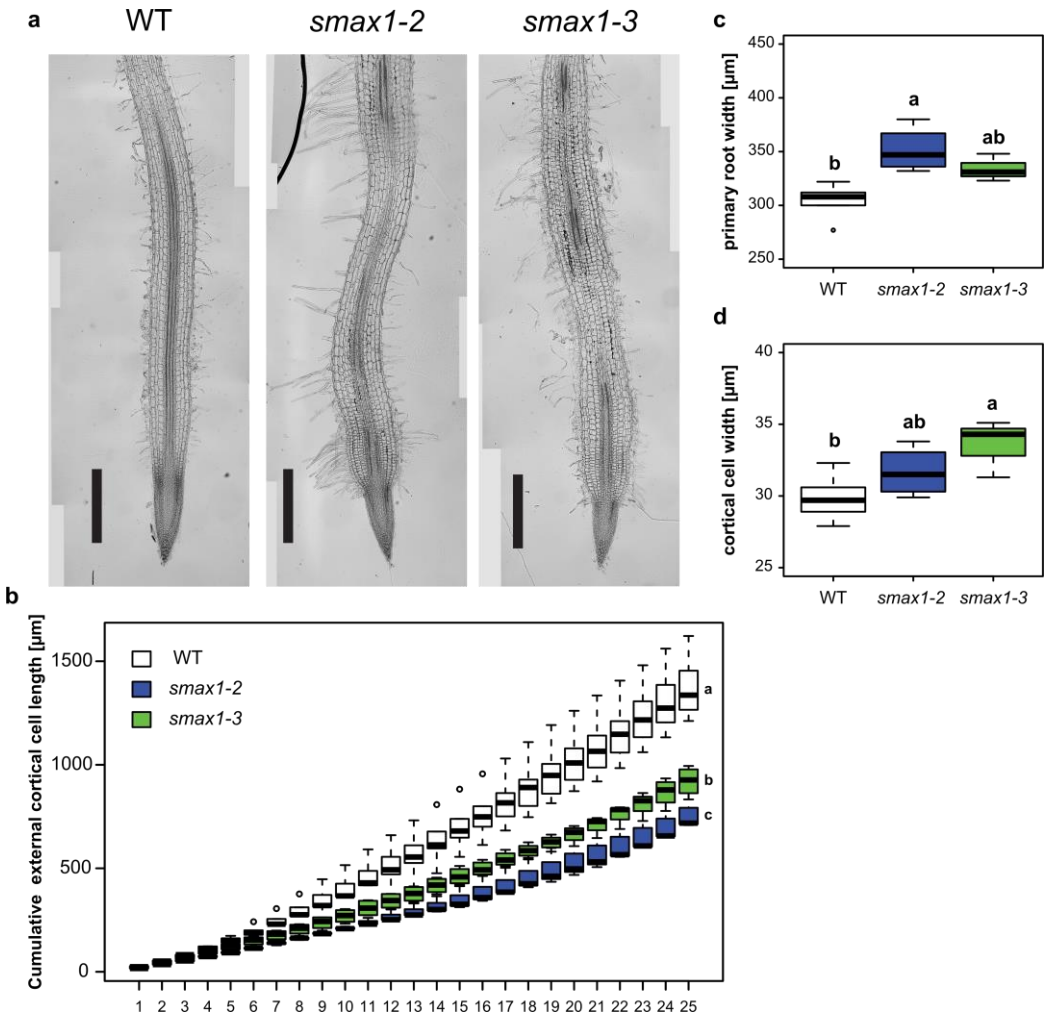

Figure 3.12: *L. japonicus smax1* mutants are perturbed in cell elongation. (a) Longitudinal sections of wild-type, *smax1-2,* and *smax1-3* grown on Petri dishes at 10 days post germination. Scale bar= 500µm. **(b)** Cumulative length of 25 external cortex cells starting from the first observable cortex cell in the meristematic zone in wild-type, *smax1-2,* and *smax1-3* (n ≥ 3). **(c)** Primary root width and **(d)** width of cortical cells in the elongation zone of wild-type, *smax1-2,* and *smax1-3* (n ≥ 3). Letters indicate significant differences (ANOVA, post-hoc Tukey test).

The short root system of the *smax1* mutants was observed on half-strength Hoagland, which is a nutrient-poor medium. In these conditions, seed reserves are an essential factor for development and growth. To investigate whether the *smax1* mutants are deprived of seed reserves, we weighed the seeds from homozygous and heterozygous *smax1* parents. Seeds from homozygous *smax1* mutants had around 25% less weight than wild-type seeds (Fig 3.13.a). Surprisingly, seeds from heterozygous parents had an intermediate weight. To investigate if this intermediate phenotype corresponds to the presence of lighter homozygous mutant seeds, we searched for sub-populations in seed size in these segregating populations. To facilitate the analysis on a high

number of seeds, we tested if the seed 2D area as measured by ImageJ after scanning the seeds is a good proxy for seed weight. Identically to weight, 2D area of *smax1* seeds was smaller than the wild-type, and the segregating population had an intermediate phenotype again (Fig 3.13.b). In addition, the linear regression between seed weight and 2D area had a high correlation coefficient (R^2=0.96) confirming that the seed 2D area is a good proxy for seed weight. Segregating populations of seeds from heterozygous mothers displayed a similar distribution than the wild-type and homozygous *smax1* seeds, despite respecting a mendelian segregation (see Chapter III, point d) (Fig 3.13.c). These results suggest that the seed reserves depend mainly on the parent plant and that *SMAX1* does likely not play a role in the intrinsic seed development but potentially in its loading. Further, the weight of small seeds of the *smax1* mutants could potentially influence the root system development at the seedling stage.

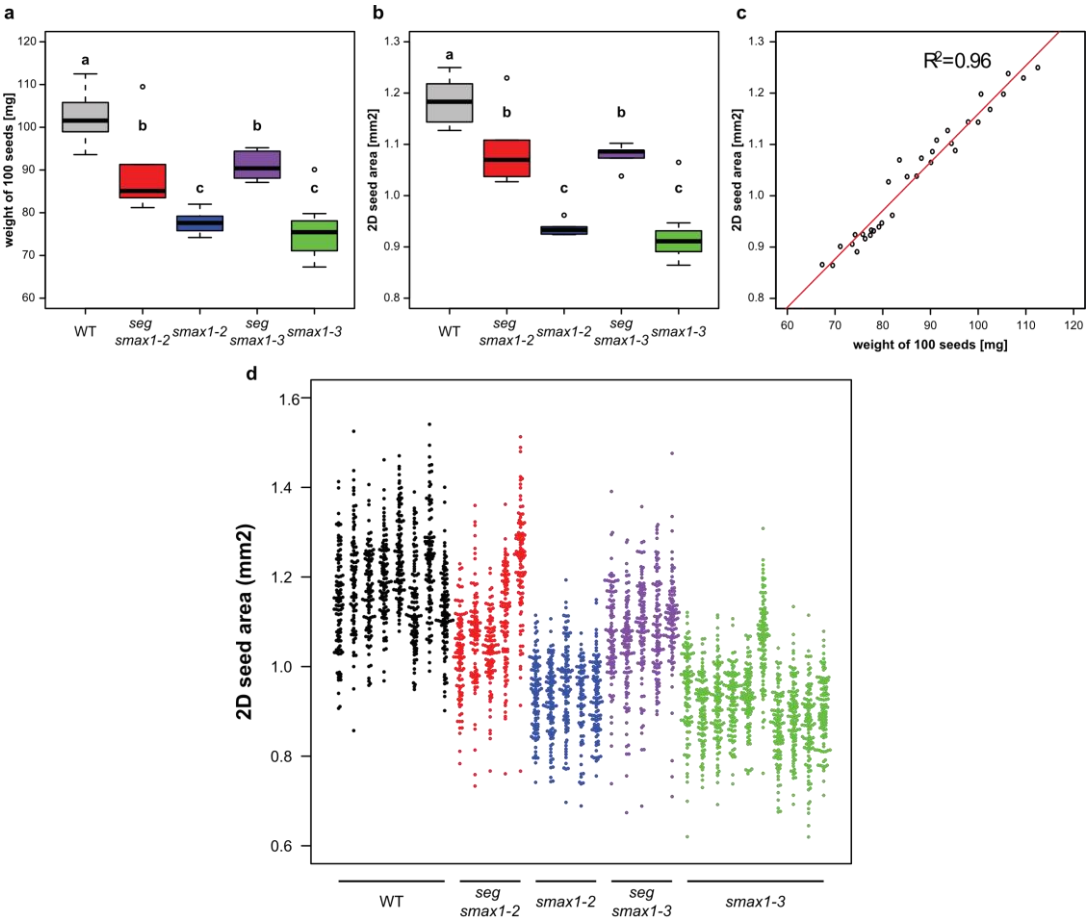

Figure 3.13: *L. japonicus smax1* mutants have smaller seeds. (a) Weight of 100 seeds in the wild-type, *smax1-2*, *smax1-3*, and segregating populations carrying the *smax1-2* or *smax1-3* mutation (n ≥ 5). **(b)** 2D area of the same seeds shown in (a) after high-resolution scanning.

(c) Linear regression of the seed weight (a) and 2D area (b). **(d)** 2D area of each single seeds used in (a-b). Letters indicate significant differences (ANOVA, post-hoc Tukey test).

e) Phosphate and sugar do not rescue the *smax1* root phenotype

To test if the smaller seeds of the *smax1* mutants are responsible for their short root system, we supplied the growth medium with 1% sugar. The presence of sugar improved the growth of the root as the PRL was increased in all backgrounds, but the effect was higher in the wild-type and moderate in the *smax1* mutants (Fig 3.14.a). However, the positive effect of sugar on growth influenced not only the primary root but also increased the PER number, which became more numerous in both *smax1* mutants than in the wild-type. Since sugar positively affected the PRL and PER number, the PER density remained unchanged, with a higher PER density in the *smax1* mutants (Fig 3.14.a).

The half-strength Hoagland medium used, contained a low amount of phosphate (2.5 µM PO_4). Several studies have reported that phosphate starvation can lead to growth decrease of the primary root by a strong reduction of primary root cell elongation and meristem arrest, accompanied by lateral root emergence (reviewed in (Péret et al. 2011)). To investigate if *smax1* is hypersensitive to phosphate starvation, we tested its growth on high phosphate medium (2.5 mM PO_4). In this condition, wild-type plants responded with reduced PRL whereas *smax1-3* remained unchanged, with a short PRL. However, low or high phosphate conditions did not affect the PER number and PER density in the wild-type or *smax1-3* mutant.

Altogether, these results indicate that the *smax1* root architecture phenotype is stable and that low nutrient availability for the *smax1* mutants is unlikely the cause of the root growth phenotype.

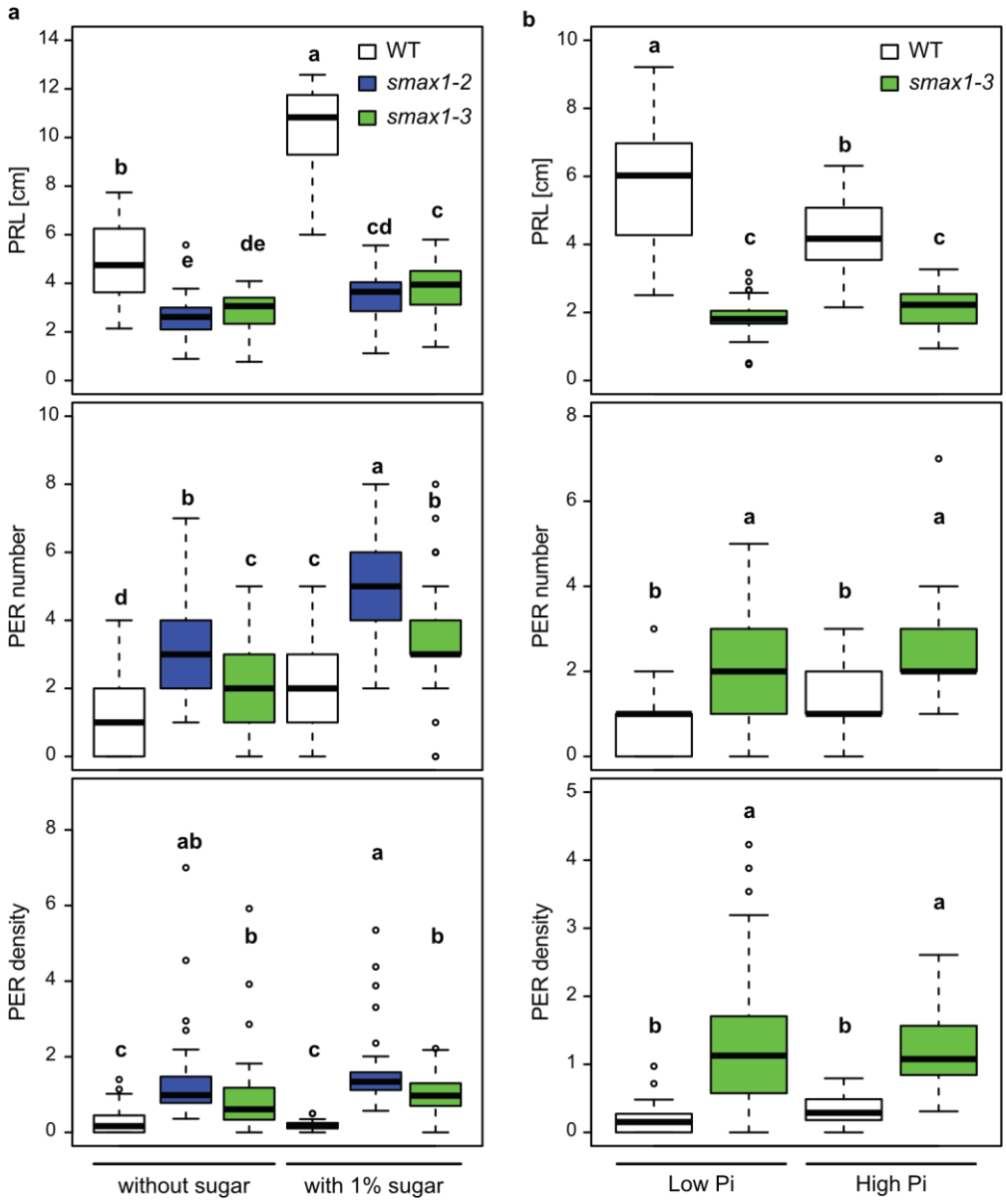

Figure 3.14: *Ljsmax1* root architecture phenotype is not rescued by phosphate or sugar. Primary root length (PRL), post-embryonic root (PER) number and PER density of wild-type **(a-b)**, *smax1-2* **(a)** and *smax1-3* **(a-b)**, after 10 days post-germination grew **(a)** with or without 1 % sugar (n ≥ 43), and **(b)** with 2.5µM (Low Pi) or 2.5uM (High Pi) phosphate (n ≥ 28). Letters indicate significant differences (ANOVA, post-hoc Tukey test).

f) RNAseq analysis shows deregulation of ethylene biosynthesis in the *smax1* mutants.

To gain insight on the impact of KL signaling in the root, we compared the root transcriptome of KL perception mutants, *kai2a-1 kai2b-1,* and *max2-4*, and the two KL repressor *smax1-2* and *smax1-3*, to wild-type plants. This experiment was conducted

with multiple goals such as: 1) Determine new positive markers of KL signaling, similar to *DLK2*, which is repressed in the KL perception mutants and de-repressed in the *smax1* mutants; 2) Find KL biosynthesis genes, as negative feedback-loop is a common mechanism in phytohormones signaling and observed in SL (Wang et al. 2015), we hoped that their expression would be induced in perception mutants, whereas repressor mutants mimicking constitutive KL signaling would lead to their downregulation; 3) find pathways disturbed in *smax1* mutants which would explain their root architecture and root-hair phenotypes.

The transcriptome analysis was performed with Illumina HighSeq 2500 with paired-end sequencing, which yielded a total of 1 379 million reads in the 20 different samples. By principal component analysis (PCA), we found that one of the four *smax1-2* biological replicates behaves as an outlier explaining around 80% of the total variance (Fig 3.15.a). After the removal of this outlier, the PCA displayed a cluster of samples belonging to the same genotype, over the two principal components explaining 56% of the total variance (Fig 3.15.b). As expected, the *smax1-2* and *smax1-3* samples fall into one group.

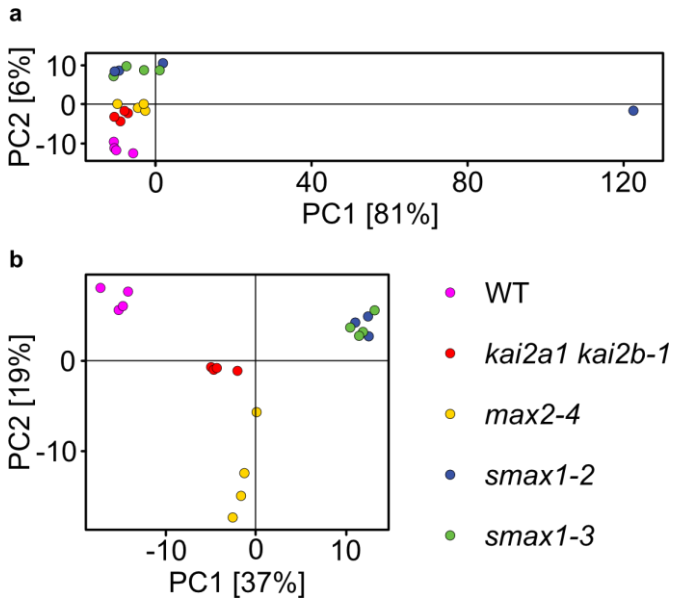

Figure 3.15: Most of the variance is explained by the differences between genotypes, apart from a *smax1-2* outlier sample. (a-b) Principal component analysis (PCA) of all reads from **(a)** all biological replicates and **(b)** after removal of the *smax1-2* outlier.

After the mapping of the reads onto the *L. japonicus* MG20 mRNA version 3.0 reference, differential expression analysis compared to the wild-type was performed, under FDR ≤ 0.01 and LogFC ≥ |0.5| thresholds. A total of unique 3148 differentially expressed genes (DEG) were discovered in the different mutants on a total on 83153

genes in the reference database, with most of them found in the *smax1* mutants (Table 3.1). The majority of the DEGs are shared between at least two mutants (2209, 70,2%), to compare with the DEGs found in only one mutant background (939, 29,9%). As expected, the DEGs in the *smax1-2* and *smax1-3* mutants are highly overlapping (74,6%) even with the loss of one biological replicate of *smax1-2* (Table 3.2). The second highest intersection is found between *max2-4* and *kai2a-1 kai2b-1* (28,5%). The high overlap in DEGs between the two KL perception and repressor mutants separately is a strong indication of their relevance.

Table 3.1. Number of DEGs per genotype with reference to the wild type and their specificity.

Genotype	Number of DEGs	Specific DEGs	Shared DEGs
kai2a-1 kai2b-1	932	220 (23,6 %)	712 (76,4 %)
max2-4	1065	339 (31,8 %)	726 (68,2 %)
smax1-2	2036	104 (5,1 %)	1932 (94,9 %)
smax1-3	2340	276 (11,8 %)	2064 (88,2 %)

Table 3.2. Proportion of co-DEG per mutant combination.

Intersection	DEG overlap
smax1-2 ∩ *smax1-3*	1870 (74,6 %)
kai2a-1 kai2b-1 ∩ *max2-4*	443 (28,5 %)
kai2a-1 kai2b-1 ∩ *smax1-3*	587 (21,9 %)
max2-4 ∩ *smax1-3*	607 (21,7 %)
kai2a-1 kai2b-1 ∩ *smax1-2*	517 (21,1 %)
max2-4 ∩ *smax1-2*	514 (19,9 %)
All mutants	290 (14,0 %)

To gain a better understanding of the pathways deregulated in the KL mutants, we performed a cluster and a gene-ontology (GO) analysis to enable a functional interpretation of these clusters (Fig 3.16). The majority of the DEGs are included in 4 out of 14 clusters: clusters 1, 2, 6 and 7. Cluster 2 groups genes, which are less expressed in all mutants as compared to wild type. The clusters 1 and 7 are mainly composed of the genes repressed and induced, respectively, in the *smax1* mutants with slight effects in the *max2-4* and *kai2a kai2b* double mutants. Whereas the cluster

6 integrates genes which are strongly expressed in the *smax1* mutants. Interestingly, there is an over-representation in cluster 6 of DEGs putatively involved in ethylene signaling. The most massively induced gene in the *smax1* mutants is a gene belonging to the *ETHYLENE-RESPONSE-FACTOR* (*ERF*) family. Also, an *ACC-SYNTHASE* (*ACS*) gene which codes for a rate-limiting ethylene biosynthesis enzyme accumulates at higher levels in the KL repressor mutants, which strongly suggest a perturbation of ethylene signaling and could potentially be causative of the *smax1* mutants root phenotype, since ethylene is known to trigger shorter roots with elongated root-hairs (reviewed in (Vandenbussche and Van Der Straeten 2012)). Unexpectedly, only few genes show an opposing expression pattern between perception and repressor mutants, which included *DLK2.* This well-known KAR marker gene in Arabidopsis belongs to cluster 6, which indicates that other KAR/KL response genes could potentially be found in the same cluster.

To confirm the DEGs found in the RNAseq analysis, we performed qPCRs analysis on a selected number of genes belonging to each cluster (Fig 3.17). The vast majority of these DEGs presents a similar expression pattern with the RNAseq. qPCR analysis confirmed that the genes related to ethylene biosynthesis and signaling were more strongly expressed in the two *smax1* mutant alleles.

Ethylene is known to affect the root system of many plant species, triggering shorter roots assorted of elongated root-hairs (reviewed in (Vandenbussche and Van Der Straeten 2012)),

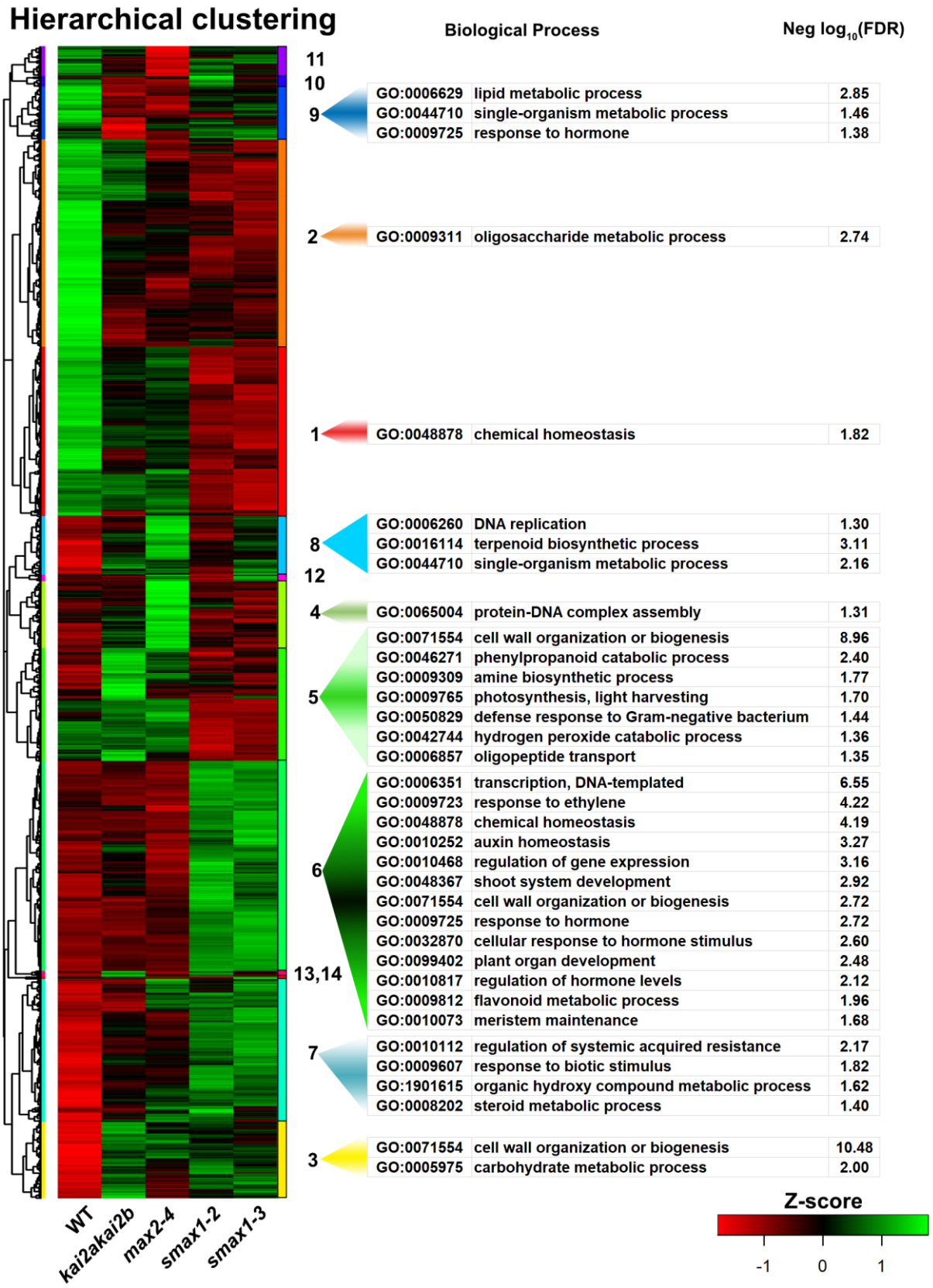

Figure 3.16: Clustering of DEGs and GO enrichment in the clusters.

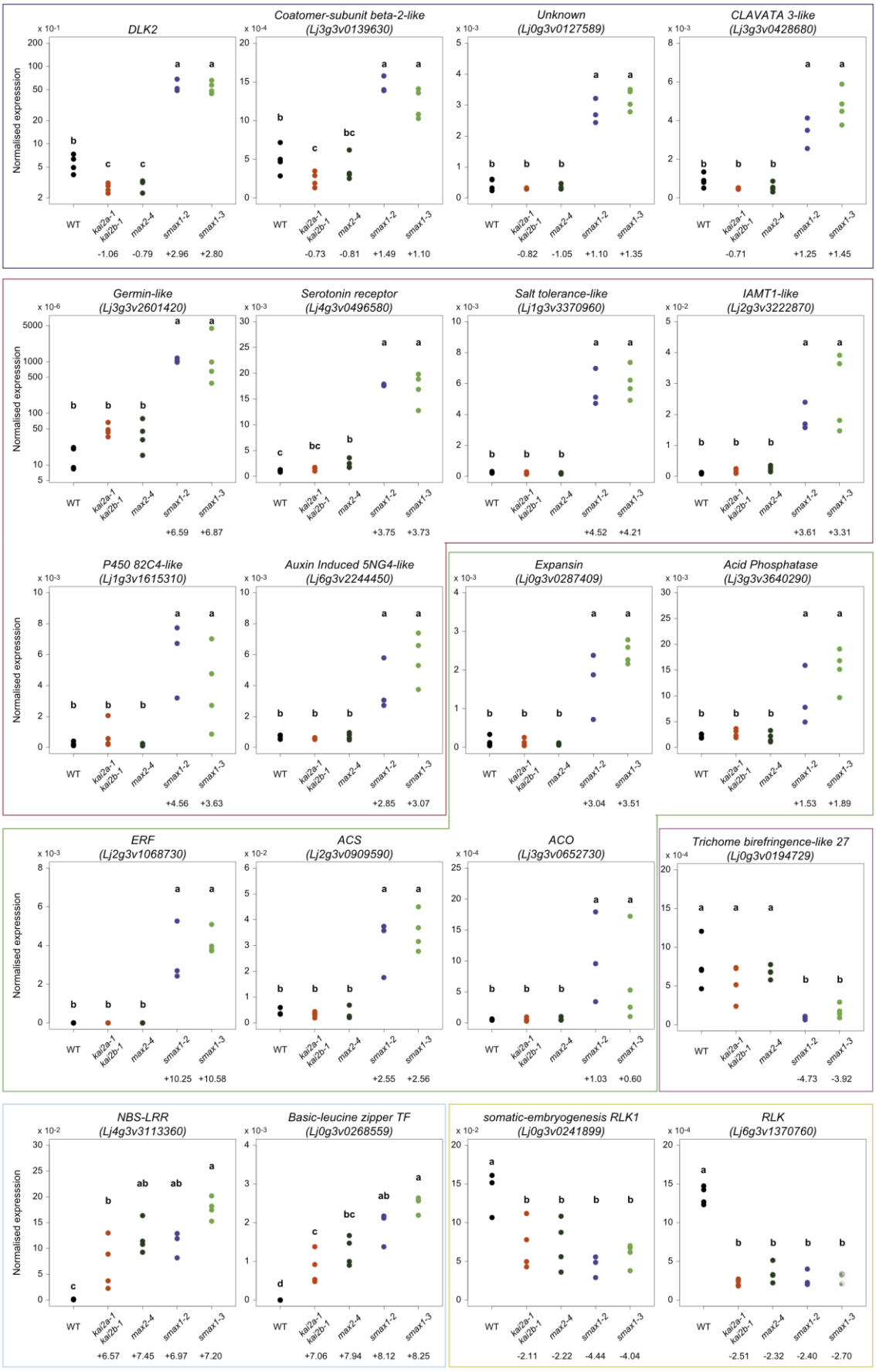

Figure 3.17: qPCRs analysis confirms RNAseq results. Normalized expression of genes in wild-type, *kai2a-1 kai2b-1*, *max2-4*, *smax1-2* and *smax1-3* (n=4). Colored boxes indicate

common patterns from the RNAseq analysis or common function. Dark blue box displays genes with opposite regulations in KL perception vs. repressor mutants, and thus putative KL marker genes. Red box displays genes with an induction only in the repressor mutants. Green box displays genes putatively linked to ethylene signaling. Light blue box displays genes induced in all mutants. Yellow box displays genes repressed in all mutants. Pink box displays a gene repressed only in *smax1* mutants. Numbers below the genotypes indicate, if significant, the log2 fold-change outcome of the RNAseq analysis. Letters indicate statistical differences between genotypes (ANOVA, post-hoc Tukey test).

g) Increased ethylene biosynthesis in the *smax1* mutants

To confirm that ethylene homeostasis is perturbed in the *smax1* mutants, we measured the ethylene accumulation in these mutants by gas-chromatography. The two alleles released around three times more ethylene than the wild-type (Fig 3.18.a). We then tested the responsiveness of the *smax1* mutants to perturbation of ethylene biosynthesis using pharmacological approaches, with the use of an ethylene precursor ACC (1-Aminocyclopropane-1-carboxylic acid) and an inhibitor of this same precursor AVG (Aminoethoxyvinylglycine). Upon inhibition of ethylene biosynthesis with AVG, ethylene accumulated less in the *smax1* mutants and to similar levels than the wild-type (Fig 3.18.b). In contrast, upon ACC treatment, ethylene production was strongly enhanced similarly in the mutants and the wild-type. Together, these results confirm that the *smax1* mutants produce more ethylene as expected by the increase transcription of the key enzyme of ethylene biosynthesis, *ACC Synthase*.

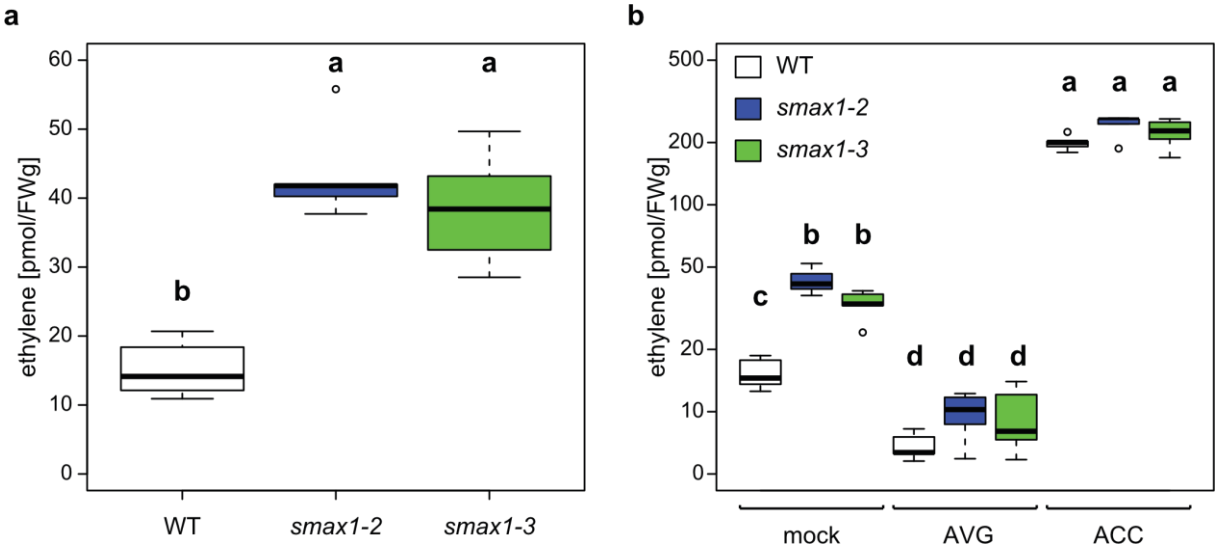

Figure 3.18: Over accumulation of ethylene in the *smax1* mutants. (a-b) Amount of ethylene released by fresh weight of *L. japonicus* seedlings. **(a)** Basal level in wild-type, *smax1-2* and *smax1-3* (n = 6). **(b)** In response to treatment with 0.1µM AVG or 1µM ACC (n = 5). Letters indicate significant differences (ANOVA, post-hoc Tukey test).

h) Inhibition of ethylene biosynthesis and perception rescues *smax1* mutants root growth phenotype

Since ethylene biosynthesis and signaling is enhanced in the *smax1* mutants, and the root phenotypes, with shorter root and root cells, resemble to ACC treated Arabidopsis (Ruzicka et al. 2007), we asked if ethylene signaling could be responsible for the root architecture phenotype observed in the KL repressor mutants. Therefore, we treated wild-type *L. japonicus* seedlings with different concentrations of the ethylene precursors ACC and Ethephon to see if this can recapitulate the *smax1* root phenotype (Fig 3.19a). Upon treatment with at least 1µM of these precursors, *L. japonicus* seedlings presented shorter primary roots, but the number of PER remained unchanged, leading to an increase of PER density. We also analyzed the effect of Ethephon treatment on the root-hair formation (Fig 3.19b). Root-hair length was increased by the treatment, and the first root-hair tended to be closer to the root apical QC. Altogether these results show that increasing ethylene recapitulates the *smax1* root-hair and root architecture phenotypes in wild-type, suggesting that these phenotypes are a direct consequence of increased ethylene production in the KL signaling repressor mutants.

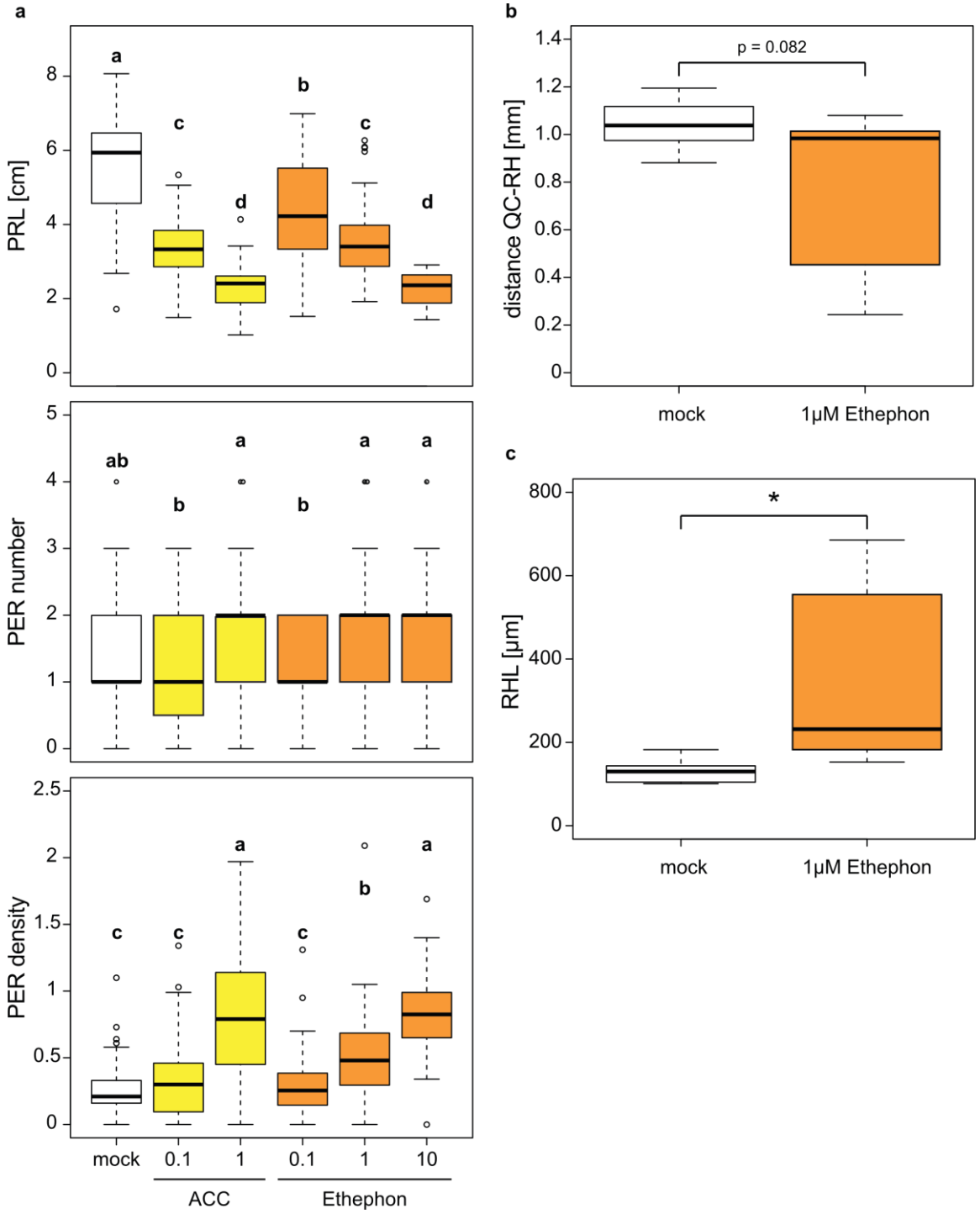

Figure 3.19: Induction of ethylene signaling prevents primary root growth in wild type. **(a)** Primary root length (PRL), post-embryonic root (PER) number and PER density of wild-type treated with ACC or ethephon at the indicated concentrations (in µM) ($n \geq 34$). **(b)** Distance of the first root-hair from the quiescent-center (QC) and **(c)** root-hair length at 1.5 to 2 mm from the apex ($n = 7$), in the wild-type upon 1µM ethephon treatment. Letters indicate significant differences (ANOVA, post-hoc Tukey test). Asterisk indicates significant differences (Welch's t.test).

To investigate whether the root developmental phenotypes of *smax1* mutants result from increased ethylene signaling, we tested if the inhibition of ethylene signaling could rescue these phenotypes. For this purpose, we used two different inhibitors. The first one is AVG, which specifically blocks the synthesis of the ethylene precursor ACC by inhibiting the ACC SYNTHASE (ACS) (Yu and Yang 1979). The second one is silver-nitrate (AgNO3), which blocks the ethylene receptor (ETHYLENE RECEPTOR 1, ETR1) (McDaniel and Binder 2012). Despite that both compounds inhibit ethylene signaling, silver nitrate treatment does not impair the synthesis of ACC which is known to have ethylene independent function in plant development (reviewed in (Van de Poel and Van Der Straeten 2014)). By consequence, the use of both compounds can be informative about the nature of the signaling, directly mediated by ACC or by ethylene (Schaller and Binder 2017). Upon AVG and silver-nitrate treatment, the PRL increased dramatically in the *smax1-3* mutant to reach wild-type level (Fig 3.20a), confirming the previous hypothesis that nutrient shortage is not causative of the weak root growth. In addition, the PER number and density decreased strongly to be statistically indifferent from the treated wild-type (Fig 3.20b). These results indicate that ethylene signaling is causative of the *smax1* root architecture phenotype.

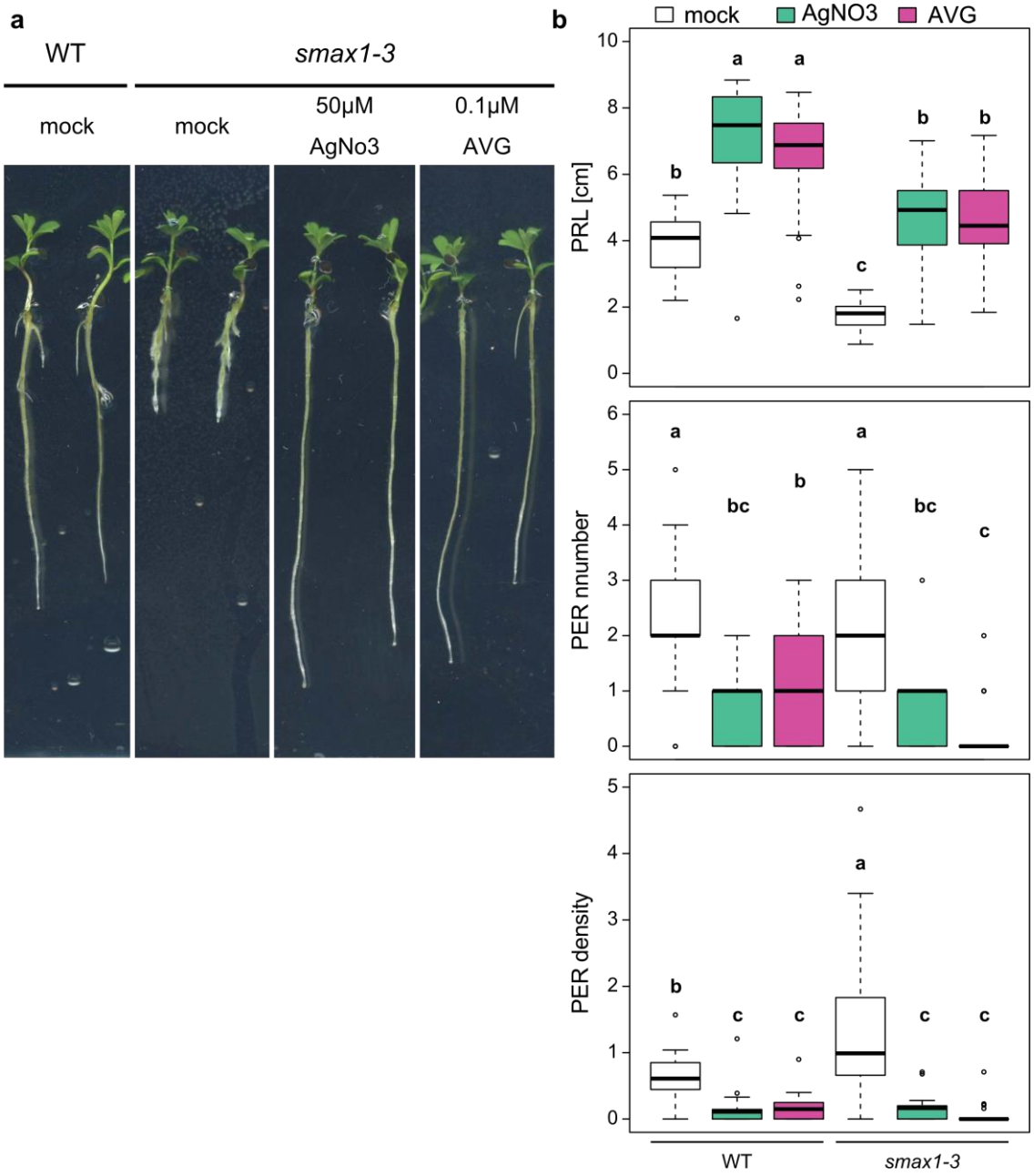

Figure 3.20: Rescue of the *smax1-3* root phenotype by ethylene inhibition. (a) Representative images and **(b)** quantification of primary root length (PRL), post-embryonic root (PER) number and PER density of wild-type and *smax1-3* in presence of 50µM silver-nitrate or 0.1µM AVG (n ≥ 24). Letters indicate significant differences (ANOVA, post-hoc Tukey test).

To gain insight into the importance of ethylene signaling for the root-hair phenotype of the *smax1* mutants, we also tested the effect of ethylene inhibition on root hair development by *smax1-3*. Upon AVG and silver-nitrate treatment, the number of root-hairs on the *smax1-3* primary root decreased (Fig 3.21a). The first root-hair emerged further away from the root apical meristem, at around 2mm (Fig 3.21b). This distance was statistically indifferent from mock-treated wild-type. In addition, when present at

the root apex, the root-hair length was strongly reduced by ethylene inhibition treatment to the wild-type level (Fig 3.21c). These results indicate that ethylene signaling is causative of the *smax1* root-hair phenotype.

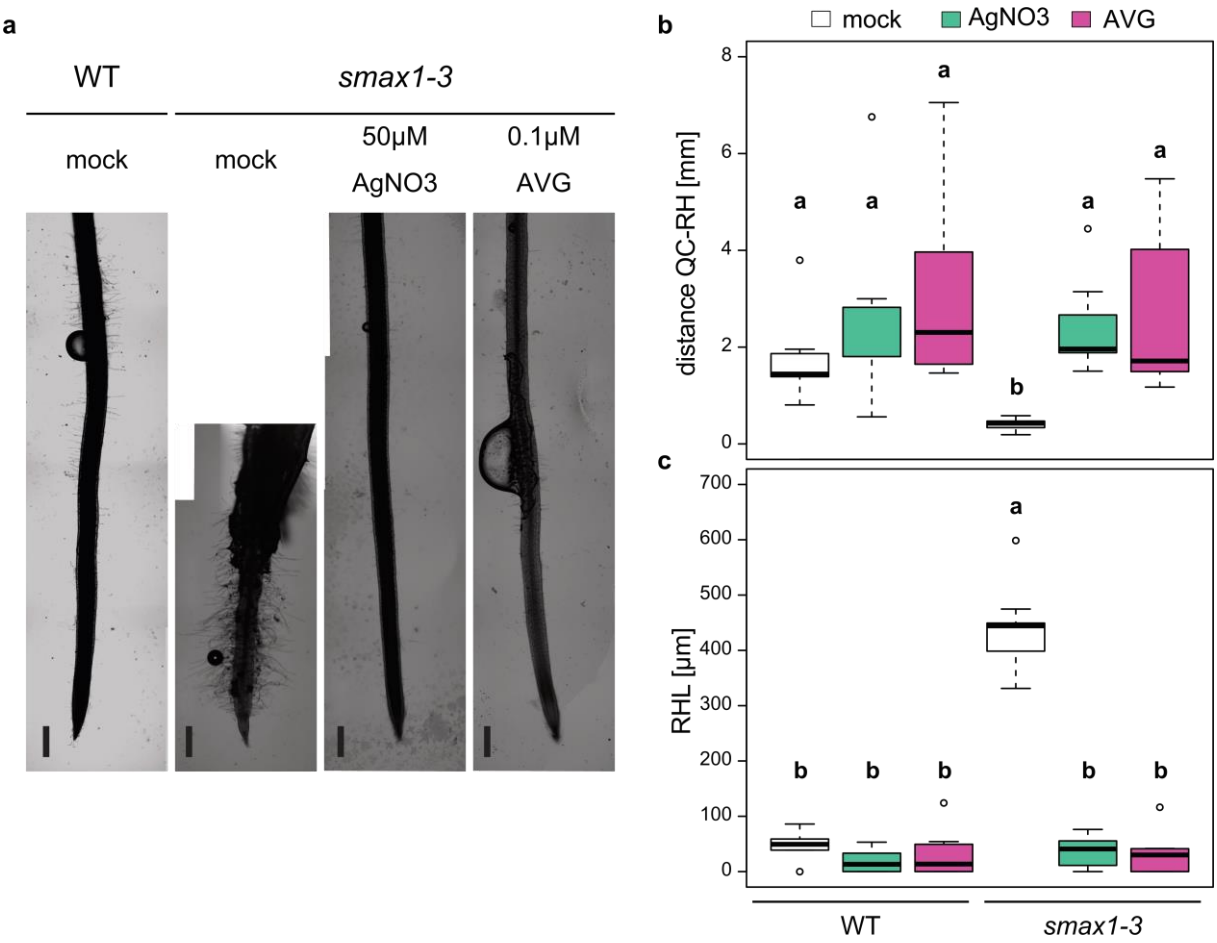

Figure 3.21: Rescue of the *smax1-3* root phenotype by ethylene inhibition. (a) Representative images, **(b)** distance between the first root-hair (RH) and the quiescent-center (QC), **(c)** and the root-hair length (RHL) of wild-type and *smax1-3* in presence of 50µM silver-nitrate or 0.1µM AVG (n ≥ 7). Scale bar= 500µm. Letters indicate significant differences (ANOVA, post-hoc Tukey test).

Taken together that the *smax1* mutants produce more ethylene, that increase ethylene signaling recapitulated the *smax1* root and root hair phenotype in wild type, and that ethylene inhibition rescues the *smax1-3* root architecture and root-hair phenotypes we demonstrate that the over-production of ethylene in the KL signaling repressor mutants, leads to the defects in root and root-hair development.

i) Ethylene signaling is required for the effect of KAR_1 on root development

Since the induction of ethylene signaling observed in the KL signaling repressor mutant is responsible for a reduction of the primary root length, we asked if the observed decrease of root growth in response to KAR_1 treatment (Fig 3.1) is mediated by ethylene signaling. To test this hypothesis, we treated wild-type plants with KAR_1 and the ethylene perception inhibitor silver-nitrate. In the absence of ethylene perception inhibition, seedlings responded to KAR_1 with a reduction of the PRL and an increase of PER density (Fig 3.22a). In contrast to KAR_1 treatment, the presence of silver nitrate leads to a long primary root with almost no PERs. In this condition, KAR_1 treatment did not affect the PRL, neither increase the PER number and the PER density of wild-type plants. In parallel, we also tested the responses to KAR_1 treatment of an ethylene-insensitive (*ein2a-2 ein2b-1*) mutant, which mimics inhibition of ethylene perception. In contrast to the wild-type, the *ein2a-2 ein2b-1* did not respond to the KAR_1 treatment and thus recapitulated the absence of KAR_1-response in the presence of the ethylene perception inhibitor (Fig 3.22b).

Taken together these results demonstrate that ethylene signaling is required for the KAR_1 effect on root architecture, and this response is likely mediated directly by ethylene signaling.

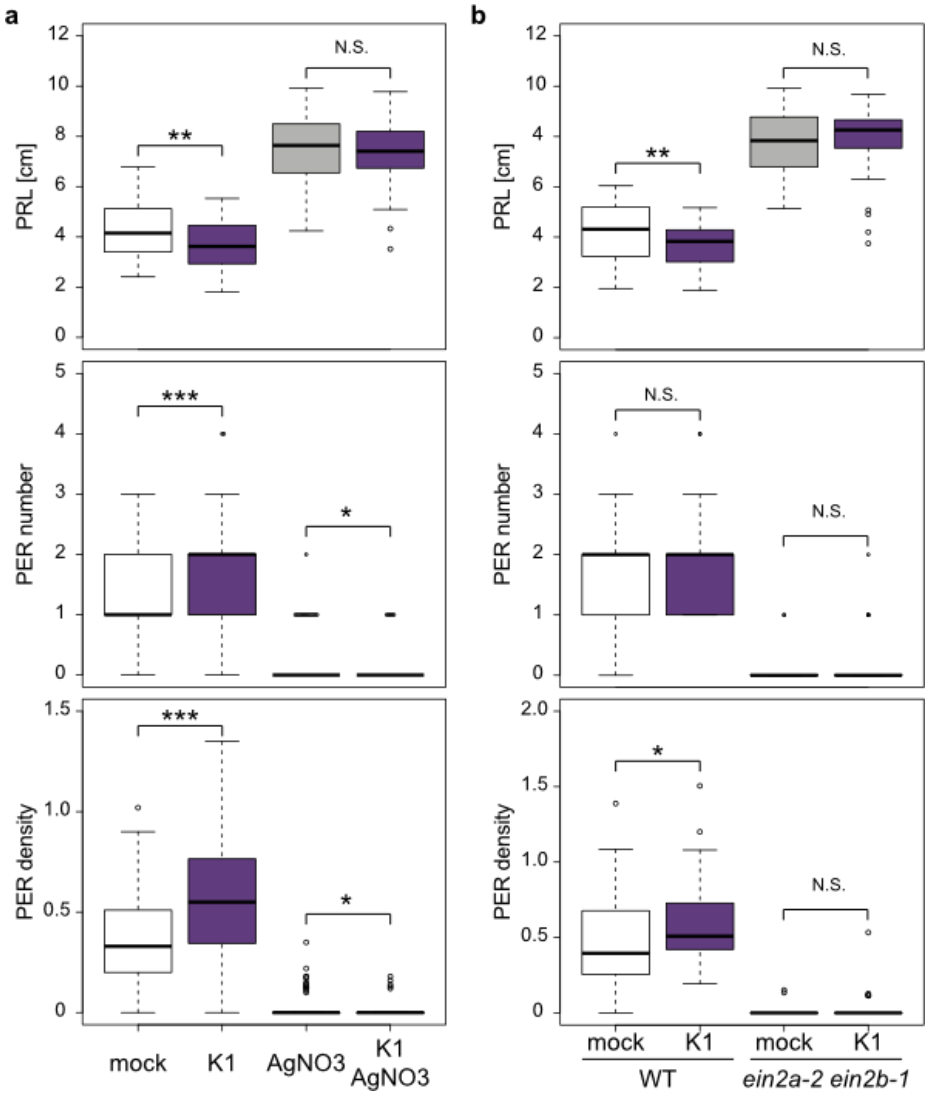

Figure 3.22: KAR_1 effect on root architecture require ethylene signaling. (a-b) Primary root length (PRL), post-embryonic root (PER) number and PER density in response to 1µM KAR_1 **(a)** in wild-type upon co-treatment with 50 µM silver-nitrate (n ≥ 57), and **(b)** in the ethylene insensitive mutant *ein2a-2 ein2b-1* (n ≥ 29). Asterisks indicate significant differences (Welch's t.test).

j) Ethylene-dependent and -independent transcriptional regulation in *smax1*-mutants

Since ethylene inhibition could rescue the abnormal root development of the *smax1* mutants, we asked if ethylene signaling or the indirect root phenotype was responsible for the deregulation of gene expression in these mutants. To examine this, we grew wild-type and both *smax1* alleles on supplemented medium with AVG or silver-nitrate, and tested the expression of few DEGs by qPCR (Fig 3.23 and 3.24). Transcript

accumulation of several genes, which was high in the *smax1* mutants, was efficiently reduced upon both AVG and silver-nitrate treatment, like the *Germin-like* (*Lj3g3v2601420*), the *IAMT1-like* (*Lj2g3v3222870*), and the *Auxin-Induced-5NG4-like* (*Lj6g3v2244450*). Surprisingly, *Expansin* (*Lj0g3v0287409*), which is known to be involved in root-hair growth mediated by ethylene signaling (Cho and Cosgrove 2002), was repressed only upon AVG but not by silver-nitrate treatment. In addition, silver-nitrate treatment leads to increased expression also in the wild-type, which suggests that *Expansin* is not regulated directly by ethylene but possibly by ACC signaling. In contrast, *DLK2* transcript over-accumulation in the *smax1* mutants was still occurring upon ethylene inhibition. Interestingly several other genes behaved in a similar fashion, like a gene of unknown function (*Lj0g3v0127589*), a serotonin receptor gene (*Lj4g3v0496580*) and unexpectedly the AP2 transcription factor annotated as *ERF* (*Lj2g3v1068730*). These genes are de-repressed by the absence of SMAX1, and not due to a downstream effect of the increase of ethylene signaling. Therefore, they are interesting candidates to be early and maybe primary targets of KL signaling.

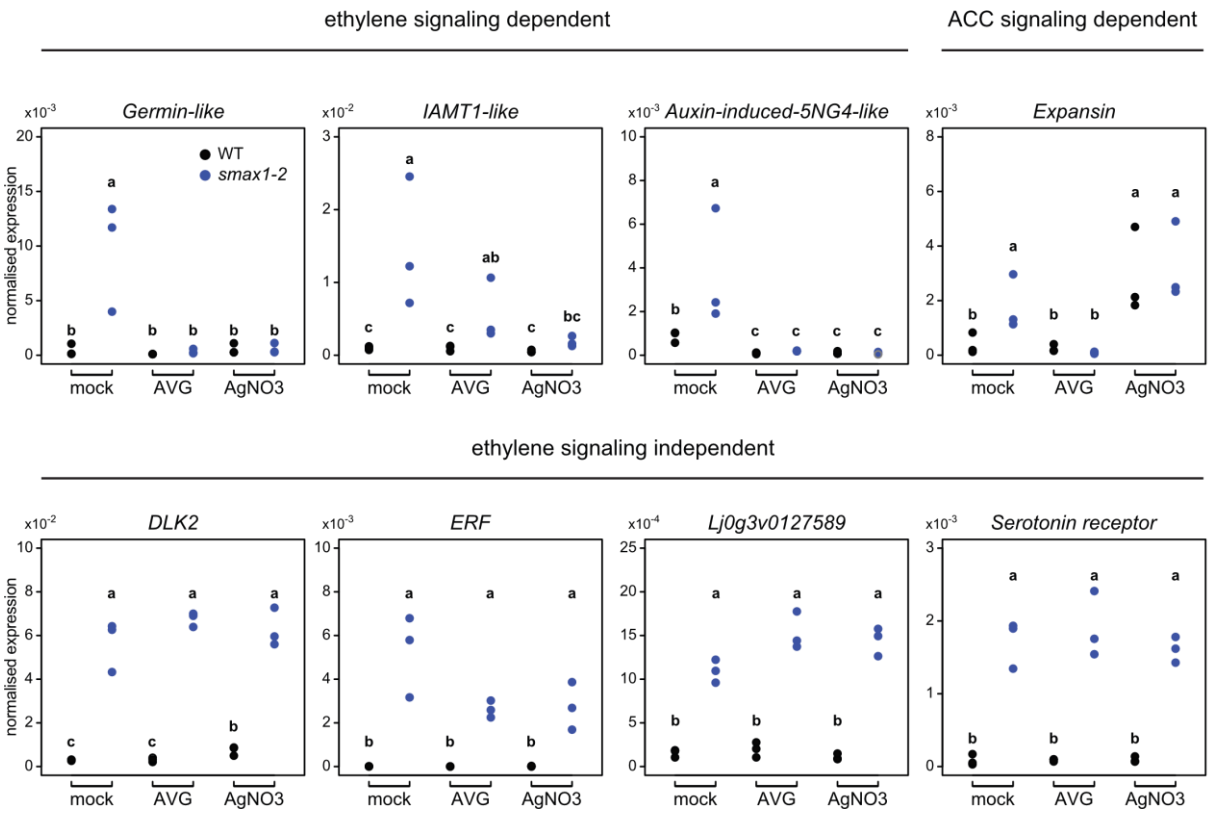

Figure 3.23: Ethylene independently and dependently regulated DEGs in *smax1-2*. Transcript accumulation of several genes in roots of wild-type (black dots) and *smax1-2* (grey dots) grown on 0.1µM AVG and 50µM silver-nitrate treatment (n=3). Letters indicate significant differences (ANOVA, post-hoc Tukey test).

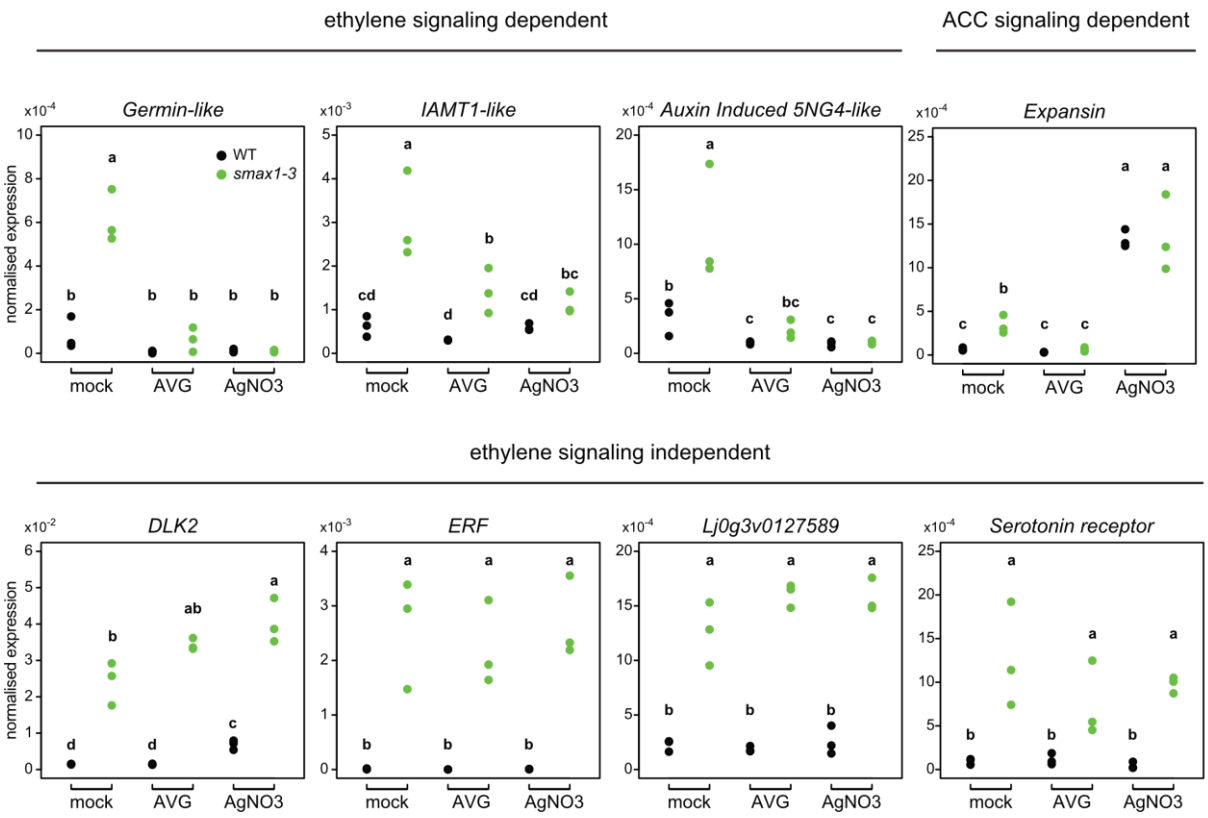

Figure 3.24: Ethylene independently and dependently DEGs in *smax1-3*. Transcript accumulation of several genes in roots of wild-type (black dots) and *smax1-3* (green dots) grown on 0.1µM AVG and 50µM silver-nitrate treatment (n=3). Letters indicate significant differences (ANOVA, post-hoc Tukey test).

k) *ERF*, a new KL/KAR marker gene

To test if these ethylene signaling independent DEGs in the *smax1* mutants are indeed early targets of KL signaling, we analyzed their possible induction by a short exogenous KAR_1 treatment on roots. After 2 hours of treatment, a strong induction of *DLK2* and *ERF* was observed in the wild-type, and this was absent in the KL perception mutants *kai2a-1 kai2b-1* and *max2-4* (Fig 3.25). A similar response pattern was observed with the *Serotonin receptor*; however, this gene was also induced in the *kai2a-1 kai2b-1* and *max2-4* mutants but with much lower intensity. In the case of the gene of unknown function (*Lj0g3v0127589)* and the *ACC synthase* (*ACS)*, a tendency of induction was detected only in the wild-type. The ethylene-dependent DEG in the *smax1* mutants, *Germin-like* was expected to be a far downstream gene and was not induced by KAR_1 treatment. Altogether, these results, confirm the discovery of a new

KL/KAR marker gene *ERF*. Furthermore, KL signaling seemed to increase transcript accumulation of *ACS*, suggesting that KAI2-mediated signaling may indeed be involved in activating ethylene biosynthesis, however, since *ACS* may be a late response gene, the incubation time of 2h may be too short to see a significant effect on *ACS* expression. Therefore, we tested the transcriptional response after 6h of KAR_1 treatment. In addition to *DLK2* and *ERF*, *ACS* was significantly induced by KAR_1 (Fig 3.26). Further, we also investigated if the absence of developmental response to *rac*-GR24 (Fig 3.1) could be related to a specific KAR_1 transcriptional response. As previously observed after 2h treatment (Fig 3.3), *DLK2* is induced by both treatments after 6h incubation time (Fig 3.26). However, *ERF* and *ACS* are specifically induced by KAR_1, and provide evidence of a specific transcriptional response to KAR_1 only which leads to *ACS* induction and promotes ethylene signaling.

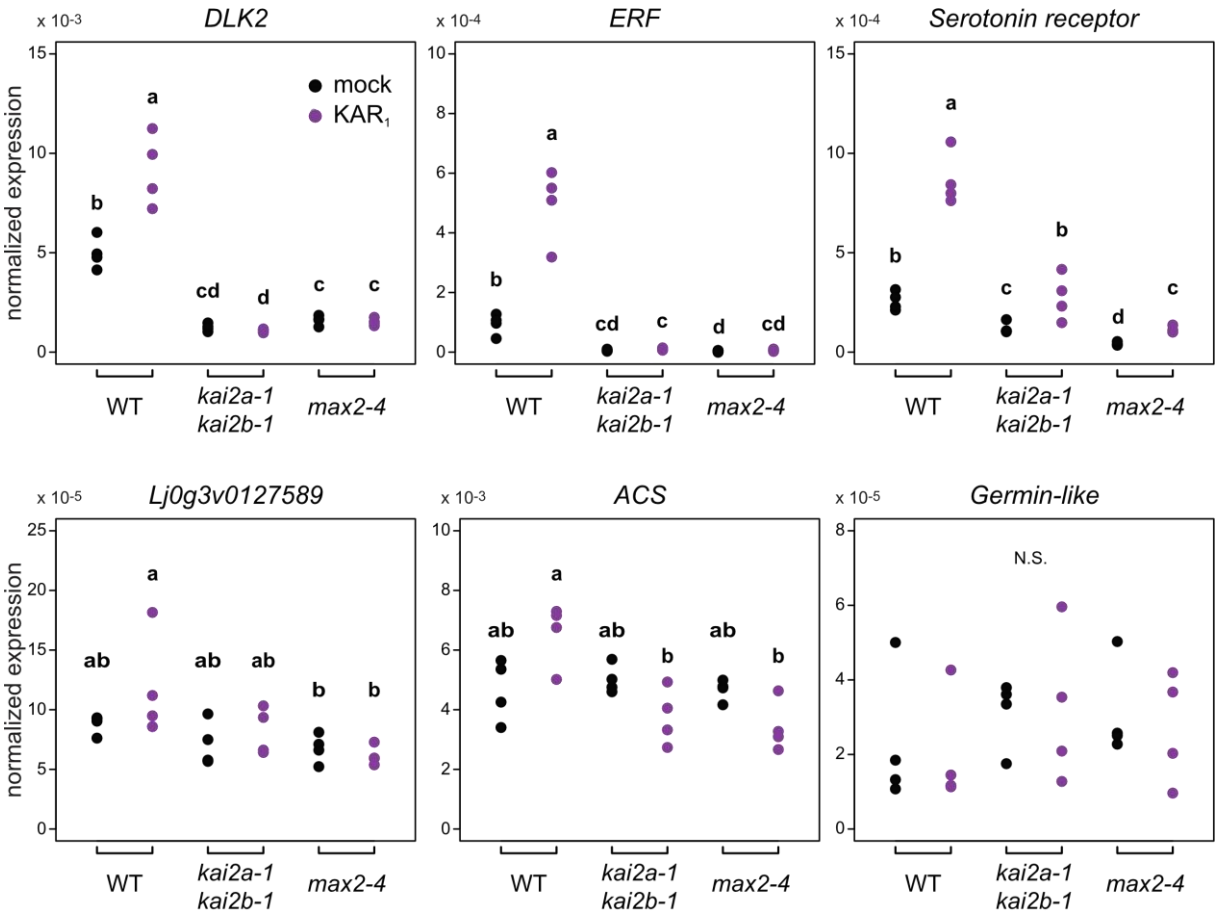

Figure 3.25: Discovery of new KL marker gene *ERF*. Transcript accumulation of several genes in roots of wild-type, *kai2a-1 kai2b-1* and *max2-4*, upon 2 hours treatment with 3µM KAR_1 (purple dots) or solvent (black dot) (n=4). Letters indicate significant differences (ANOVA, post-hoc Tukey test).

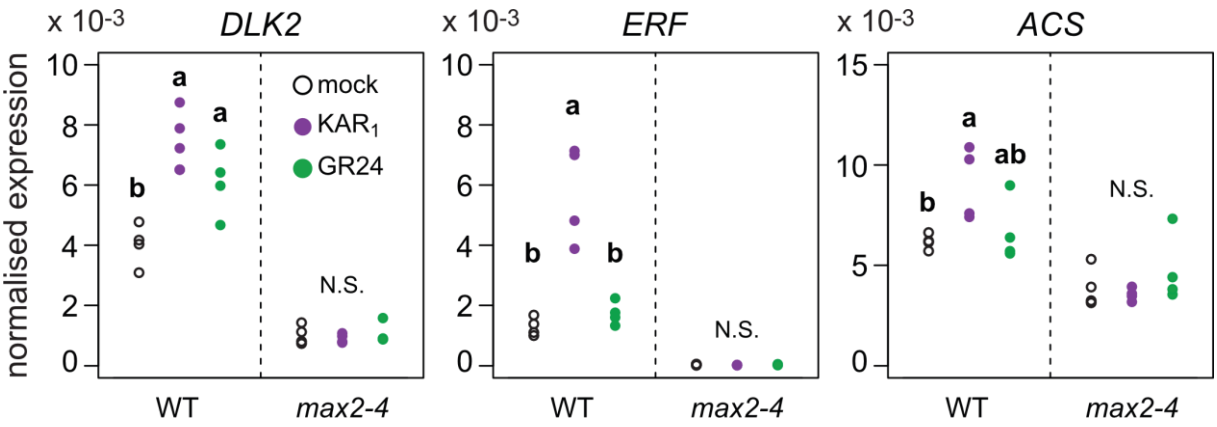

Figure 3.26: *ERF* and *ACS* are specifically induced by KAR_1. Transcript accumulation of *DLK2, ERF,* and *ACS* in roots of wild-type and *max2-4*, upon 6 hours treatment with 1µM KAR_1, 1µM *rac*-GR24 or solvent (n=4). Letters indicate significant differences (ANOVA, post-hoc Tukey test).

VIII. Materials and methods

a) Plant material

A. thaliana kai2-2 (Ler background) and *d14-1* (Col-0 background) mutants were provided by Mark Waters (Waters et al. 2012), *d14-1 kai2-2* (Col-0 background) were provided by Tom Bennett (Bennett et al. 2016).

The *L. japonicus* Gifu *max2-1, max2-2, max2-3, max2-4, kai2a-1, kai2b-3, smax1-1, smax1-3, smxl3a-1, smxl3b-1* and *smxl4-1* mutations are caused by a LORE1 retrotransposon insertion. Seeds, segregating for each insertion were obtained from the Lotus Base (https://lotus.au.dk, (Urbanski et al. 2012)) or Makoto Hayashi (NIAS, Tsukuba, Japan, (Fukai et al. 2012) for *max2-2*. The *d14-1, kai2b-1,* and *kai2b-2* were obtained by TILLING (Perry et al. 2003) at RevGenUK (https://www.jic.ac.uk/technologies/genomic-services/revgenuk-tilling-reverse-genetics/). The *ein2a-2 ein2b-1* double mutant was provided by Dugald Reid and Jens Stougaard (Reid et al. 2018).

Table 1: *L. japonicus* mutant used in this study.

allele	type	reference	position from ATG	comments
d14-1	EMS	SL4580	C685T (Q > stop)	-
kai2a-1	LORE1 insertion	30008990	387	-
kai2b-1	EMS	SL1281	C640T (Q > stop)	-
kai2b-2	EMS	SL2723	G462A (W > stop)	no seed produced
kai2b-3	LORE1 insertion	30034333	535	-
max2-1	LORE1 insertion	30031159	83	handful of seeds
max2-2	LORE1 insertion	P0860_3	504	handful of seeds
max2-3	LORE1 insertion	30019601	1132	produce few seeds
max2-4	LORE1 insertion	30049531	1230	produce few seeds
smax1-1	*LORE1* insertion	30056261	498	No seeds
smax1-2	*LORE1* insertion	30039146	601	
smax1-3	*LORE1* insertion	30015424	917	
smxl3a-1	*LORE1* insertion	30020916	283	
smxl3b-1	*LORE1* insertion	30019975	1953	
smxl4-1	*LORE1* insertion	30049271	98	

ein2a-2 *ein2b-1*	*LORE1* insertions	Characterized in (Reid et al. 2018)

b) Seed germination

A. thaliana seeds were surface sterilized with 70% ethanol. For synchronizing the germination, seeds were placed on ½ MS 1% agar medium and maintained at 4°C in dark for 72 hours.

L. japonicus seeds were manually scarified with sand-paper, surface sterilized with 1% NaClO, washed 4 times and incubated 2 hours in sterile water. Imbibed seeds were germinated on 1/2 Hoagland medium containing 2.5µM PO_4^{3-} and 0.4% Gelrite (www.duchefa-biochemie.com), at 24°C for 3 days in the dark, or on ½ MS 0.8% agar at 4°C for 3 days in dark (only for the experiment in Fig 1.7).

c) DNA extraction

L. japonicus leaves were collected in tubes containing 2 metal beads and frozen in liquid nitrogen. Tissues were lysed using a TissueLyser (Qiagen) at 30Hz for 1min. 300µL of 65°C preheated extraction buffer (2% CTAB, 100mM Tris, 1.4M NaCl, 20mM EDTA) and 2µL of Beta-mercaptoethanol was added, and quickly vortexed. Samples were incubated at 65°C for 30min. 170µL of Chloroform was added and mixed by repeated inversion for 5min. Following incubation, samples were centrifuged 15min at 13000rpm. Supernatants were recovered in new tubes, to which 200µL of isopropanol and 20µL of 3M pH5.2 sodium-acetate were added for DNA precipitation. After mixing by inversion, samples were centrifuged 15min at 13000rpm. Pellets were washed one time in 70% ethanol, and samples centrifuged 5min at 13000rpm. Supernatants were discarded, and ethanol evaporated at 65°C. Dried DNA pellets were suspended in Millipore filtered water.

d) Plant genotyping

Following DNA extraction, homozygous mutants were identified by PCR. Mutants originating from a *LORE1* insertion were identified by the use of two primer pairs: one forward and reverse flanking the insertion site, and the second using the forward and a specific primer to the *LORE1* sequence (CCATGGCGGTTCCGTGAATCTTAGG). Primers are indicated in Table 2.

Table 2: Primers used for LORE1 insertion mutant genotyping.

allele	Forward		Reverse	
Ljkai2a-1	Sc403	TATGGTCTCTCACGCTGTTTCCGCCATGATCG	Sc283	TCCACAATAGACACGCCACC
Ljkai2b-3	Sc285	CCTCCGTTGACATGACCTCC	Sc17	TTGAAGACTACCCCTTAAACA AGGGGTTTGAG
Ljmax2-1	Sc130	ATGAAGACTTTACGGGTCTCACACCATGAGTA ACGCTGCTGAAAC	CG416	CAGTAGAAGCTCCGGCAAAC
Ljmax2-2	CG383	TTGGGGAGGGGTTTAATAGG	CG424	CGATTTCGTGAGACTTGAAGC
Ljmax2-3	Sc163	TCACCTCGCTGGATCTCTC	Sc131	TTGAAGACTACCACCTCCCAT GTTGTCATC
Ljmax2-4	Sc131	TTGAAGACTACCACCTCCCATGTTGTCATC	Sc163	TCACCTCGCTGGATCTCTC
Ljsmax1-1	Sc189	CGACGCTTCTAGCTTCGCCGTCTG	Sc190	CACATGGCCATTGCTGAAAACCCC
Ljsmax1-2	Sc191	CACATGGCCATTGCTGAAAACCCC	Sc192	CGACGCTTCTAGCTTCGCCGTCTG
Ljsmax1-3	Sc193	GGCACTGCCTGAAGATCCCAATCA	Sc194	TACCGCGCCGAGCAGGAATTTGTA
Ljsmxl3a-1	Sc195	TGCAACAAGGCCTAACTGCCGAGG	Sc196	GACTCGCCAAATTCTCCACCACGC
Ljsmxl3b-1	Sc199	TGTGATGCCTTGGAGAAGAAGGTTCC	Sc200	TCCATGAAGAACACCCTGTGGGGG
Ljsmxl4-1	Sc201	GAGGCTGCTGTTGCTGCTGCTCAA	Sc202	TTGAGGGTGGGGTGGTGGTGATTG

EMS derived mutants were identified by amplification of the mutated sites, followed by digestion with restriction enzymes which cut specifically the WT locus. Products were separated on a 3% agarose gel. Primers and enzyme used are indicated in Table 3.

Table 3: Primers used for EMS mutant genotyping.

allele	Forward		Reverse		Site
Ljd14-1	Sc429	GCCGGCGGCGGCCGCGAGGTACCT G	Sc242	TTTCGTCTCACCTTGTGTGCCCCCGCC AGTGC	PstI (Cut WT)
Ljkai2b-1	Sc431	GGTAACTGTGCCATGTCACAGTATA	Sc285	CCTCCGTTGACATGACCTCC	AccI (Cut WT)

e) Plasmid generation

Genes and promoter regions were amplified using Phusion PCR according to standard protocols and using primers indicated in Table 4. Plasmids were constructed by Golden Gate cloning (Binder et al. 2014) as indicated in Table 5.

Table 4: Primers used for cloning.

Use	Primers	
cloning promoter *AtD14* in LI	Sc224	TTTCGTCTCAGCGGGTCTACACATTCATCAATCTCGC
	Sc225	TTTCGTCTCACAGATTTTTTATGTGTTTGGGTTTGAG
cloning promoter *AtKAI2* fragment 1 in LI	Sc232	TTTCGTCTCAGCGGGGCGATTCAGTGCCATGATT
	Sc233	TTTCGTCTCACGATTCGTTCAGATTCTCGCT
cloning promoter *AtKAI2* fragment 2 in LI	Sc234	TTTCGTCTCAATCGACTCGAATTTGATGGATCTTTC
	Sc235	TTTCGTCTCACAGACTCTCTAAAGAAGATTCTTC
cloning genomic *AtD14* in LI	Sc236	TTTCGTCTCACACCATGAGTCAACACAACATCTTAGAAG
	Sc237	TTTCGTCTCACCTTTCACCGAGGAAGAGCTCGCC
cloning genomic *AtKAI2* in LI	Sc238	TTTCGTCTCACACCATGGGTGTGGTAGAAGAAG
	Sc239	TTTCGTCTCACCTTTCACATAGCAATGTCATTACGAATG
cloning genomic *LjD14* in LI	Sc240	TTTCGTCTCACACCATGGCCACTTCAATCCTCGACG
	Sc241	TTTCGTCTCACCTTTCAGTGTGCCCCCGCCAGTG
cloning genomic *LjKAI2a* in LI	Sc243	TTTCGTCTCACACCATGGGGATAGTGGAGGAAGCTCAC
	Sc244	TTTCGTCTCACCTTTTACACCCCACTAAATTTTACATCAC
cloning genomic *LjKAI2b* in LI	Sc246	TTTCGTCTCACACCATGGGGATAGTGGAAGAAGCTC
	Sc247	TTTCGTCTCACCTTTCAAGCTGCAATATCATGGCAAATG
cloning cDNA *LjKAI2a* (3b) fragment 1 in L0	Sc505	ATGAAGACTTCCATCGGAGCCCACCCTAAAC
	ST161	ATGAAGACTTTACGTCGTCTCACACCATGGG
cloning cDNA *LjKAI2a* (3b) fragment 2 in L0	ST163	ATGAAGACTTATGGCGGTGGGTGGAGACATG
	ST164	ATGAAGACTTCGCAAAACGGTTAGAGCAATATC
cloning cDNA *LjKAI2a* (3b) fragment 3 in L0	ST165	ATGAAGACTTTGCGGACCATTTTTCAGAGC
	Sc498	ATGAAGACTACAGACGTCTCACCTTTTACACCCCACTAAATTTTAC
cloning cDNA *LjKAI2b* (3a) fragment 1 in L0	Sc506	ATGAAGACTTCCAGCGGGGCAAAGCCTGAAC
	ST169	ATGAAGACTTTACGTCGTCTCACACCATGGG
cloning cDNA *LjKAI2b* (3a) fragment 2 in L0	ST171	ATGAAGACTTCTGGCTATCGGAGGAGACATG
	ST172	ATGAAGACTTTGCGATACGCTTAAGGCTATG
cloning cDNA *LjKAI2b* (3a) fragment 3 in L0	ST173	ATGAAGACTTCGCAGACAATTTTTCAAAGTG
	Sc503	ATGAAGACTACAGACGTCTCACCTTTCAAGCTGCAATATC
cloning promoter *LjMAX2* in LI	Sc128	TTTGGTCTCAGCGGCAGCGTGAGAGGAATCAGC
	Sc129	TTTGGTCTCACAGACGCCGGTAAGATGATGATTC
cloning genomic *LjMAX2* in L0	Sc130	ATGAAGACTTTACGGGTCTCACACCATGAGTAACGCT GCTGAAAC
	Sc131	TTGAAGACTACCACCTCCCATGTTGTCATC
	Sc132	TTGAAGACTAGTGGACTTCTCAATTTTGACCTG

	Sc133	TTGAAGACTATCTTCACATTCCTCATCCC
	Sc134	TTGAAGACTAAAGATCCAAGCAAAAGGAAGAGG
	Sc135	TTGAAGACTAAGACCAAATTCACTCTCAGC
	Sc136	TTGAAGACTAGTCTAAGCATCCTGGCTTGTTATC
	Sc137	ATGAAGACTTCAGAGGTCTCACCTTTCAATCACAGATA TGACGC
LI *gLjD14* wo ATG	MK1	AAGGTCTCACACCGCCACTTCAATCCTCGAC
	Sc12	TTGAAGACTACAGAGGTCTCTCCTTTCAGTGTGCCCCCGCCAGTG
LI *gLjKAI2a* wo ATG	MK2	AAGGTCTCACACCGGGATAGTGGAGGAAGCTCA
	Sc14	TTTGGTCTCTCCTTTTACACCCCACTAAATTTTACATCAC
LI *gLjKAI2b* wo ATG	MK3	AAGGTCTCACACCGGGATAGTGGAAGAAGCTCAC
	Sc18	TTGAAGACTACAGAGGTCTCTCCTTTCAAGCTGCAATATCATGGCA AATG
LI *gLjMAX2* wo ATG	MK4	AAGGTCTCACACCAGTAACGCTGCTGAAACCAC
	Sc137	ATGAAGACTTCAGAGGTCTCACCTTTCAATCACAGATATGACGC
LI Esp3i *LjSMAX1* A	Sc249	TTTCGTCTCACACCATGAGAGCGGGTCTCAGCACCATCC
	Sc274	TTTCGTCTCATAGTTCCGCATACACTGGGGA
LI Esp3i *LjSMAX1* B	Sc275	TTTCGTCTCAACTACGAGCAAGAAGTAGCAGAAATG
	Sc250	TTTCGTCTCACCTTACACTGTTCCGCCACCAGTCTC
LI Esp3i *gLjSMXL3* A	MK5	TATCGTCTCACACCATGAGAACTGGAAACTGTGCTG
	MK6	TATCGTCTCAGTAGTTGCTTTATTCTCATTCTTATACTG
LI Esp3i *gLjSMXL3* B	MK7	TATCGTCTCACTACCTACAATCATCAGGTCTTGA
	MK8	TATCGTCTCACCTTTAAGTTCTGAAATTTGAAGATAAACATT
LI Esp3i *gLjSMXL4* A	MK13	TATCGTCTCACACCATGCGCTCAGGAGCTTG
	MK14	TATCGTCTCAGTGCTTCTTTTTCATAATTTGAGG
LI Esp3i *gLjSMXL4* B	MK15	TATCGTCTCAGCACAGTTGTTCAAACCAGG
	MK16	TATCGTCTCACCTTATCCATGAAGTAGTTAACTTGGATG
LI Esp3i *gLjSMXL9* A	MK9	TATCGTCTCACACCATGAGGGGAGGAATTTGC
	MK10	TATCGTCTCACTCCTACTCTATCTTCAAAAGGCA
LI Esp3i *gLjSMXL9* B	MK11	TATCGTCTCAGGAGCAAGGAAGAATCTAACTTG
	MK12	TATCGTCTCACCTTAAAGTTAAAACTAATTTGCTTATCAACTAAC
LI Esp3i *gLjSMXL8* A	Sc253	TTTCGTCTCACACCATGCCAACGCCGGTAGGAGTAG
	Sc254	TTTCGTCTCATCTCCACTCTCCACCTCCTTCC
LI Esp3i *gLjSMXL8* B	Sc255	TTTCGTCTCAGAGATGGCGAGGCCGTCGGTGC
	Sc276	TTTCGTCTCACCACGGAAGCAGAAAAGA
LI Esp3i *gLjSMXL8* C	Sc277	TTTCGTCTCAGTGGCTGATCCCTACCAATCT
	Sc256	TTTCGTCTCATCTGGATCGCAAAATTCATTGTC
LI Esp3i *gLjSMXL8* D	Sc257	TTTCGTCTCACAGAAACGCCTAAAAGGGCACATACA
	Sc258	TTTCGTCTCACCTTTTCTACAATTATCCTTGGAGGAAGG

Table 5: Plasmids.

Name	Description
Golden Gate Level 0	
L0 *cLjKAI2a(3b)* A	PCR amplification of *L. japonicus* Gifu cDNA with primers Sc505 +ST161. Assembly by StuI cut ligation into L0-Amp (BB01)
L0 *cLjKAI2a(3b)* B	PCR amplification of *L. japonicus* Gifu cDNA with primers ST163 +ST164. Assembly by StuI cut ligation into L0-Amp (BB01)
L0 *cLjKAI2a(3b)* C	PCR amplification of *L. japonicus* Gifu cDNA with primers ST165 +Sc498. Assembly by StuI cut ligation into L0-Amp (BB01)
L0 *cLjKAI2b(3a)* A	PCR amplification of *L. japonicus* Gifu cDNA with primers Sc506 +ST169. Assembly by StuI cut ligation into L0-Amp (BB01)
L0 *cLjKAI2b(3a)* B	PCR amplification of *L. japonicus* Gifu cDNA with primers ST171 +ST172. Assembly by StuI cut ligation into L0-Amp (BB01)
L0 *cLjKAI2b(3a)* C	PCR amplification of *L. japonicus* Gifu cDNA with primers ST173 +Sc503. Assembly by StuI cut ligation into L0-Amp (BB01)
L0 g*MAX2* A	PCR amplification with primers Sc130 + Sc131. Assembly by StuI cut ligation into L0-Amp (BB01)
L0 g*MAX2* B	PCR amplification with primers Sc132 + Sc133. Assembly by StuI cut ligation into L0-Amp (BB01)
L0 g*MAX2* C	PCR amplification with primers Sc134 + Sc135. Assembly by StuI cut ligation into L0-Amp (BB01)
L0 g*MAX2* D	PCR amplification with primers Sc136 + Sc137. Assembly by StuI cut ligation into L0-Amp (BB01)
Golden Gate Level I	
LI Esp3I p*AtKAI2* A	PCR amplification of *L. japonicus* Gifu genomic DNA with primers Sc232 + Sc233. Assembly by StuI cut ligation into LI-pUC57 (BB02)
LI Esp3I p*AtKAI2 B*	PCR amplification of *L. japonicus* Gifu genomic DNA with primers Sc234 + Sc235. Assembly by StuI cut ligation into LI-pUC57 (BB02)
LI Esp3I p*AtD14*	PCR amplification of *L. japonicus* Gifu genomic DNA with primers Sc224 + Sc225. Assembly by StuI cut ligation into LI-pUC57 (BB02)
LI Esp3I *gAtKAI2*	PCR amplification of *L. japonicus* Gifu genomic DNA with primers Sc238 + Sc239. Assembly by StuI cut ligation into LI-pUC57 (BB02)
LI Esp3I *gAtD14*	PCR amplification of *L. japonicus* Gifu genomic DNA with primers Sc237 + Sc238. Assembly by StuI cut ligation into LI-pUC57 (BB02)
LI Esp3I *gLjKAI2a*	PCR amplification of *L. japonicus* Gifu genomic DNA with primers Sc243 + Sc244. Assembly by StuI cut ligation into LI-pUC57 (BB02)
LI Esp3I *gLjKAI2b*	PCR amplification of *L. japonicus* Gifu genomic DNA with primers Sc246 + Sc247. Assembly by StuI cut ligation into LI-pUC57 (BB02)
LI Esp3I *gLjD14*	PCR amplification of *L. japonicus* Gifu genomic DNA with primers Sc240 + Sc241. Assembly by StuI cut ligation into LI-pUC57 (BB02)
LI Esp3I *cLjKAI2a*	PCR amplification of *L. japonicus* Gifu coding DNA with primers Sc243 + Sc244. Assembly by StuI cut ligation into LI-pUC57 (BB02)
LI Esp3I c*LjKAI2b*	PCR amplification of *L. japonicus* Gifu cDNA with primers Sc246 + Sc248. Assembly by StuI cut ligation into LI-pUC57 (BB02)
LI Esp3I c*LjKAI2a (3b)*	Assembled by BpiI cut ligation from: L0 *cLjKAI2a (3b)* A + L0 *cLjKAI2a (3b)* B + L0 *cLjKAI2a (3b*) C + LI-BpiI (BB03)
LI Esp3I c*LjKAI2b (3a)*	Assembled by BpiI cut ligation from: L0 *cLjKAI2b (3a)* A + L0 *cLjKAI2b (3a*) B + L0 *cLjKAI2b (3a*) C + LI-BpiI (BB03)
LI *pMAX2*	PCR amplification with primers Sc128 + Sc129. Assembly by StuI cut ligation into LI-pUC57 (BB02)

LI g*MAX2*	Assembled by BpiI cut ligation from: L0 g*MAX2* A + L0 g*MAX2* B + L0 g*MAX2* C + L0 g*MAX2* D + LI-BpiI (BB03)
LI *gLjD14* wo ATG	PCR amplification of LI gLjD14 with primers MK1 and Sc12. Assembly into LI-pUC57 (BB02). Assembly by StuI cut ligation into LI-pUC57 (BB02)
LI *gLjKAI2a* wo ATG	PCR amplification of LI gLjKAI2a with primers MK2 and Sc14. Assembly into LI-pUC57 (BB02). Assembly by StuI cut ligation into LI-pUC57 (BB02)
LI *gLjKAI2b* wo ATG	PCR amplification of LI gLjKAI2b with primers MK3 and Sc18. Assembly into LI-pUC57 (BB02). Assembly by StuI cut ligation into LI-pUC57 (BB02)
LI *gLjMAX2* wo ATG	PCR amplification of LI gLjMAX2 with primers MK4 and Sc137. Assembly into LI-pUC57 (BB02). Assembly by StuI cut ligation into LI-pUC57 (BB02)
LI Esp3i *LjSMAX1* A	PCR amplification of *L. japonicus* Gifu genomic DNA with primers Sc249 and Sc274. Assembly by StuI cut ligation into LI-pUC57 (BB02)
LI Esp3i *LjSMAX1* B	PCR amplification of *L. japonicus* Gifu genomic DNA with primers Sc275 and Sc250. Assembly by StuI cut ligation into LI-pUC57 (BB02)
LI Esp3i *gLjSMXL3a* A	PCR amplification of *L. japonicus* Gifu genomic DNA with primers MK5 and MK6. Assembly by SmaI cut ligation into LI-pUC57 (BB02)
LI Esp3i *gLjSMXL3a* B	PCR amplification of *L. japonicus* Gifu genomic DNA with primers MK7 and MK8. Assembly by SmaI cut ligation into LI-pUC57 (BB02)
LI Esp3i *gLjSMXL4* A	PCR amplification of *L. japonicus* Gifu genomic DNA with primers MK13 and MK14. Assembly by SmaI cut ligation into LI-pUC57 (BB02)
LI Esp3i *gLjSMXL4* B	PCR amplification of *L. japonicus* Gifu genomic DNA with primers MK15 and MK16. Assembly by SmaI cut ligation into LI-pUC57 (BB02)
LI Esp3i *gLjSMXL3b* A	PCR amplification of *L. japonicus* Gifu genomic DNA with primers MK9 and MK10. Assembly by SmaI cut ligation into LI-pUC57 (BB02)
LI Esp3i *gLjSMXL3b* B	PCR amplification of *L. japonicus* Gifu genomic DNA with primers MK11 and MK12. Assembly by SmaI cut ligation into LI-pUC57 (BB02)
LI Esp3i *gLjSMXL8* A	PCR amplification of *L. japonicus* Gifu genomic DNA with primers Sc253 and Sc254. Assembly by SmaI cut ligation into LI-pUC57 (BB02)
LI Esp3i *gLjSMXL8* B	PCR amplification of *L. japonicus* Gifu genomic DNA with primers Sc255 and Sc276. Assembly by SmaI cut ligation into LI-pUC57 (BB02)
LI Esp3i *gLjSMXL8* C	PCR amplification of *L. japonicus* Gifu genomic DNA with primers Sc277 and Sc256. Assembly by SmaI cut ligation into LI-pUC57 (BB02)
LI Esp3i *gLjSMXL8* D	PCR amplification of *L. japonicus* Gifu genomic DNA with primers Sc257 and Sc258. Assembly by SmaI cut ligation into LI-pUC57 (BB02)
Golden Gate Level II	
LIIc F 1-2 POI:GOI:*HygroR*	Assembled by BsaI cut ligation from: LI A-B POI (G082) + LI B-C dy (BB06) + LI C-D GOI + LI D-E dy (BB08) + LI E-F nos-T (G006) + LI F-G HygroR (G095) + LIIc F 1-2 (BB30)
LIIc R 3-4 p*35S*:*mCherry*	Assembled by BsaI cut ligation from: LI A-B p*35S* (G005) + LI B-C dy (BB06) + LI C-D *mCherry* (G023) + LI D-E dy (BB08) + LI E-F 35S-T (G059) + LI F-G dy (BB09) + LIIc R 3-4 (BB34)
LIIc F 1-2 *pMAX2:MAX2*	Assembled by BsaI cut ligation from: LI *pMAX2* + LI B-C dy (BB06) + LI gMAX2 + LI D-E dy (BB08) + LI E-F nos-T (G006) + LI F-G dy (BB09) + LIIc F 1-2 (BB30)
LIIc R 3-4 p*35S*:*mCherry*	Assembled by BsaI cut ligation from: LI A-B p*35S* (G005) + LI B-C dy (BB06) + LI C-D *mCherry* (G023) + LI D-E dy (BB08) + LI E-F 35S-T (G059) + LI F-G dy (BB09) + LIIc R 3-4 (BB34)
LIIc F1-2 *pUbi:*GOI_*GFP*	Assembled by BsaI cut ligation from: LI *pUbi* (G7) + LI B-C dy (BB06) + LI dy POI (G83) + LI D-E *GFP* (G11) + LI E-F nos-T (G6) + LI F-G dy (BB09) + LIIc F 1-2 (BB30)
LIIc F4-5 *pUbi:HA_gLjD14*	Assembled by BsaI cut ligation from: LI A-B *pUbi* (G7) + LI B-C *HA* (G67) + LI C-D *gLjD14* wo ATG+ LI D-E dy (BB8) + LI E-F HSP-T (G45) + LI F-G dy (BB09) + LIIc F4-5 (BB35)
LIIc F4-5 *pUbi:HA_gLjKAI2a*	Assembled by BsaI cut ligation from: LI A-B *pUbi* (G7) + LI B-C *HA* (G67) + LI C-D *gLjKAI2a* wo ATG + LI D-E dy (BB8) + LI E-F HSP-T (G45) + LI F-G dy (BB09) + LIIc F4-5 (BB35)

LIIc F4-5 *pUbi:HA_gLjKAI2b*	Assembled by BsaI cut ligation from: LI A-B *pUbi* (G7) + LI B-C *HA* (G67) + LI C-D *gLjKAI2b* wo ATG + LI D-E dy (BB8) + LI E-F HSP-T (G45) + LI F-G dy (BB09) + LIIc F4-5 (BB35)
LIIc F5-6 p*35S:MYC_MAX2*	Assembled by BsaI cut ligation from: LI A-B p*35S* (G005) + LI B-C *MYC* (G069) + LI C-D *gLjMAX2* wo ATG + LI D-E dy (BB08) + LI E-F 35S-T (G059) + LI F-G dy (BB09) + LIIc F5-6 (BB37)
Golden Gate Level III	
LIIIβ POI:GOI:*HygroR*	Assembled by BpiI cut ligation from: LIIc F 1-2 POI:GOI:HygroR + LII 2-3 ins (BB43) + LIIc R 3-4 p35S:*mCherry* + LII 4-6 dy (BB41) + LIIIβ F A-B (BB53)
LIIIβ p*AtKAI2:gAtKAI2*	Assembled by Esp3I cut ligation from: LIIIβ F A-B POI:GOI:HygroR + LI Esp3I *pAtKAI2* A + LI Esp3I *pAtKAI2* A + LI Esp3I *gAtKAI2*
LIIIβ p*AtKAI2:gAtD14*	Assembled by Esp3I cut ligation from: LIIIβ F A-B POI:GOI:HygroR + LI Esp3I *pAtKAI2* A + LI Esp3I *pAtKAI2* A + LI Esp3I *gAtD14*
LIIIβ p*AtKAI2:gLjKAI2a*	Assembled by Esp3I cut ligation from: LIIIβ F A-B POI:GOI:HygroR + LI Esp3I *pAtKAI2* A + LI Esp3I *pAtKAI2* A + LI Esp3I *gLjKAI2a*
LIIIβ p*AtKAI2:gLjKAI2b*	Assembled by Esp3I cut ligation from: LIIIβ F A-B POI:GOI:HygroR + LI Esp3I *pAtKAI2* A + LI Esp3I *pAtKAI2* A + LI Esp3I *gLjKAI2b*
LIIIβ p*AtKAI2:gLjD14*	Assembled by Esp3I cut ligation from: LIIIβ F A-B POI:GOI:HygroR + LI Esp3I *pAtKAI2* A + LI Esp3I *pAtKAI2* A + LI Esp3I *gLjD14*
LIIIβ p*AtD14:gAtD14*	Assembled by Esp3I cut ligation from: LIIIβ F A-B POI:GOI:HygroR + LI Esp3I *pAtKD14* + LI Esp3I *gAtD14*
LIIIβ p*AtD14:gAtKAI2*	Assembled by Esp3I cut ligation from: LIIIβ F A-B POI:GOI:HygroR + LI Esp3I *pAtKD14* + LI Esp3I *gAtKAI2*
LIIIβ p*AtD14:gLjD14*	Assembled by Esp3I cut ligation from: LIIIβ F A-B POI:GOI:HygroR + LI Esp3I *pAtKD14* + LI Esp3I *gLjD14*
LIIIβ p*AtD14:gLjKAI2a*	Assembled by Esp3I cut ligation from: LIIIβ F A-B POI:GOI:HygroR + LI Esp3I *pAtKD14* + LI Esp3I *gLjKAI2a*
LIIIβ p*AtD14:gLjKAI2b*	Assembled by Esp3I cut ligation from: LIIIβ F A-B POI:GOI:HygroR + LI Esp3I *pAtKD14* + LI Esp3I *gLjKAI2b*
LIIIβ *pMAX2:MAX2*	Assembled by BpiI cut ligation from: LIIc F 1-2 pMAX2:MAX2 + LII 2-3 ins (BB43) + LII R 3-4 p35s:mCherry + LII 4-6 dy (BB41) + LIIIβ F A-B (BB53)
LIIIβ empty vector	Assembled by BpiI cut ligation from: LII 1-2 dy (BB63) + LII 2-3 ins (BB43) + LII R 3-4 p35s:mCherry + LII 4-6 dy (BB41) + LIIIβ F A-B (BB53)
LIIIβ *pUbi:*GOI_*GFP* p*35S:mCherry* *pUbi:HA_gLjD14* p*35S:MYC_MAX2*	Assembled by BpiI cut ligation from: LIIc F 1-2 *pUbi:*GOI_*GFP* + LII 2-3 ins (BB43) + LIIc R 3-4 p35S:*mCherry* + LII 4-5 *pUbi:HA_gLjD14* + LII 5-6 p*35S:MYC_MAX2* + LIIIβ F A-B (BB53)
LIIIβ *pUbi:*GOI_*GFP* p*35S:mCherry* *pUbi:HA_gLjKAI2a* p*35S:MYC_MAX2*	Assembled by BpiI cut ligation from: LIIc F 1-2 *pUbi:*GOI_*GFP* + LII 2-3 ins (BB43) + LIIc R 3-4 p35S:*mCherry* + LII 4-5 *pUbi:HA_gLjKAI2a* + LII 5-6 p*35S:MYC_MAX2* + LIIIβ F A-B (BB53)
LIIIβ *pUbi:*GOI_*GFP* p*35S:mCherry* *pUbi:HA_gLjKAI2b* p*35S:MYC_MAX2*	Assembled by BpiI cut ligation from: LIIc F 1-2 *pUbi:*GOI_*GFP* + LII 2-3 ins (BB43) + LIIc R 3-4 p35S:*mCherry* + LII 4-5 *pUbi:HA_gLjKAI2b* + LII 5-6 p*35S:MYC_MAX2* + LIIIβ F A-B (BB53)
LIIIβ *pUbi:gLjSMAX1_GFP* p*35S:mCherry* *pUbi:HA_gLjD14* p*35S:MYC_MAX2*	Assembled by Esp3I cut ligation from: LIIIβ *pUbi:*GOI_*GFP* p*35S:mCherry pUbi:HA_gLjD14* p*35S:MYC_MAX2* + LI Esp3I *gLjSMAX1* A + LI Esp3I *gLjSMAX1* B
LIIIβ *pUbi:gLjSMAX1_GFP*	Assembled by Esp3I cut ligation from: LIIIβ *pUbi:*GOI_*GFP* p*35S:mCherry pUbi:HA_gLjKAI2a* p*35S:MYC_MAX2* + LI Esp3I *gLjSMAX1* A + LI Esp3I *gLjSMAX1* B

p*35S:mCherry* *pUbi:HA_gLjKAI2a* p*35S:MYC_MAX2*	
LIIIβ *pUbi:gLjSMAX1_GFP* p*35S:mCherry* *pUbi:HA_gLjKAI2b* p*35S:MYC_MAX2*	Assembled by Esp3I cut ligation from: LIIIβ *pUbi:*GOI*_GFP* p*35S:mCherry pUbi:HA_gLjKAI2b* p*35S:MYC_MAX2* + LI Esp3I *gLjSMAX1* A + LI Esp3I *gLjSMAX1* B
LIIIβ *pUbi:gLjSMXL3a_GFP* p*35S:mCherry* *pUbi:HA_gLjD14* p*35S:MYC_MAX2*	Assembled by Esp3I cut ligation from: LIIIβ *pUbi:*GOI*_GFP* p*35S:mCherry pUbi:HA_gLjD14* p*35S:MYC_MAX2* + LI Esp3I *gLjSMXL3a* A + LI Esp3I *gLjSMXL3a* B
LIIIβ *pUbi:gLjSMXL3a_GFP* p*35S:mCherry* *pUbi:HA_gLjKAI2a* p*35S:MYC_MAX2*	Assembled by Esp3I cut ligation from: LIIIβ *pUbi:*GOI*_GFP* p*35S:mCherry pUbi:HA_gLjKAI2a* p*35S:MYC_MAX2* + LI Esp3I *gLjSMXL3a* A + LI Esp3I *gLjSMXL3a* B
LIIIβ *pUbi:gLjSMXL3a_GFP* p*35S:mCherry* *pUbi:HA_gLjKAI2b* p*35S:MYC_MAX2*	Assembled by Esp3I cut ligation from: LIIIβ *pUbi:*GOI*_GFP* p*35S:mCherry pUbi:HA_gLjKAI2b* p*35S:MYC_MAX2* + LI Esp3I *gLjSMXL3a* A + LI Esp3I *gLjSMXL3a* B
LIIIβ *pUbi:gLjSMXL3b_GFP* p*35S:mCherry* *pUbi:HA_gLjD14* p*35S:MYC_MAX2*	Assembled by Esp3I cut ligation from: LIIIβ *pUbi:*GOI*_GFP* p*35S:mCherry pUbi:HA_gLjD14* p*35S:MYC_MAX2* + LI Esp3I *gLjSMXL3b* A + LI Esp3I *gLjSMXL3b* B
LIIIβ *pUbi:gLjSMXL3b_GFP* p*35S:mCherry* *pUbi:HA_gLjKAI2a* p*35S:MYC_MAX2*	Assembled by Esp3I cut ligation from: LIIIβ *pUbi:*GOI*_GFP* p*35S:mCherry pUbi:HA_gLjKAI2a* p*35S:MYC_MAX2* + LI Esp3I *gLjSMXL3b* A + LI Esp3I *gLjSMXL3b* B
LIIIβ *pUbi:gLjSMXL3b_GFP* p*35S:mCherry* *pUbi:HA_gLjKAI2b* p*35S:MYC_MAX2*	Assembled by Esp3I cut ligation from: LIIIβ *pUbi:*GOI*_GFP* p*35S:mCherry pUbi:HA_gLjKAI2b* p*35S:MYC_MAX2* + LI Esp3I *gLjSMXL3b* A + LI Esp3I *gLjSMXL3b* B
LIIIβ *pUbi:gLjSMXL4_GFP* p*35S:mCherry* *pUbi:HA_gLjD14* p*35S:MYC_MAX2*	Assembled by Esp3I cut ligation from: LIIIβ *pUbi:*GOI*_GFP* p*35S:mCherry pUbi:HA_gLjD14* p*35S:MYC_MAX2* + LI Esp3I *gLjSMXL4* A + LI Esp3I *gLjSMXL4* B
LIIIβ *pUbi:gLjSMXL4_GFP* p*35S:mCherry* *pUbi:HA_gLjKAI2a* p*35S:MYC_MAX2*	Assembled by Esp3I cut ligation from: LIIIβ *pUbi:*GOI*_GFP* p*35S:mCherry pUbi:HA_gLjKAI2a* p*35S:MYC_MAX2* + LI Esp3I *gLjSMXL4* A + LI Esp3I *gLjSMXL4* B
LIIIβ *pUbi:gLjSMXL4_GFP* p*35S:mCherry* *pUbi:HA_gLjKAI2b* p*35S:MYC_MAX2*	Assembled by Esp3I cut ligation from: LIIIβ *pUbi:*GOI*_GFP* p*35S:mCherry pUbi:HA_gLjKAI2b* p*35S:MYC_MAX2* + LI Esp3I *gLjSMXL4* A + LI Esp3I *gLjSMXL4* B
LIIIβ *pUbi:gLjSMXL8_GFP* p*35S:mCherry* *pUbi:HA_gLjD14* p*35S:MYC_MAX2*	Assembled by Esp3I cut ligation from: LIIIβ *pUbi:*GOI*_GFP* p*35S:mCherry pUbi:HA_gLjD14* p*35S:MYC_MAX2* + LI Esp3I *gLjSMXL8* A + LI Esp3I *gLjSMXL8* B + LI Esp3I *gLjSMXL8* C + LI Esp3I *gLjSMXL8* D

LIIIβ *pUbi:gLjSMXL8_GFP* p*35S:mCherry* *pUbi:HA_gLjKAI2a* p*35S:MYC_MAX2*	Assembled by Esp3I cut ligation from m: LIIIβ *pUbi:*GOI*_GFP* p*35S:mCherry pUbi:HA_gLjD14* p*35S:MYC_MAX2* + LI Esp3I *gLjSMXL8* A + LI Esp3I *gLjSMXL8* B + LI Esp3I *gLjSMXL8* C + LI Esp3I *gLjSMXL8* D
LIIIβ *pUbi:gLjSMXL8_GFP* p*35S:mCherry* *pUbi:HA_gLjKAI2b* p*35S:MYC_MAX2*	Assembled by Esp3I cut ligation from: LIIIβ *pUbi:*GOI*_GFP* p*35S:mCherry pUbi:HA_gLjD14* p*35S:MYC_MAX2* + LI Esp3I *gLjSMXL8* A + LI Esp3I *gLjSMXL8* B + LI Esp3I *gLjSMXL8* C + LI Esp3I *gLjSMXL8* D
LIIIβ *pUbi:*GOI*_GFP* p*35S:mCherry* *pUbi:HA_gLjD14*	Assembled by BpiI cut ligation from: LIIc F 1-2 *pUbi:*GOI*_GFP* + LII 2-3 ins (BB43) + LIIc R 3-4 p35S*:mCherry* + LII 4-5 *pUbi:HA_gLjD14* + LII 5-6 *dy* (BB65) + LIIIβ F A-B (BB53)
LIIIβ *pUbi:*GOI*_GFP* p*35S:mCherry* *pUbi:HA_gLjKAI2a*	Assembled by BpiI cut ligation from: LIIc F 1-2 *pUbi:*GOI*_GFP* + LII 2-3 ins (BB43) + LIIc R 3-4 p35S*:mCherry* + LII 4-5 *pUbi:HA_gLjKAI2a* + LII 5-6 *dy* (BB65)+ LIIIβ F A-B (BB53)
LIIIβ *pUbi:*GOI*_GFP* p*35S:mCherry* *pUbi:HA_gLjKAI2b*	Assembled by BpiI cut ligation from: LIIc F 1-2 *pUbi:*GOI*_GFP* + LII 2-3 ins (BB43) + LIIc R 3-4 p35S*:mCherry* + LII 4-5 *pUbi:HA_gLjKAI2b* + LII 5-6 *dy* (BB65)+ LIIIβ F A-B (BB53)
LIIIβ *pUbi:SMXL8_GFP* p*35S:mCherry* *pUbi:HA_gLjD14*	Assembled by Esp3I cut ligation from: LIIIβ *pUbi:*GOI*_GFP* p*35S:mCherry pUbi:HA_gLjD14* + LI Esp3I *gLjSMXL8* A + LI Esp3I *gLjSMXL8* B + LI Esp3I *gLjSMXL8* C + LI Esp3I *gLjSMXL8* D
LIIIβ *pUbi:SMAX1_GFP* p*35S:mCherry* *pUbi:HA_gLjKAI2a*	Assembled by Esp3I cut ligation from: LIIIβ *pUbi:*GOI*_GFP* p*35S:mCherry pUbi:HA_gLjKAI2a* + LI Esp3I *gLjSMAX1* A + LI Esp3I *gLjSMAX1* B
LIIIβ *pUbi:SMAX1_GFP* p*35S:mCherry* *pUbi:HA_gLjKAI2b*	Assembled by Esp3I cut ligation from: LIIIβ *pUbi:*GOI*_GFP* p*35S:mCherry pUbi:HA_gLjKAI2b* + LI Esp3I *gLjSMAX1* A + LI Esp3I *gLjSMAX1* B
Protein induction	
pSUMO *LjKAI2a*	PCR amplification from LI Esp3I *cLjKAI2a* with primers MW1002 + MW1003. Assembly by Gibson cloning
pSUMO *LjKAI2b*	PCR amplification from LI Esp3I *cLjKAI2b* with primers MW1002 + MW1004. Assembly by Gibson cloning
pSUMO *LjKAI2a (3b)*	PCR amplification from LI Esp3I *cLjKAI2a (3b)* with primers MW1002 + MW1003. Assembly by Gibson cloning
pSUMO *LjKAI2b (3a)*	PCR amplification from LI Esp3I *cLjKAI2b (3a)* with primers MW1002 + MW1004. Assembly by Gibson cloning

f) *A. thaliana* transformation

kai2-2 and *d14-1* mutants were transformed by a floral dip in *Agrobacterium tumefaciens* AGL1 suspension. Transgenic seedlings were selected by mCherry fluorescence and resistance to 20 µg/mL hygromycin-B in the growth medium.

Experiments were performed using T2 or T3 generations, with transformed plants determined by mCherry fluorescence.

g) *L. japonicus* transformation

Three days post-germination, seedlings were cut at the base of the hypocotyl and dipped into a fresh and concentrated solution of *Agrobacterium rhizogenes* AR1193 before to be placed on B5 medium in the dark for 3 days. Seedlings were transferred successively on new plates containing B5 medium supplied with 1% sugar and cefotaxime, at 24˚C, 60% humidity, with 16h-light-8h-dark cycles. After 3 weeks, transformed roots were screened with the mCherry transformation marker on a stereomicroscope (Leica MZ16 FA).

h) Shoot branching assay

A. thaliana and *L. japonicus* were grown in soil in a greenhouse at 16h/8h light/dark cycles for 4 and 7 weeks, respectively. Branches with length superior to 1cm were counted.

i) Hypocotyl elongation assay

A. thaliana were grown for 5 days on half-strength Murashige and Skoog (MS) medium containing 1% agar (BD). *L. japonicus* seedlings were grown for 6 days on half-strength Hoagland medium containing 2.5µM PO_4^{3-} and 0.4% Gelrite (www.duchefa-biochemie.com), or on half-strength MS containing 0.8% agar (only for the experiment in Fig 1.7) containing different compounds or equal amount of solvent (see Table 3.5). Long-day conditions with 16h/8h light/dark cycles were used to test the cross-species complementation (Fig 1.4). Short-day conditions at 8h/16h light/dark cycles were used to test hormone responsiveness. After high-resolution scanning, the hypocotyl length was measured with Fiji (http://fiji.sc/).

j) Root system architecture assay

L. japonicus germinated seeds were transferred onto new Petri dishes with half-strength Hoagland medium at 2.5µM PO_4^{3-} and 0.4% Gelrite, containing different compounds or equal amount of the solvent (see Table 6). Petri dishes were partially covered with black paper to keep the roots in the dark, and placed at 24°C with 16-h-light/8-h-dark cycles for 2 weeks. After high-resolution scanning, post-embryonic root number was counted, and primary root length measured with Fiji (http://fiji.sc/).

Table 6: Compounds used in this study.

compound	Supplier	Solvent	Stock Concentration
Karrikin 1	Olchemim	75% Methanol	10 mM
Karrikin 2	Olchemim	75% Methanol	10 mM
rac-GR24	Chiralix	100% Acetone	10 mM
ACC	Sigma	water	10 mM
Ethephon	Sigma	water	10 mM
AVG	Sigma	water	10 mM
Silver nitrate	Sigma	water	50 mM

k) Root-hair assay

Images of root tips were taken on the same roots used for the root architecture assays. Before root-hair imaging, a Biofolie 25 film (Lumox) was placed on top of a water layer on the roots. Multiple images per root apical meristem were taken with a Leica DM6 B microscope equipped with a Leica DFC9000 GT camera. Stitching of the root images was performed with the Fiji plugin MosaicJ. Fiji was used for all quantifications. The root-hair length was determined as the average of all the complete observable root-hairs (approximately 10-30 in mock condition and 2 to 5 with ethylene inhibitors) a distance from 1.5 to 2 mm from the root apex per biological replicate.

l) Longitudinal root tip sections

Images of root tips were taken on the same roots used for the root architecture assays. Root tips of 1 to 2 cm were fixed by vacuum infiltration in 2.5 % glutaraldehyde in 0.1M potassium phosphate buffer pH 7. After embedding in 5% low-melt agarose, sections

of 45 µm were created with a Vibratome VT1100S (Leica). Multiple images per root apical meristem samples were taken with a Leica DM6 B microscope equipped with a Leica DFC9000 GT camera. Stitching of the root images was performed with the Fiji plugin MosaicJ. Fiji was used for all quantifications, and analysis was performed in the transition zone. For the cortical cell length, the cortical cell layer below the epidermis of both sides was selected as this was the most visible cell layer in the root tip. The cell lengths were measured from the first observable cell after the quiescent center and averaged with the cell at the same developmental stage of the other side of the root. For cortical cell width, 10 random cells in all cortical layers were measured and averaged.

m) Degradation assay in *Nicotiana benthamiana*

Nicotiana benthamiana leaves were transiently transformed by infiltration with *Agrobacterium tumefaciens* strain AGL1 as described in (Yano et al., 2008 PNAS). Plasmids contained in *A. tumefaciens* were constructed by golden gate cloning (Binder et al., 2015) as indicated in (Table 5) from genes sequences amplified using Phusion PCR according to standard protocols and using primers indicated in (Table 4). Sequential scanning for the green (excited: 488 nm, detected: 500-550 nm) and red fluorescence (excited: 561 nm, detected: 570-625 nm) was carried out simultaneously with bright field image acquisition using a confocal microscope Leica SP5. Images were acquired using LAS AF software.

n) Seed 2D area measurement

Seeds were randomly placed into an empty petri-dish, paying attention that the seeds do not touch each other. After a high-resolution scan, images were transformed in grey-scale 8-bit. In Fiji, after threshold adjustment, the area was measured with the “analyze particle” tool.

o) Ethylene measurement

Seedlings were grown on plates, 7 days post-germination with if indicated 0.1µM AVG or 50µM silver-nitrate, and then, transferred into 25ml vials containing identical medium

with 0.2% gelrite. Vials were sealed with rubbers septa, and placed in a growth chamber at 24°C with 16-h-light/8-h-dark cycles. After 3 days, 1mL volume of air contained in the vial was injected by syringe in a Gas Chromatography VARIAN 3300. Ethylene peaks were recorded by an integrator Shimadzu CR6A chromatopac.

p) Treatment for gene expression analysis

For KAR responses, seedlings were placed for 2 hours in a solution of 1/2 Hoagland with 2.5µM PO_4^{3-} containing as indicated 1 or 3 µM karrikin1, karrikin2, rac-GR24 or equal amounts of the corresponding solvents. For ethylene inhibition responses, seedlings were grown 10 days on growth medium containing as indicated 0.1µM AVG or 50µM silver-nitrate.

q) Gene expression analysis

Plant tissue was harvested and rapidly shock-frozen in liquid nitrogen. RNA was extracted using the Spectrum Plant Total RNA Kit (www.sigmaaldrich.com). Residual DNA was removed by DNase I treatment (www.signaaldrich.com). RNA purity was tested by PCR. cDNA synthesis on 1µg of RNA was performed using the Superscript III kit (www.invitrogen.com). qPCR reactions were carried out either with a mix of SYBR Green I (Invitrogen S7563), GoTaq G2 polymerase and colorless GoTaq buffer (www.promega.com) or with a ready-mix EvaGreen (www.Metabion.com). qPCR reactions were run on an iCycler (Biorad, www.bio-rad.com) or on QuantStudio5 (applied biosystem, www.thermofisher.com). Thermal cycler conditions were: 95°C 2 min, 45 cycles of 95°C 15 sec, 60°C 15 sec, 72°C 20 sec, followed by a dissociation curve analysis. Expression values were calculated according to the ΔΔCt method (Marzec et al. 2016). Expression values were normalized to the expression level of the housekeeping gene *Ubiquitin*. For each condition 3 to 4 technical and biological replicates were performed. Primers are indicated in Table 7.

Table 7: qPCR primers.

Use	**Primers**	
qPCR *Ubiquitin*	Ubi F	ATGCAGATCTTCGTCAAGACCTTG
	Ubi R	ACCTCCCCTCAGACGAAG

qPCR *LjMAX2*	Sc302	GAATGTTACACCCTGAGGAAGC
	Sc303	TCAGGTTTGGGATCTTGAGG
qPCR *LjKAI2a*	Sc282	CGGTGCAGGAGTTTAGCAGA
	Sc283	TCCACAATAGACACGCCACC
qPCR *LjKAI2b*	Sc284	AAGAAAGACCTGGCGGTTCC
	Sc285	CCTCCGTTGACATGACCTCC
qPCR *LjDLK2*	MG027	CTCCTTGGTGCTTCTCCCAG
	MG028	AAAGCCGAAGCCAGTTTTCA
qPCR *LjD14*	D14_qPCR_F	ACAGCGTCCGAGAAAACTC
	D14_qPCR_R	AGCAATGGAGGCCAACTAC
qPCR *SMAX1*	Sc114	TGACAAGATTGCCAGTGGAG
	Sc115	CTAACCAGCAGCGAACAAGAC
qPCR *SMXL3a*	Sc138	GAAATTGCAAGCACCGTTTT
	Sc139	TCTGCGAAACTGCTCAGAGA
qPCR *SMXL3b*	Sc140	TCTCTGTGATGCCTTGGAGA
	Sc141	TCTTTGGCCTGAGAATCCAC
qPCR *SMXL4*	Sc142	CAAGAGAAGGGCTGAACTGG
	Sc143	AGGGATCGGCTATGGTTTCT
qPCR *SMXL6/7a*	Sc112	GAGGTAATGGCACAGATACTCG
	Sc113	AGGGTGGGTTTTCTGCTTAG
qPCR *SMXL6/7b*	Sc146	CCAAAGCATCAGTGCAGCTA
	Sc147	ACAAACCTTGCAACCAAAGG
qPCR *SMXL8*	Sc144	TGCATGGTTATCGGACAAGA
	Sc145	AGCTGGAAGGCACACTCCTA
qPCR *ERF* (*Lj2g3v1068730*)	Sc507	ACCTGAGTGCTTGAAGTTCAC
	Sc508	CCCTTGCTGCCATCATGTAC
qPCR *Germin-like* (*Lj3g3v2601420*)	Sc509	CCCTGGCCTTCAAATCCTTG
	Sc510	TGCCACCAAGAACACCCTTA
qPCR *Serotonin receptor* (*Lj4g3v0496580*)	Sc523	AGCACTGTCAAGCACTACCT
	Sc524	TCCACTACCCGTTGTTTCGA
qPCR *IAMT1-like* (*Lj2g3v3222870*)	Sc527	AACATTCCGGTTTATGCGCC
	Sc528	GCCCTGCCTACTTCACTAGC
qPCR *auxin-induced 5NG4-like* (*Lj6g3v2244450*)	Sc533	TGCGTCTGTTTTCAACCCTC
	Sc534	CCATGTACAAGCCACACACA
qPCR *coatomer subunit Beta-2-like (Lj3g3v0139630)*	Sc577	GGTCTGGAGAGAGTGTGGAG
	Sc578	TGGCAGCTTCCAGATTCAGT
qPCR *Lj0g3v0127589*	Sc575	CCAAACATGCTAACCGGTGT
	Sc576	CTTGCTTCTTGTGCTGTCCA

qPCR *CLAVATA3-like (Lj3g3v0428680)*	Sc581	AGTTCTGGCATTGCTTGTGG
	Sc582	GGTGACACTCTCTCAAGCCT
qPCR *P450 N-monooxoagenase2 (Lj3g3v0744710)*	Sc525	TGATGGCTTGAAGACCGTTG
	Sc526	TTGCGCCTTGATTTCCTTCA
qPCR *Salt-tolerance-like (Lj1g3v3370960)*	Sc519	TCCCTGGTTACTGCTTCGAA
	Sc520	CGAATGGCTAAGTTGAGGGG
qPCR *ACC Synthase (Lj2g3v0909590)*	Sc595	CGCTCGGAGGATGTCAAGTT
	Sc596	CCCTGCATTCCCTTCCAAGT
qPCR *ACC Oxidase (Lj3g3v0652730)*	Sc593	TGGTCCATTGCCTCAAGTCC
	Sc594	AGCATGTTCAATGGTCGCCT
qPCR *Expansin (Lj0g3v0287409)*	Sc601	CGGGGATGTGAAGGCTGTAT
	Sc602	CTGGTTTCTGAGGTCTGCGT
qPCR *Acid Phosphatase (Lj3g3v3640290)*	Sc591	GCTGTTATTGGCATGGCTGG
	Sc592	AACTGTCCTTAACTTCCCTGGT
qPCR *NBS-LRR (Lj4g3v3113360)*	Sc563	AGCCAGCTTTCACGGTAAAA
	Sc564	TAGTCACCAGCAACGCCATA
qPCR *Basic-leucine-zipper TF (Lj0g3v0268559)*	Sc561	TGATGCCATGGGAAGGAAAC
	Sc562	TCCAAACATGCATGCAGTGT
qPCR *somatic embryogenesis RLK1 (Lj0g3v0241899)*	Sc569	TGGATCTGTGTGGACCAGTC
	Sc570	GACACATGGAGGAGGAGGAG
qPCR *RLK (Lj6g3v1370760)*	Sc571	CTGGACAACTTGGGGAGCTA
	Sc572	GGCTTGGGAATTTCATCGGA
qPCR *Trichome birefringence-like 27 (Lj0g3v0194729)*	Sc535	AGAGGAAAGCAGCTCAAGGA
	Sc536	CACCCTTATCCCACGAACCT

r) Gene expression analysis by RNAseq

Root tissue was harvested and rapidly shock-frozen in liquid nitrogen. RNA was extracted using the Spectrum Plant Total RNA Kit (Sigma). DNA was removed by DNAse I treatment on column (Sigma). Residual DNA was removed by LiCl precipitation. The RNA purity was tested by PCR. The RNA quality was tested on an Agilent Bioanalyzer, and samples with RIN>6.7 were processed further. Libraries were created with TruSeq® Stranded mRNA LT (RS-122-2101, Illumina) after selection with AMPure XP beads (NEB). Sequencing was performed on a Highseq 2500 with 2x100bp paired-end (Illumina). Raw fastq files obtained from the sequencing facility were tested for quality with FastQC (Babraham Institute). Data were processed with quasi-transcript mapping approach in Salmon (Patro et al. 2017). Salmon operation

was carried out in Conda environment inside Linux terminal (https://anaconda.org/bioconda/salmon). Reads were mapped on the *L. japonicus* MG20 mRNA version 3.0 reference (Lotusjaponicus_MG20_v3.0_cdna.fa) downloaded from *LOTUS* BASE (Mun et al. 2016). Read counts were obtained for *L. japonicus* transcripts at the gene level. Read counts were further processed through tximport in R/Bioconductor (Soneson et al. 2015) for input into DESeq2 for data exploratory analysis and differential expression analysis (wild-type versus mutants), with FDR ≤ 0.01 and LogFC ≥ |0.5| thresholds. Heatmaps were prepared using the pheatmap package in R/Bioconductor (Soneson et al. 2015). AgriGO was utilized to find enriched GO terms for the differentially expressed genes (Du et al. 2010).

s) Protein alignment, phylogenetic tree, and synteny analysis

Protein sequences were retrieved using tBLASTn with *AtKAI2*, *AtDLK2, AtMAX2,* and *AtSMAX1,* against the NCBI database, the plantGDB database, and the Lotus genome V2.5 (http://www.kazusa.or.jp/lotus). The presence of *MAX2-like* was identified by tBLASTn in an in-house genome generated by next-generation sequencing using CLC Main Workbench (Pimprikar et al. 2016). Pea sequences were found by BLASTn on "Pisum sativum v2" database with AtKAI2 as query (https://www.coolseasonfoodlegume.org). The MAFFT alignment (https://mafft.cbrc.jp) of the protein sequences was used to generate a Maximum-likelihood tree with 1000 bootstrap replicates in MEGA7 (Kumar et al. 2016). For the synteny analysis of *MAX2* and *MAX2-like*, flanking sequences were retrieved from the same in-house genome.

t) Bacterial protein expression and purification

Full-length coding sequences were cloned into pE-SUMO Amp. Clones were sequence-verified and transformed into Rosetta DE3 pLysS cells (Novagen). Subsequent protein expression and purification were performed as described previously (Waters et al. 2015b), with the following modifications: the lysis and column wash buffers contained 10 mM imidazole, and a cobalt-charged affinity resin was used (TALON, Takara Bio).

u) Differential scanning fluorimetry

DSF assays were performed as described previously (Waters et al. 2015b). Assays were performed in 384-well format on a Roche LightCycler 480, with excitation 483 nm and emission 640 nm. Raw fluorescence values were transformed by calculating the first derivation of fluorescence over temperature. These data were then imported into GraphPad Prism 8.0 software for plotting. Data presented are the mean of three super-replicates from the same protein batch; each super-replicate comprised four technical replicates at each ligand concentration. Experiments were performed at least twice.

v) Protein modeling

Protein 3D structures were modeled using SWISS-MODEL tool (https://swissmodel.expasy.org) with the *A. thaliana* KAI2 (4JYM) templates.

w) AM inoculation

Pots were prepared with a sand-vermiculite mix (2:1) containing a layer of 500 *Rhizophagus irregularis* DAOM197198 (Agronutrition) spores per plant. Plantlets were then transferred from plates to pots (5-7 per pot) and grown at 24˚C, 60% humidity, with 16h-light-8h-dark cycles. Pots were fertilized once a week with 30 mL of modified half-strength B&D (reference) containing 5 µM phosphate and watered twice a week with a 1:1 mix of tap and deionized water. After 6 weeks post-inoculation, plants were harvested for fungal colonization quantification.

x) AM quantification

Prior to quantification, in the case of hairy-root transformation, transformed roots expressing the mCherrry transformation marker were separated from non-transformed roots by fluorescence microscopy (Leica MZ16 FA). Fungal structures in colonized roots were stained with the acid-ink method (Vierheilig et al. 1998). Root length colonization was quantified using the gridline intersect method (McGonigle et al. 1990) on a light microscope (Leica, 020-518500 DM/LS) with 10 to 20 root pieces.

y) Wheat-germ-agglutinin staining

Roots were placed in 50% ethanol for 4 hours, before being soaked for 2 days in a 20% KOH solution. After 3 washes with water, roots were acidified in a 0.1M HCl solution for 2 hours. Then, roots were gently washed with PBS (phosphate-buffered saline) and incubated in dark for a minimum of 6 hours in a PBS solution containing 2 µg/mL wheat-germ-agglutinin-AlexaFluor488. Imaging was performed with a GFP filter on a fluorescent microscope (Leica DMI6000B).

z) Statistical analysis

Statistical analyses were performed using Rstudio (www.rstudio.com). For equal variance, gene expression data were log-transformed prior to analysis. Statistical results from the ANOVAs are indicated in Table 8.

Table 8: Results of statistical analysis.

Figure	Condition	P value	F value
Fig 1.4.a	-	≤ 0.001	$F_{14/1438} = 125.3$
Fig 1.4.b	-	≤ 0.001	$F_{11/132} = 45.6$
Fig 1.5.b	*KAI2a*	≤ 0.001	$F_{5/18} = 39.5$
	KAI2b	≤ 0.001	$F_{5/18} = 33.7$
Fig 1.6.b	-	≤ 0.001	$F_{6/103} = 35$
Fig 1.7	-	≤ 0.001	$F_{6/605} = 26.5$
Fig 1.8	KAR_1	≤ 0.001	$F_{3/396} = 33.1$
	KAR_2	≤ 0.001	$F_{3/390} = 16.5$
	rac-Gr24	≤ 0.001	$F_{3/392} = 35$
Fig 1.9.left	WT	≤ 0.001	$F_{2/313} = 30$
	kai2a-1	= 0.08	$F_{2/234} = 2.51$
	kai2b-1	≤ 0.001	$F_{2/302} = 29.3$
	kai2b-3	≤ 0.001	$F_{2/308} = 14.2$
	kai2a-1 kai2b-1	= 0.99	$F_{2/272} = 0.01$
Fig 1.9.right	WT	≤ 0.001	$F_{2/246} = 51$
	d14-1	≤ 0.001	$F_{2/260} = 74.3$
	max2-4	= 0.25	$F_{2/204} = 1.38$
Fig 1.10.a	-	≤ 0.001	$F_{4/10} = 148$
Fig 1.10.b	WT	≤ 0.001	$F_{3/8} = 28.4$
	kai2a-1	≤ 0.001	$F_{3/8} = 53$
	kai2b-3	≤ 0.001	$F_{3/8} = 26$
	kai2a-1 kai2b-1	≤ 0.001	$F_{3/8} = 105.8$
	max2-4	= 0.99	$F_{3/8} = 0.04$
Fig 1.11.a	WT (Ler)	≤ 0.001	$F_{2/311} = 244$
	kai2-2	= 0.18	$F_{2/300} = 1.71$
	AtKAI2 #1	≤ 0.001	$F_{2/122} = 31.9$
	AtKAI2 #3	≤ 0.001	$F_{2/303} = 116.4$
	LjKAI2a #10b	≤ 0.001	$F_{2/316} = 65.7$

	LjKAI2a #11b	≤ 0.001	$F_{2/313} = 42$
	LjKAI2b #1b	≤ 0.001	$F_{2/296} = 33.4$
	LjKAI2b #5b	≤ 0.001	$F_{2/288} = 87.4$
Fig 1.11.b	WT (Col)	≤ 0.001	$F_{2/311} = 158.3$
	K02821	≤ 0.001	$F_{2/353} = 100.3$
	WT (Ler)	≤ 0.001	$F_{2/384} = 499.6$
	htl-2	≤ 0.05	$F_{2/391} = 3.2$
	#18	≤ 0.001	$F_{2/383} = 104.8$
	#23	≤ 0.001	$F_{2/253} = 127$
Fig 1.11.c	WT (Col)	≤ 0.001	$F_{2/415} = 1008$
	d14-1 kai2-2	= 0.22	$F_{2/353} = 1.54$
	LjKAI2a #32	≤ 0.001	$F_{2/287} = 50$
	LjKAI2a #46	≤ 0.001	$F_{2/184} = 85$
	LjKAI2b #29	≤ 0.001	$F_{2/283} = 9.4$
	LjKAI2b #31	≤ 0.05	$F_{2/244} = 3.9$
Fig 2.2.a	Total	≤ 0.01	$F_{3/32} = 6.51$
	Hyphopodia	≤ 0.05	$F_{3/32} = 3.38$
Fig 2.3	-	≤ 0.001	$F_{6/63} = 6.24$
Fig 2.4	-	≤ 0.001	$F_{2/17} = 11.6$
Fig 3.1.a	KAR_1 PRL	≤ 0.001	$F_{3/209} = 7.40$
	KAR_1 PER	≤ 0.001	$F_{3/209} = 11.1$
	KAR_1 PER density	≤ 0.01	$F_{3/209} = 5.51$
	KAR_2 PRL	= 0.51	$F_{3/217} = 0.77$
	KAR_2 PER	= 0.18	$F_{3/217} = 1.64$
	KAR_2 PER density	= 0.72	$F_{3/217} = 0.44$
	rac-GR24 PRL	= 0.74	$F_{3/203} = 0.42$
	rac-GR24 PER	= 0.07	$F_{3/203} = 2.45$
	rac-GR24 PER density	= 0.43	$F_{3/203} = 0.92$
Fig 3.1.b	-	≤ 0.01	$F_{3/188} = 4.1$
Fig 3.3.a	WT	≤ 0.001	$F_{2/9} = 30.7$
	max2-4	= 0.20	$F_{2/9} = 1.97$
Fig 3.9.b	-	≤ 0.001	$F_{4/10} = 113.2$
Fig 3.9.c	*SMAX1*	≤ 0.001	$F_{4/10} = 80.6$
	SMXL3a	≤ 0.001	$F_{4/10} = 21.2$
	SMXL3b	≤ 0.001	$F_{4/10} = 15.8$
	SMXL4	≤ 0.05	$F_{4/10} = 5.84$
Fig 3.10.b	PRL	≤ 0.001	$F_{2/106} = 39.3$
	PER	= 0.26	$F_{2/106} = 1.37$
	PER density	≤ 0.001	$F_{2/106} = 20.3$
Fig 3.10.c	PRL	≤ 0.001	$F_{2/69} = 10.4$
	PER	≤ 0.001	$F_{2/69} = 8.1$
	PER density	≤ 0.001	$F_{2/69} = 23.8$
Fig 3.11.b	-	≤ 0.01	$F_{2/19} = 8.47$
Fig 3.11.c	-	≤ 0.001	$F_{2/19} = 12.5$
Fig 3.12.b	-	≤ 0.001	$F_{2/225} = 315.3$
Fig 3.12.c	-	≤ 0.01	$F_{2/9} = 8.4$
Fig 3.12.d	-	= 0.054	$F_{2/9} = 4.12$

Fig 3.13.a	-	≤ 0.001	$F_{4/28} = 21.3$
Fig 3.13.b	-	≤ 0.001	$F_{4/28} = 36.1$
Fig 3.14.a	PRL	≤ 0.001	$F_{5/319} = 272.3$
	PER	≤ 0.001	$F_{5/319} = 66.3$
	PER density	≤ 0.001	$F_{5/319} = 28.8$
Fig 3.14.b	PRL	≤ 0.001	$F_{3/136} = 87.4$
	PER	≤ 0.001	$F_{3/136} = 17.5$
	PER density	≤ 0.001	$F_{3/136} = 22$
Fig 3.17	*DLK2*	≤ 0.001	$F_{4/14} = 230.7$
	Coatomer-subunit-beta-2-like	≤ 0.001	$F_{4/14} = 21.3$
	Unknown	≤ 0.001	$F_{4/14} = 83.3$
	CLAVATA 3-like	≤ 0.001	$F_{4/14} = 48.1$
	Germin-like	≤ 0.001	$F_{4/14} = 36.9$
	Serotonin receptor	≤ 0.001	$F_{4/14} = 123.6$
	Salt tolerance-like	≤ 0.001	$F_{4/14} = 240.7$
	IAMT1-like	≤ 0.001	$F_{4/14} = 54.3$
	P450 82C4-like	≤ 0.001	$F_{4/14} = 17.2$
	Auxin induced 5NG4-like	≤ 0.001	$F_{4/14} = 60.9$
	Expansin	≤ 0.001	$F_{4/14} = 28.2$
	Acid Phosphatase	≤ 0.001	$F_{4/14} = 22.2$
	ERF	≤ 0.001	$F_{4/14} = 2516$
	ACS	≤ 0.001	$F_{4/14} = 39.7$
	ACO	≤ 0.001	$F_{4/14} = 12.5$
	Trichome birefringence-like 27	≤ 0.001	$F_{4/14} = 20.4$
	NBS-LRR	≤ 0.001	$F_{4/14} = 80.1$
	Basic-leucine zipper TF	≤ 0.001	$F_{4/14} = 515.6$
	Somatic-embryogenesis RLK1	≤ 0.01	$F_{4/14} = 5.42$
	RLK	≤ 0.001	$F_{4/14} = 31.9$
Fig 3.18.a	-	≤ 0.001	$F_{2/15} = 51.5$
Fig 3.18.b	-	≤ 0.001	$F_{8/36} = 174.9$
Fig 3.19.a	PRL	≤ 0.001	$F_{5/286} = 74$
	PER	≤ 0.001	$F_{5/286} = 7.8$
	PER density	≤ 0.001	$F_{5/286} = 24.8$
Fig 3.20.b	PRL	≤ 0.001	$F_{5/169} = 73.3$
	PER	≤ 0.001	$F_{5/169} = 26.2$
	PER density	≤ 0.001	$F_{5/169} = 30.7$
Fig 3.21.b	-	≤ 0.001	$F_{5/43} = 19.1$
Fig 3.21.c	-	≤ 0.001	$F_{5/42} = 122.6$
Fig 3.23	*Germin-like*	≤ 0.001	$F_{5/12} = 11.5$
	IAMT1-like	≤ 0.001	$F_{5/12} = 18.8$
	Auxin-induced 5NG4-like	≤ 0.001	$F_{5/12} = 27.9$

	Expansin	≤ 0.001	$F_{5/12} = 18.9$
	DLK2	≤ 0.001	$F_{5/12} = 148.3$
	ERF	≤ 0.001	$F_{5/12} = 22.3$
	Lj0g3v0127589	≤ 0.001	$F_{5/12} = 57.6$
	Serotonin receptor	≤ 0.001	$F_{5/12} = 47.8$
Fig 3.24	*Germin-like*	≤ 0.001	$F_{5/12} = 12.5$
	IAMT1-like	≤ 0.001	$F_{5/12} = 24.2$
	Auxin-induced 5NG4-like	≤ 0.001	$F_{5/12} = 20$
	Expansin	≤ 0.001	$F_{5/12} = 113.1$
	DLK2	≤ 0.001	$F_{5/12} = 283.8$
	ERF	≤ 0.001	$F_{5/12} = 109.8$
	Lj0g3v0127589	≤ 0.001	$F_{5/12} = 49.3$
	Serotonin receptor	≤ 0.001	$F_{5/12} = 23.1$
Fig 3.25	*DLK2*	≤ 0.001	$F_{5/18} = 137.6$
	ERF	≤ 0.001	$F_{5/18} = 56.1$
	Serotonin receptor	≤ 0.001	$F_{5/18} = 72.4$
	Lj0g3v0127589	≤ 0.05	$F_{5/18} = 4.17$
	ACS	≤ 0.01	$F_{5/18} = 6.1$
	Germin-like	= 0.65	$F_{5/18} = 0.67$
Fig 3.26	*DLK2* WT	≤ 0.01	$F_{2/9} = 14.6$
	DLK2 max2-4	= 0.73	$F_{2/9} = 0.32$
	ERF WT	≤ 0.001	$F_{2/9} = 38.5$
	ERF max2-4	= 0.83	$F_{2/9} = 0.19$
	ACS WT	≤ 0.05	$F_{2/9} = 5.08$
	ACS max2-4	= 0.34	$F_{2/9} = 1.22$

IX. Discussion

1) KL signaling and hypocotyl elongation

KL signaling is known in Arabidopsis and rice, to inhibit hypocotyl and mesocotyl elongation, respectively (Nelson et al. 2011; Waters et al. 2012; Gutjahr et al. 2015). Since these two species are evolutionary quite distinct from each other but have both retained a function of KL signaling in inhibiting the growth of similar organs, it can be assumed that this function would be conserved among a large number of plant species. Surprisingly, in *L. japonicus*, no elongated hypocotyl phenotype is observed in the single KL receptors mutants used in this study, neither for the *kai2a-1 kai2b-1* mutant nor for the two allelic *max2* mutants tested (Fig 1.7). The strong repression of the well-known KAR marker *DLK2* in these mutants (Fig 1.9) and the robust *max2* shoot branching phenotype (Fig 1.6), indicate that they are real knock-out mutants, and it is unlikely that some KL signaling is still occurring. *De facto*, we can also exclude any major function of SL signaling in hypocotyl development in *L. japonicus*. Notably, under sub-optimal conditions, with a growth medium with low phosphate levels and without sugar supplement, used to test responsiveness to KAR, the hypocotyl length was, in general, shorter than the wild-type, which could be explained by overall smaller seeds (data not shown). Also, hypocotyl elongation is regulated by light and several hormones (auxin, ethylene, gibberellic acid) (Collett et al. 2000), with KL signaling presumably acting as one of their modulators. The diversity in light optima among plants and the complexity of hormone signaling interactions increase the scope for functional diversification in different plant species. In pea, in which SL signaling function has been extensively studied, there is to my knowledge no information in the literature concerning an eventual hypocotyl phenotype of the *rms4/max2* mutant. However, pea is a hypogeal plant, in which the epicotyl has a major role in seedling development to reach the light, therefore it is not always comparable. To confirm the widespread function of KL signaling in photo-morphogenesis in the angiosperms, with maybe an exception in legumes, would be essential to look at the KL perception mutants in other legumes, like *M. truncatula*, and in Solanaceae species like tomato, potato or petunia.

Despite the absence of hypocotyl phenotype in KL perception mutants, *L. japonicus* hypocotyl responds to KAR (Fig 1.8 and 1.9). The developmental response to KAR_1 requires *KAI2a* and *MAX2*, indicating that the KL pathway has the potential to inhibit hypocotyl elongation. Therefore, it is possible that in our tested conditions, no significant amounts of KL ligand are present in the hypocotyl tissue, preventing the observation of a longer hypocotyl phenotype in the KL receptor mutants. Also, *KAI2b* is not required for the transcriptional and developmental hypocotyl response to KAR_1 in *L. japonicus*, although being able to mediate KAR_1 responses in roots. Possibly, *KAI2b* is not sufficiently expressed in hypocotyl (Fig 1.3b) or in different cells than *KAI2a* required for the responses, demonstrating the functional divergence of the two paralogs.

2) Receptor specificity and ligand diversity

a) Determinants of ligand perception

Two *KAI2* copies remained functional in *L. japonicus* after a duplication which occurred before the legumes diversification, suggesting a positive selection pressure on the two genes and their functional divergence. Indeed, they show specificity in ligand perception with *KAI2a* mediating responses to KAR_1, KAR_2, and $GR24^{ent\text{-}5DS}$, whereas *KAI2b* responds preferentially to KAR_1 and hardly to KAR_2. This specificity is due to very few residues inside the pocket, as their ligand specificity towards $GR24^{ent\text{-}5DS}$ can be reversed with the exchange of only three amino acids. In parasitic weeds, multiple gene duplications of the KL receptor has occurred, followed by a neo-functionalization (Conn et al. 2015). The authors reported that substitution of 4 residues in the cavity by smaller hydrophobic amino acids have modified their ligand-binding specificity, to allow them to perceive the SLs in host-root-exudates (Conn et al. 2015). In the weed *Brassica tournefortii*, it has been reported that the two KAI2 copies have different preferences towards KARs and GR24, which are determined by two different amino acids in their binding pocket changing the hydrophobicity of the cavity (Sun et al. 2019). Interestingly, the residues determining the ligand specificity are different between *L. japonicus* and *B. tournefortii*, implying strong plasticity of these receptors. These

reported independent events indicate that upon duplication, one of the KAI2 copy is likely to evolve and gain specificity towards ligand recognition.

b) Organ-specific perception of KARs

L. japonicus responds transcriptionally and developmentally to treatments with diverse KAR molecules, in hypocotyls and roots. However, our results demonstrate different levels of specificity in the response, which are dependent on the receptors but also on the organs. Despite triggering responses in the hypocotyl, KAR_2 treatments did not generate any developmental or transcriptional responses in the root, regardless of the capacity of *KAI2a* in mediating KAR_1 responses in this tissue and mediating KAR_2 responses in hypocotyl. These results indicate that the effect on root architecture is a local response likely through local perception, independent of the hypocotyl response and independent of receptor-ligand specificity. The discrepancy in response to different KAR molecules among different plant organs has to our knowledge never been previously observed. However, this inconsistency could explain why a transcriptomic analysis of KAR_2-treated rice roots found no differentially expressed genes, whereas rice mesocotyl could developmentally respond to KAR_2 (Gutjahr et al. 2015). The absence of binding of KARs to AtKAI2 in DSF-assay suggests that the receptors do not directly perceive KARs, but first, need to be metabolized (Waters et al. 2015b). Therefore, it is possible that the enzymes involved in KAR metabolism differ between hypocotyls and roots and have different substrate-specificities. Also, the transport of the KAR_2-derived metabolic product could be limited in the root system. Finally, specific catabolism for KAR_2-derivatives might occur in the root, limiting the response due to decreasing amounts of the ligand. This organ specificity response is an important discovery for the design of future experiments in *L. japonicus* but also in other plants.

c) Several KL molecules *in planta*?

Phytohormone classes are often composed of multiple endogenous active molecules. For example, 3 molecules are commonly regarded as endogenous auxins (Enders and Strader 2015), whereas 4 bioactive GAs are found *in planta* (Shinjiro 2008). In the case of Strigolactones, the diversification is extreme with more than 25 SLs identified in different plant species, with one species producing usually many different SLs and

different SL cocktails being produced by different plants (Abe et al. 2014; Charnikhova et al. 2017; Kohlen et al. 2013; Yoneyama et al. 2015). Most SLs were discovered in roots or in root exudates, where they act as stimulants of AM fungi. In this condition, the SL diversification is possibly a way for the plants to selectively promote the AM symbionts or other rhizosphere microbes and avoid recognition from parasitic plants (Wang and Bouwmeester 2018). Although, it is still unclear if all exuded SLs plays an additional role in plant development.

The multiplicity of bioactive molecules per class of phytohormones is mirrored in their perception, with a diversification of the receptors. In the case of auxin, there are 6 homologs of the TRANSPORT INHIBITOR1 / AUXIN-SIGNALLING F-BOX PROTEINS (TIR1/AFB) family in Arabidopsis (Mockaitis and Estelle 2008). It is postulated that the different members of this family have distinct auxin specificities, and associated with a particular set of Aux/IAA repressors, it would allow the plant to fine-tune auxin responses (Enders and Strader 2015; Mockaitis and Estelle 2008; Simon and Petrášek 2011). Similarly, the GA receptor GIBBERELLIN INSENSITIVE DWARF1 (GID1) is present in 3 functional and partially redundant copies in Arabidopsis (Sun 2011). Surprisingly, their ligand selectivity was similar towards bioactive GAs and solely differed in the binding affinity (Nakajima et al. 2006). However, evolutionary studies revealed that in eudicots, one type of GID1 showed higher nonsynonymous-to-synonymous divergence in the region determining GA_4 affinity, suggesting ongoing receptor selection in binding preference for certain GAs (Yoshida et al. 2018).

Concerning KL, our results demonstrated that the duplication of the KAR receptor has led to their sub-functionalization in *L. japonicus*, with different organ expression profiles and more interestingly a specificity in ligand perception. This result could reflect the presence of several endogenous ligands KL(s), which would be perceived specifically by the two receptors possibly to control different developmental functions. Further, the presence of multiple KL molecules with complex biosynthesis pathways could also explain why forward genetic screens failed so far to discover the genes involved in their production. The major challenge in the field remains to find the endogenous KL molecule(s), and its (their) biosynthesis pathway(s).

3) KL function in AMS

a) A *L. japonicus* or legume specificity?

In this thesis, we investigated the role of KL signaling in AMS in *L. japonicus.* KL signaling mutants have a reduction of colonization corresponding to half of the wild-type level. This phenotype is close to the described *rms4/max2* in pea, which also had a 50% reduction of AM colonization (Foo et al. 2013). In contrast, in Petunia and rice, perception components of KL signaling were described as crucial for the establishment of AMS, especially for early stages (Gutjahr et al. 2015; Liu et al. 2019). Experimental conditions, like harvesting time, inoculum strength or nutrient conditions, are factors which are unlikely to explain these important differences. Thus, the function of KL signaling during AMS emerges as species-specific or more likely phylogenetic-group-specific. Analysis of KL perception mutant in other species will give additional information on the conserved function of KL signaling in AMS.

Phylogenetic analyses revealed that the perception components of KAR signaling, *MAX2,* and *KAI2*, are present in Charales, prior to the land colonization and AMS (Bythell-Douglas et al. 2017). Therefore, a tempting hypothesis is that the function of KL signaling in AMS was acquired early in evolution, and possibly participated in the conquest of lands by plants. With the advent of CRISPR-Cas9 and the improvement of transformation techniques, basal plants, which are susceptible to AM fungi such as *Marchantia paleacea* or *Lunularia cruciata*, could be used to test this hypothesis (Ishizaki et al. 2015).

b) A local requirement of KL signaling

In *L. japonicus*, AM colonization of *max2* was rescued to wild-type level when expressing *MAX2* in roots under its own promoter (Fig 2.3). In contrast, the non-transformed roots from the same *max2* plants showed low levels of colonization. This result indicates that *MAX2* mediated signaling is required locally for optimal root colonization by AM fungi. By extension, it indicates that no root to root, or shoot to root communications are involved downstream of *MAX2* mediated signaling to regulate AMS. In Arabidopsis, the increased adventitious root number of *max2* has been shown

to be rescued by ectopic expression of *MAX2* in xylem (Rassmussen et al., 2012). A partial rescue was also observed when *MAX2* was expressed under phloem and procambium specific promoters (Rassmussen et al., 2012). Adventitious roots are originated from pericycle tissue, suggesting that *MAX2* mediated signaling can act in a non-cell autonomous to regulate adventitious root formation. This conclusion was then confirmed with the expression of *MAX2* under endodermal promoter which rescued the sensitivity of *max2* mutant to rac-GR24 in regulating lateral root formation but also root-hair elongation (Koren et al. 2013). Similarly, tissue-specific promoters could be used to define in which root tissue *MAX2* is required for AM colonization.

c) Downstream of KL signaling in control of AMS

Despite phenotypic variation in different species, the positive function of KL signaling in AMS discovered in rice (Gutjahr et al. 2015) and suggested in pea with the lower colonization of *max2* (Foo et al. 2013), is now also observed in petunia (Liu et al. 2019) and *L. japonicus*. All these observations are based solely on the use of mutants of the KL perception complex. The involvement of the downstream elements of the signaling pathway has not been tested so far. Since there is no evidence of SMAX1-degradation-independent signal transduction to mediate KL responses, SMAX1 is likely a negative regulator of AMS, and thus the absence of SMAX1 is expected to support higher root colonization by AM fungi. Accordingly, a *smax1* mutation should suppress the root colonization phenotype of the *kai2* and *max2* mutants. In theory, expression of a gain of function resistant to degradation SMAX1, alike *d53*, would lead to a decrease in root colonization by AMF. In a long-term perspective, mutated SMAX1 versions could become a tool to promote or inhibit AMS.

The different phases of AMS are accompanied by massive cell-autonomous transcriptional reprogramming (reviewed in (Pimprikar and Gutjahr 2018)). Many transcription factors (TF) from different families, sometimes associated in multimeric complexes (Pimprikar et al. 2016; Floss et al. 2017), have been discovered to be important and even specialized in AMS (reviewed in (Pimprikar and Gutjahr 2018)). Yet, the research focused mainly on GRAS TF, but three members of the ERF / AP2-Domain Transcription Factors family (WRINKLED 5) were shown in *M. truncatula* to promotes fatty-acid biosynthesis and transport for the symbiont (Jiang et al. 2018; Luginbuehl et al. 2017) suggesting that other undiscovered members of this family

could play a role during AMS. The new KL marker gene *ERF* encoding a transcription factor could be a major regulator interconnecting symbiosis and KL signaling. Supporting this hypothesis and consistent with genes involved in AMS (Delaux et al. 2013), phylogenetic analysis (data not shown) revealed the absence of homologous *ERF* in the AM-incompetent species Arabidopsis. Also, ERF shares high homology with ERN1 (Ethylene Response Factor Required for Nodulation 1), a TF required for the RNS (Cerri et al. 2017; Kawaharada et al. 2017), which suggest a function in symbiosis due to the high overlap in signaling components observed between the two type of symbiosis (Parniske 2008). Root colonization of the *erf* mutant and, similarly to the approach used in Pimprikar et al. 2016 (Pimprikar et al. 2016), analysis of the potential induction of AM marker genes in non-inoculated roots ectopically expressing ERF could reveal a potential function of ERF in AMS.

Intriguingly, AMS is known to promote root-hair elongation and density (Chun-Yan Liu et al., 2018 Scientific report), as well as lateral root growth and density (Gutjahr and Paszkowski 2013). Thus, there is a correlation in root developmental responses between KL signaling and AMS, suggesting that KL signaling could influence AMS through regulation of ethylene signaling. However, ethylene was shown to have an inhibitory effect on early transcriptional responses to spores exudates as well on intraradical colonization (Mukherjee and Ané 2011; Martín-Rodríguez et al. 2011). Further, rice *kai2/d14l* mutant, despite being impaired in root colonization, had root architecture changes in response to AMF (Chiu et al. 2018). Therefore, the positive function of KL signaling on AMS is unlikely due to an increase in ethylene signaling.

Plants control the degree of AM colonization depending on their nutritional status (Carbonnel and Gutjahr 2014). Under high phosphate supply, AM development is repressed at early developmental stages (Balzergue et al. 2011; Balzergue et al. 2013; Breuillin et al. 2010). Biosynthesis and exudation of SL are known to be induced by phosphate starvation (Yoneyama et al. 2007; Breuillin et al. 2010; Balzergue et al. 2013; Balzergue et al. 2011; Lopez-Raez et al. 2008) but exogenous application of GR24 failed to rescue the root colonization under high phosphate availability (Balzergue et al. 2011; Breuillin et al. 2010), indicating that low level of SL exudation is not the main reason for low AM colonization. Due to the common origin of SL and KL signaling, an attractive idea is that KL could mediate phosphate homeostasis signals. Supporting this hypothesis, in our RNAseq analysis, one phosphate transporter (*Lj1g3v4483780*) and three genes coding for proteins with SPX-domain

(*Lj0g3v0310179, Lj0g3v0064419, Lj1g3v2626310*), a sensor of phosphate homeostasis (reviewed in (Jung et al. 2018)), were found to be specifically induced in the *smax1* mutants. Similarly, a homologous gene of the SL exporter *PLEITROPIC DRUG RESISTANCE 1* (*PDR1*, *Lj1g3v1914990*), important for AM colonization in Petunia (Kretzschmar et al. 2012), was induced in the *smax1* mutants. Further analysis on the relation between phosphate homeostasis and KL signaling would be an interesting topic of research in the near future.

4) KL and ethylene signaling to control root development

a) KL signaling affects root architecture development

Species preferences towards different KARs have been described in the literature for seed germination (Chiwocha et al. 2009). In our hands, *L. japonicus* roots respond transcriptionally and developmentally to KAR_1, but not to KAR_2. This root response is mediated by *KAI2* and *MAX2*, indicating for the first time that KL signaling can affect root architecture development (Fig 3.2). KAR_1 treatment leads to a shorter primary root and an increase in post-embryonic root number. It is, however, unclear if KL signaling is involved directly in the two effects. Indeed, the arrest of primary root growth could also induce lateral root formation, as it is known for several decades (Torrey 1950). Previous to this thesis nothing was known about the function of KL signaling in root development; in contrast, several analyses described a function of SL in roots. SL biosynthesis and perception mutants display increased adventitious root number in pea and Arabidopsis (Rasmussen et al. 2012). Accordingly, treatment with GR24 reduces the number of adventitious roots in the same species (Rasmussen et al. 2012). rac-GR24 was also shown to increase primary root length in Arabidopsis (Ruyter-Spira et al. 2011) and rice crown-root length (Arite et al. 2012). Lateral root density is also decreased in Arabidopsis and Medicago by rac-GR24 treatment at low phosphate levels (Ruyter-Spira et al. 2011; Jiang et al. 2016; De Cuyper et al. 2015). In summary, SL signaling appears as a positive regulator of primary root growth, and a negative regulator of lateral and adventitious root development. In roots, the known SL function would oppose the observed effects of KAR treatment in *L. japonicus*. However, rac-

GR24 treatment, even at high concentrations, neither affected primary root length nor post-embryonic root number in *L. japonicus* (Fig 3.1). Nevertheless, Lotus roots were still able to respond transcriptionally to rac-GR24 leading to the transcriptional activation of *DLK2* (Fig 3.3). This surprising result indicates that *DLK2* is likely not involved in the root developmental response, and suggest that specific downstream responses to KAR_1 treatment should occur. Also, a different spatial distribution inside the plant of the hormone-like compounds, associated with a particular tissue involved in the developmental response, would explain this specific response to KAR_1 versus *rac*-GR24.

b) *SMAX1*, a single copy in *L. japonicus*

Loss-of-function mutants in phytohormone signaling repressors are powerful tools to understand better the role of the hormones in plant development or responses to biotic/abiotic stresses but their use is often limited by a high level of redundancy requiring higher-order mutants. For example in Arabidopsis, there are 29 AUX/IAAs and 5 DELLAs, auxin and gibberellin repressors, respectively (Gan et al. 2007; Luo et al. 2018). Also, in jasmonate signaling, the JAZ repressor family consists of 13 members in *A. thaliana*, from which the single mutants do not display strong phenotypes (Chini et al. 2016). Only mutants defective in multiple *JAZ* genes showed delayed growth and reproduction (Guo et al. 2018). Similarly, the three SL repressors found in Arabidopsis are functionally redundant (Soundappan et al. 2015). In KL signaling, the number of SMAX1 repressor copies is limited (Stanga et al. 2013), which is a real opportunity for quick and relatively easy reverse genetics in more complex organisms like *L. japonicus*.

Due to the effect of KAR treatment on root growth, we hypothesized that a KL repressor mutant which would mimic constitutive KL signaling would exhibit a root phenotype. Phylogenetic analysis revealed that SMAX1 and the SMXLs are distributed in four different well-conserved clades in the Angiosperms, with a single copy of SMAX1 in *L. japonicus* (Fig 3.4). This unique *LjSMAX1* copy is ubiquitously expressed in leaf, stem, flower, and root (Fig 3.5) suggesting pleiotropic functions in plant development. When ectopically expressed in *N. benthamiana* leaves, SMAX1-GFP, like the other SMXLs, localized in the nucleus (Fig 3.6). Nuclear localization of phytohormone signaling repressors is expected as they possess an EAR motif (Ethylene-responsive element

binding factor-associated amphiphilic repression), which allow interaction with TOPLESS proteins for direct transcriptional repression by chromatin compacting (reviewed in (Kagale and Rozwadowski 2014)). This mechanism is conserved in many hormonal signaling pathways like auxin, jasmonic acid, brassinosteroids and SL (Pauwels et al. 2010; Shyu et al. 2012; Tiwari et al. 2004; Oh et al. 2014; Ma et al. 2017). The specific degradation of SMAX1 when co-expressed with KAI2a and KAI2b (Fig 3.6), in a MAX2 dependent-manner (Fig 3.7) confirmed that SMAX1 is a specific target of the KL perception components, likely leading to its ubiquitination followed by proteasomal degradation (Jiang et al. 2013; Zhou et al. 2013).

c) *SMAX1* a gene with pleiotropic roles

The two *L. japonicus smax1* mutant alleles present several developmental phenotypes, exposing *SMAX1* as a gene with pleiotropic functions. Particularly, *smax1* mutants stably displayed a short primary root without a decrease in PER number (Fig 3.10 and 3.14). This phenotype is associated with a perturbation of cortical cell-elongation in the RAM (Fig 3.12), and long root-hairs (Fig 3.11). In Arabidopsis, where *SMAX1* was discovered, no root developmental phenotype was described for the mutant (Stanga et al. 2013; Soundappan et al. 2015). Recently in Arabidopsis, similarly to Lotus, the KL repressor mutant was shown to have a root-hair phenotype (Villaecija Aguilar et al. 2019), whereas *kai2* and *max2* present less and shorter root-hairs (Villaecija Aguilar et al. 2019; Kapulnik et al. 2011; Koren et al. 2013). *SMAX1* is duplicated in Arabidopsis, with a close homolog *SMXL2* which has been described to be partially redundant with SMAX1 (Stanga et al. 2016). However, the Arabidopsis double mutant *Atsmax1 smxl2* have similar root length than the wild-type (personal communication from José Villaecija-Aguilar). This result suggests species specificity functions or ethylene biosynthesis influence of *SMAX1* in plant development. Description of *smax1* mutants in other species will be required to determine if the promoting function of *SMAX1* in root development is common or peculiar in land plants.

d) What is the KL biosynthesis pathway?

To gain indications of downstream pathways affected by KL signaling, we performed an RNAseq analysis. Despite a substantial overlap in DEG between perception and

repressor mutants (Table 3.2), the results were surprising. Indeed, we speculated that opposite regulation would be observed, but occurred only for few DEGs which included the known KAR marker gene *DLK2* (Fig 3.17). To our knowledge, comparative transcriptional analysis between perception or biosynthesis versus repressor mutants of the same hormone has never been carried out. However, SL biosynthesis genes are known to be induced in *d14* and *max2* mutants due to a negative feedback loop of SL signaling on its biosynthesis (reviewed in (Dun et al. 2006)). In the RNAseq analysis, no genes following feedback loop mechanism could be found and possibly assigned to KL biosynthesis. Also, it is possible that in our tested conditions, the endogenous KL molecule is present in low amounts, which led to small variation of expression in KAR response genes between the wild-type and the KL perception mutants. In Arabidopsis *DLK2* transcripts accumulate at higher levels in dark-grown plants, indicating more KL signaling and possibly increase KL biosynthesis (Végh et al. 2017). Also, the organ is primordial for the visible feedback loop. Transcripts of SL biosynthesis genes were induced up to 75 fold in basal cauline internodes, compared to the 3 fold observed in hypocotyls of the same Arabidopsis *max2* mutant (Hayward et al. 2009). It is possible that KL biosynthesis might primarily occur in other organs than roots.

e) Ethylene is epistatic to KL

Nevertheless, our GO analysis revealed an enrichment of DEG related to another hormone: ethylene (Fig 3.16 and 3.17). Particularly, the expression of the ethylene biosynthesis enzymes *ACS* and *ACO* were upregulated in the *smax1* mutants (Fig 3.17). Supporting the GO analysis, these mutants were shown to release around 3 times more ethylene than the wild-type (Fig 3.18). Ethylene is known to affect the root system of many plant species, triggering shorter roots assorted of elongated root-hairs (reviewed in (Vandenbussche and Van Der Straeten 2012)), and inhibiting the root cell elongation in Arabidopsis (Ruzicka et al. 2007). In *L. japonicus* wild type, ethylene treatment caused the same responses producing a phenocopy of the *smax1* mutant root phenotypes (Fig 3.19). Upon inhibition of ethylene biosynthesis and perception, the root and root-hair phenotypes were rescued in the *smax1* mutants (Fig 3.21). In addition, ethylene signaling was required for root developmental responses to KAR_1 treatment (Fig 3.22). In Arabidopsis, it has been shown that GR24 treatment leads to

increase root-hair length in a *MAX2* dependent fashion, which was abolished in presence of AVG (Kapulnik et al. 2011). At that time, the authors concluded that ethylene was epistatic to SLs, but in the light of our results, ethylene is a major factor for developmental processes regulated by KL signaling.

f) A connection KL – ethylene, and auxin?

Ethylene is known to act on the root and root-hair development but is often associated in these effects with another hormone: auxin (reviewed in (Qin and Huang 2018; Muday et al. 2012). Auxin treatment also leads to a short primary root, higher lateral root density, and increased root-hair growth (reviewed in (Overvoorde et al. 2010)). Ethylene and auxin positively interact with each other at different levels, ethylene influences auxin biosynthesis and distribution (Ruzicka et al. 2007; Strader et al. 2010) and auxin stimulates ethylene biosynthesis (Tsuchisaka and Theologis 2004). The tight connection between auxin and ethylene is supported by a transcriptional analysis, which revealed a large overlap in response to the two hormones in Arabidopsis epidermal cells (Bruex et al. 2012). In the clade 6 of the GO analysis, which corresponds to the genes induced in *smax1* mutants, auxin responses are indeed also over-represented but at a lower extent than ethylene responses (Fig 3.16). These auxin-related responses are possibly due to the over-production of ethylene in the *smax1* mutants (Fig 3.18). But there is also a possibility that these responses are independent of ethylene signaling, and could even be causative of the increased ethylene biosynthesis. Interestingly, similar ongoing work in *A. thaliana*, suggested auxin transport to be influenced by KL signaling to control lateral root and root-hair development (Villaecija Aguilar et al. 2019). Further analyses will be required to shed light on the epistasis between ethylene and auxin downstream of KL signaling.

g) The ethylene independent response to the removal of SMAX1

Inhibition of ethylene biosynthesis and perception rescued root growth in *smax1* mutants, but also the expression of some genes differentially regulated between *smax1* mutant and the wild type (Fig 3.23 and 3.24), allowing to differentiate indirect effects from potential direct targets of KL signaling. Two of the tested genes rescued by ethylene inhibition, *IAMT1-like* and *Auxin-induced 5NG4-like*, are related to auxin

signaling. *IAMT1-like* codes for an *Indole-3-acetate O-methyltransferase 1,* which transforms IAA into Me-IAA, another bioactive form of auxin (Qin et al. 2005). The *Auxin-Induced 5NG4-like* encodes for a transmembrane protein related to Nodulin21 induced by IAA treatment (Busov et al. 2004). This result suggests that at least part of the auxin perturbation found in the GO analysis in the *smax1* mutants are an indirect effect of perturbed ethylene homeostasis. *Expansin* expression is also rescued by the inhibition of the biosynthesis of the ethylene precursor ACC and is known in *Arabidopsis* to be induced by ACC treatment and to be involved in root-hair elongation (Cho and Cosgrove 2002). However, several DEGs were shown to be ethylene independently regulated in the *smax1* mutants (Fig 3.23 and 3.24), including *DLK2* and *ERF* indicating that *ERF* although annotated as an *ETHYLENE RESPONSE FACTOR* gene, does not really act as such. These results indicate that regulation of ethylene signaling controls only part of the downstream responses to SMAX1 degradation. An additional transcriptomic analysis after inhibition of ethylene biosynthesis and perception in the *smax1* mutants would provide the magnitude of ethylene dependency downstream of SMAX1. Also, it would refine potential direct targets of KL signaling, which could be coupled with a ChIP-seq analysis with SMAX1 used as bait.

Formerly, a minimal number of KAR marker genes were discovered in Arabidopsis, and they were also shown to be induced by GR24 in a D14 dependent manner (Waters et al. 2012). In addition to *DLK2*, it was the case for *SALT TOLERANCE 7* (*STH7*) a B-box domain transcription factor, and *KAR-UP F-BOX 1* (*KUF1*) an F-box protein. In our RNAseq analysis, homologs of these genes in Lotus are either not differentially expressed in any mutants like *LjSTH7* (*Lj5g3v0165540*), or not strongly induced in the *smax1* mutants, with only 2-fold change for *LjKUF1* (*Lj2g3v1549980*). Our results showed that *DLK2* and *ERF*, which are ethylene independently regulated genes, are induced in roots by a short KAR_1 treatment (Fig 3.25), indicating that they are early KAR responses genes. In contrast to *DLK2,* which is a very well described KAR marker gene, this is the first-time that *ERF* is related to KL signaling. Despite several analyses, there is no clear function of *DLK2* in developmental responses to KAR (Végh et al. 2017), which indicates that downstream developmental responses are controlled by another primary target (s). Since *ERF* encodes a transcription factor, specifically induced by KAR_1 (Fig 3.26), it is possible that this protein is a key regulator of secondary KAR responses, which potentially includes the transcriptional activation of

ACS required for the biosynthesis of ethylene. Characterization of an *erf* mutant would provide meaningful elements of response to this hypothesis.

Altogether, our results show that KL signaling can influence root architecture development through the regulation of SMAX1, which acts as an inhibitor of ethylene signaling via the regulation of its biosynthesis (Fig 5). However, it remains unclear in which organ, tissue or even cell-type this regulation occurs, and how far downstream to KL signaling ethylene biosynthesis is situated. Collectively these results open new frontiers of research on the relation between KL and ethylene signaling and the transcriptional cascade responding to KL/KAR.

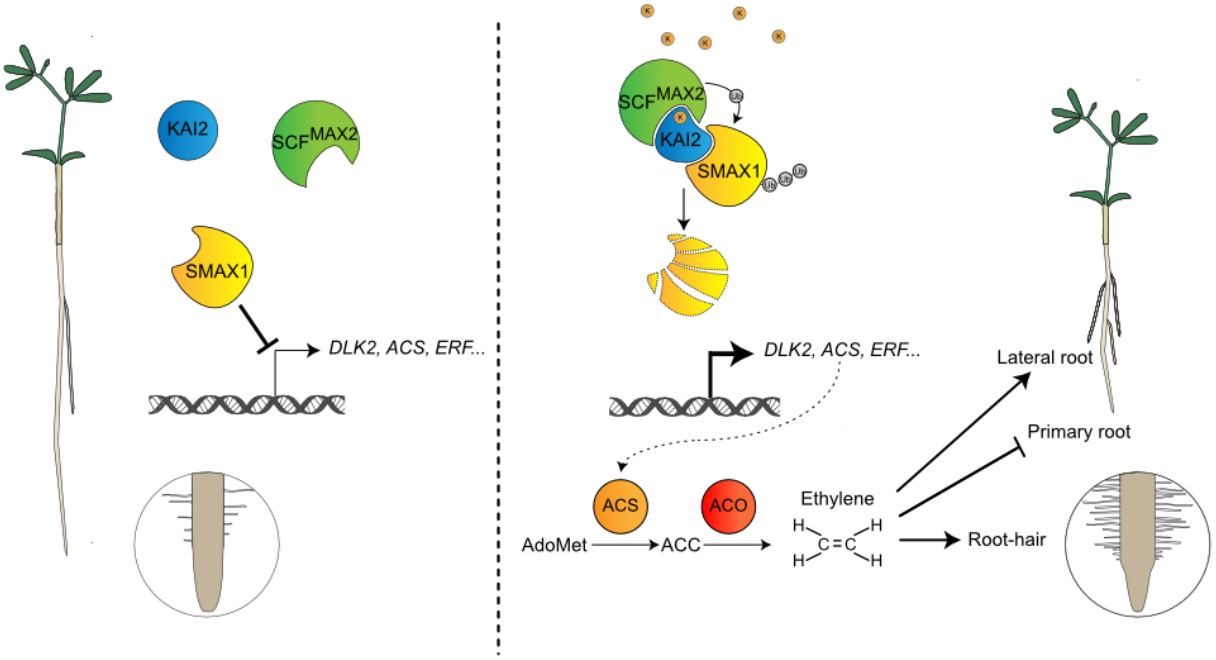

Figure 5: Schematic model of KL signaling regulating root-hairs and root architecture through ethylene biosynthesis.

X. References

Abe, S., A. Sado, K. Tanaka, T. Kisugi, K. Asami, S. Ota, H. I. Kim, K. Yoneyama, X. Xie, T. Ohnishi, Y. Seto, S. Yamaguchi, K. Akiyama, K. Yoneyama, and T. Nomura. 2014. Carlactone is converted to carlactonoic acid by MAX1 in Arabidopsis and its methyl ester can directly interact with AtD14 in vitro. *Proc Natl Acad Sci U S A* 111 (50):18084-18089.

Akiyama, K., K. Matsuzaki, and H. Hayashi. 2005. Plant sesquiterpenes induce hyphal branching in arbuscular mycorrhizal fungi. *Nature* 435 (7043):824-827.

Al-Babili, S., and H. J. Bouwmeester. 2015. Strigolactones, a novel carotenoid-derived plant hormone. *Annu Rev Plant Biol* 66:161-186.

Arite, T., H. Iwata, K. Ohshima, M. Maekawa, M. Nakajima, M. Kojima, H. Sakakibara, and J. Kyozuka. 2007. DWARF10, an RMS1/MAX4/DAD1 ortholog, controls lateral bud outgrowth in rice. *Plant J* 51 (6):1019-1029.

Arite, T., H. Kameoka, and J. Kyozuka. 2012. Strigolactone positively controls crown root elongation in rice. *J Plant Growth Reg* 31 (2):165-172.

Arite, T., M. Umehara, S. Ishikawa, A. Hanada, M. Maekawa, S. Yamaguchi, and J. Kyozuka. 2009. *d14*, a strigolactone-insensitive mutant of rice, shows an accelerated outgrowth of tillers. *Plant Cell Physiol* 50 (8):1416-1424.

Balzergue, C., M. Chabaud, D. G. Barker, G. Bécard, and S. F. Rochange. 2013. High phosphate reduces host ability to develop arbuscular mycorrhizal symbiosis without affecting root calcium spiking responses to the fungus. *Front Plant Sci* 4:426-426.

Balzergue, C., V. Puech-Pagès, G. Bécard, and S. F. Rochange. 2011. The regulation of arbuscular mycorrhizal symbiosis by phosphate in pea involves early and systemic signalling events. *J Exp Bot* 62 (3):1049-1060.

Bennett, T., G. Hines, and O. Leyser. 2014. Canalization: what the flux? *Trends Genet* 30 (2):41-48.

Bennett, T., Y. Liang, M. Seale, S. Ward, D. Müller, and O. Leyser. 2016. Strigolactone regulates shoot development through a core signalling pathway. *Biol Open* 5 (12):1806-1820.

Bennett, T., T. Sieberer, B. Willett, J. Booker, C. Luschnig, and O. Leyser. 2006. The Arabidopsis MAX pathway controls shoot branching by regulating auxin transport. *Curr Biol* 16 (6):553-563.

Besserer, A., G. Becard, A. Jauneau, C. Roux, and N. Sejalon-Delmas. 2008. GR24, a synthetic analog of strigolactones, stimulates the mitosis and growth of the arbuscular mycorrhizal fungus *Gigaspora rosea* by boosting its energy metabolism. *Plant Physiol* 148 (1):402-413.

Besserer, A., V. Puech-Pages, P. Kiefer, V. Gomez-Roldan, A. Jauneau, S. Roy, J. C. Portais, C. Roux, G. Becard, and N. Sejalon-Delmas. 2006. Strigolactones stimulate arbuscular mycorrhizal fungi by activating mitochondria. *PLoS Biol* 4 (7):e226.

Beveridge, C. A., J. J. Ross, and I. C. Murfet. 1996. Branching in pea (action of genes *Rms3* and *Rms4*). *Plant Physiol* 110 (3):859-865.

Binder, A., J. Lambert, R. Morbitzer, C. Popp, T. Ott, T. Lahaye, and M. Parniske. 2014. A modular plasmid assembly kit for multigene expression, gene silencing and silencing rescue in plants. *PLoS One* 9 (2):e88218.

Breuillin, F., J. Schramm, M. Hajirezaei, A. Ahkami, P. Favre, U. Druege, B. Hause, M. Bucher, T. Kretzschmar, E. Bossolini, C. Kuhlemeier, E. Martinoia, P. Franken, U. Scholz, and D. Reinhardt. 2010. Phosphate systemically inhibits development of arbuscular

mycorrhiza in *Petunia hybrida* and represses genes involved in mycorrhizal functioning. *Plant J* 64 (6):1002-1017.

Bruex, A., R. M. Kainkaryam, Y. Wieckowski, Y. H. Kang, C. Bernhardt, Y. Xia, X. Zheng, J. Y. Wang, M. M. Lee, P. Benfey, P. J. Woolf, and J. Schiefelbein. 2012. A gene regulatory network for root epidermis cell differentiation in Arabidopsis. *PLoS Genet* 8 (1):e1002446.

Bu, Q., T. Lv, H. Shen, P. Luong, J. Wang, Z. Wang, Z. Huang, L. Xiao, C. Engineer, T. H. Kim, J. I. Schroeder, and E. Huq. 2014. Regulation of drought tolerance by the F-box protein MAX2 in Arabidopsis. *Plant Physiol* 164 (1):424-439.

Busov, V. B., E. Johannes, R. W. Whetten, R. R. Sederoff, S. L. Spiker, C. Lanz-Garcia, and B. Goldfarb. 2004. An auxin-inducible gene from loblolly pine (*Pinus taeda* L.) is differentially expressed in mature and juvenile-phase shoots and encodes a putative transmembrane protein. *Planta* 218 (6):916-927.

Bythell-Douglas, R., C. J. Rothfels, D. W. D. Stevenson, S. W. Graham, G. K. Wong, D. C. Nelson, and T. Bennett. 2017. Evolution of strigolactone receptors by gradual neo-functionalization of KAI2 paralogues. *BMC Biol* 15 (1):52.

Carbonnel, S., and C. Gutjahr. 2014. Control of arbuscular mycorrhiza development by nutrient signals. *Front Plant Sci* 5:462-462.

Cerri, M. R., Q. Wang, P. Stolz, J. Folgmann, L. Frances, K. Katzer, X. Li, A. B. Heckmann, T. L. Wang, J. A. Downie, A. Klingl, F. de Carvalho-Niebel, F. Xie, and M. Parniske. 2017. The *ERN1* transcription factor gene is a target of the CCaMK/CYCLOPS complex and controls rhizobial infection in *Lotus japonicus*. *New Phytol* 215 (1):323-337.

Charnikhova, T. V., K. Gaus, A. Lumbroso, M. Sanders, J. P. Vincken, A. De Mesmaeker, C. P. Ruyter-Spira, C. Screpanti, and H. J. Bouwmeester. 2017. Zealactones. Novel natural strigolactones from maize. *Phytochemistry* 137:123-131.

Chevalier, F., K. Nieminen, J. C. Sanchez-Ferrero, M. L. Rodriguez, M. Chagoyen, C. S. Hardtke, and P. Cubas. 2014. Strigolactone promotes degradation of DWARF14, an alpha/beta hydrolase essential for strigolactone signaling in Arabidopsis. *Plant Cell* 26 (3):1134-1150.

Chini, A., S. Gimenez-Ibanez, A. Goossens, and R. Solano. 2016. Redundancy and specificity in jasmonate signalling. *Curr Opi Plant Biol* 33:147-156.

Chiu, C. H., J. Choi, and U. Paszkowski. 2018. Independent signalling cues underpin arbuscular mycorrhizal symbiosis and large lateral root induction in rice. *New Phytol* 217 (2):552-557.

Chiwocha, S. D. S., K. W. Dixon, G. R. Flematti, E. L. Ghisalberti, D. J. Merritt, D. C. Nelson, J. M. Riseborough, S. M. Smith, and J. C. Stevens. 2009. Karrikins: A new family of plant growth regulators in smoke. *Plant Sci*
177 (4):252-256.

Cho, H. T., and D. J. Cosgrove. 2002. Regulation of root hair initiation and expansin gene expression in Arabidopsis. *Plant Cell* 14 (12):3237-3253.

Collett, C. E., N. P. Harberd, and O. Leyser. 2000. Hormonal interactions in the control of Arabidopsis hypocotyl elongation. *Plant Physiol* 124:553-561.

Conn, C. E., R. Bythell-Douglas, D. Neumann, S. Yoshida, B. Whittington, J. H. Westwood, K. Shirasu, C. S. Bond, K. A. Dyer, and D. C. Nelson. 2015. Convergent evolution of strigolactone perception enabled host detection in parasitic plants. *Science* 349 (6247):540-543.

Conn, C. E., and D. C. Nelson. 2016. Evidence that KARRIKIN-INSENSITIVE2 (KAI2) receptors may perceive an unknown signal that is not karrikin or strigolactone. *Front. Plant. Sci.* 6:1219.

De Cuyper, C., J. Fromentin, R. E. Yocgo, A. De Keyser, B. Guillotin, K. Kunert, F. D. Boyer, and S. Goormachtig. 2015. From lateral root density to nodule number, the strigolactone analogue GR24 shapes the root architecture of *Medicago truncatula*. *J Exp Bot* 66 (1):137-146.

De Lange, J. H., and C. Boucher. 1990. Autecological studies on *Audouinia capitata* (Bruniaceae). I. Plant-derived smoke as a seed germination cue. *South African J Bot* 56 (6):700-703.

Delaux, P. M., N. Séjalon-Delmas, G. Bécard, and J. Ané. 2013. Evolution of the plant–microbe symbiotic 'toolkit'. *Trends Plant Sci* 18 (6):298-304.

Delaux, P. M., X. Xie, R. E. Timme, V. Puech-Pages, C. Dunand, E. Lecompte, C. F. Delwiche, K. Yoneyama, G. Becard, and N. Sejalon-Delmas. 2012. Origin of strigolactones in the green lineage. *New Phytol* 195 (4):857-871.

Dixon, K. W., D. J. Merritt, G. R. Flematti, and E. L. Ghisalberti. 2009. Karrikinolide : a phytoreactive compound derived from smoke with applications in horticulture, ecological restoration and agriculture. *Acta Horticulturae* (813):155-170.

Du, Z., X. Zhou, Y. Ling, Z. Zhang, and Z. Su. 2010. agriGO: a GO analysis toolkit for the agricultural community. *Nucleic Acids Research* 38 (suppl_2):W64-W70.

Dun, E. A., A. De Saint Germain, C. Rameau, and C. A. Beveridge. 2012. Antagonistic action of strigolactone and cytokinin in bud outgrowth control. *Plant Physiol* 158 (1):487-498.

Dun, E. A., B. J. Ferguson, and C. A. Beveridge. 2006. Apical dominance and shoot branching. Divergent opinions or divergent mechanisms? *Plant Physiol* 142 (3):812.

Enders, T. A., and L. C. Strader. 2015. Auxin activity: Past, present, and future. *American J Bot* 102 (2):180-196.

Flematti, G. R., E. L. Ghisalberti, K. W. Dixon, and R. D. Trengove. 2004. A compound from smoke that promotes seed germination. *Science* 305 (5686):977.

———. 2009. Identification of alkyl substituted 2H-furo[2,3-c]pyran-2-ones as germination stimulants present in smoke. *J Agric Food Chem* 57 (20):9475-9480.

Floss, D. S., S. K. Gomez, H. Park, A. M. MacLean, L. M. Müller, K. K. Bhattarai, V. Lévesque-Tremblay, I. E. Maldonado-Mendoza, and M. J. Harrison. 2017. A transcriptional program for arbuscule degeneration during AM symbiosis is regulated by MYB1. *Curr Biol* 27 (8):1206-1212.

Foo, E., K. Yoneyama, C. J. Hugill, L. J. Quittenden, and J. B. Reid. 2013. Strigolactones and the regulation of pea symbioses in response to nitrate and phosphate deficiency. *Mol Plant* 6 (1):76-87.

Fukai, E., T. Soyano, Y. Umehara, S. Nakayama, H. Hirakawa, S. Tabata, S. Sato, and M. Hayashi. 2012. Establishment of a *Lotus japonicus* gene tagging population using the exon-targeting endogenous retrotransposon *LORE1*. *Plant J* 69 (4):720-730.

Gan, Y., H. Yu, J. Peng, and P. Broun. 2007. Genetic and molecular regulation by DELLA proteins of trichome development in Arabidopsis. *Plant Physiol* 145 (3):1031-1042.

Gomez-Roldan, V., S. Fermas, P. B. Brewer, V. Puech-Pages, E. A. Dun, J. P. Pillot, F. Letisse, R. Matusova, S. Danoun, J. C. Portais, H. Bouwmeester, G. Becard, C. A. Beveridge, C. Rameau, and S. F. Rochange. 2008. Strigolactone inhibition of shoot branching. *Nature* 455 (7210):189-194.

Guan, J. C., K. E. Koch, M. Suzuki, S. Wu, S. Latshaw, T. Petruff, C. Goulet, H. J. Klee, and D. R. McCarty. 2012. Diverse roles of strigolactone signaling in maize architecture and the uncoupling of a branching-specific subnetwork. *Plant Physiol* 160 (3):1303-1317.

Guo, Q., Y. Yoshida, I. T. Major, K. Wang, K. Sugimoto, G. Kapali, N. E. Havko, C. Benning, and G. A. Howe. 2018. JAZ repressors of metabolic defense promote growth and reproductive fitness in Arabidopsis. *Proc Natl Acad Sci U S A* 115 (45):E10768-E10777.

Guo, Y., Z. Zheng, J. J. La Clair, J. Chory, and J. P. Noel. 2013. Smoke-derived karrikin perception by the alpha/beta-hydrolase KAI2 from Arabidopsis. *Proc Natl Acad Sci U S A* 110 (20):8284-8289.

Gutjahr, C., E. Gobbato, J. Choi, M. Riemann, M. G. Johnston, W. Summers, S. Carbonnel, C. Mansfield, S. Yang, M. Nadal, I. Acosta, M. Takano, W. Jiao, K. Schneeberger, K. A. Kelly, and U. Paszkowski. 2015. Rice perception of symbiotic arbuscular mycorrhizal fungi requires the karrikin receptor complex. *Science* 350 (6267):1521-1524.

Gutjahr, C., and U. Paszkowski. 2013. Multiple control levels of root system remodeling in arbuscular mycorrhizal symbiosis. *Front Plant Sci* 4 (204).

Gutjahr, C., D. Radovanovic, J. Geoffroy, Q. Zhang, H. Siegler, M. Chiapello, L. Casieri, K. An, G. An, E. Guiderdoni, C. S. Kumar, V. Sundaresan, M. J. Harrison, and U. Paszkowski. 2012. The half-size ABC transporters STR1 and STR2 are indispensable for mycorrhizal arbuscule formation in rice. *Plant J* 69 (5):906-920.

Halouzka, R., P. Tarkowski, B. Zwanenburg, and S. Cavar Zeljkovic. 2018. Stability of strigolactone analog GR24 toward nucleophiles. *Pest Manag Sci* 74 (4):896-904.

Hamiaux, C., R. S. Drummond, B. J. Janssen, S. E. Ledger, J. M. Cooney, R. D. Newcomb, and K. C. Snowden. 2012. DAD2 is an alpha/beta hydrolase likely to be involved in the perception of the plant branching hormone, strigolactone. *Curr Biol* 22 (21):2032-2036.

Hayward, A., P. Stirnberg, C. Beveridge, and O. Leyser. 2009. Interactions between auxin and strigolactone in shoot branching control. *Plant Physiol* 151 (1):400-412.

Hur, Y., J. Kim, D. Lee, K. M. Chung, and H. R. Woo. 2012. Overexpression of *AtCHX24*, a member of the cation/H+ exchangers, accelerates leaf senescence in *Arabidopsis thaliana*. *Plant Sci* 183:175-182.

Ishikawa, S., M. Maekawa, T. Arite, K. Onishi, I. Takamure, and J. Kyozuka. 2005. Suppression of tiller bud activity in tillering dwarf mutants of rice. *Plant Cell Physiol* 46 (1):79-86.

Ishizaki, K., R. Nishihama, T. Kohchi, and K. T. Yamato. 2015. Molecular genetic tools and techniques for *Marchantia polymorpha* research. *Plant Cell Physiol* 57 (2):262-270.

Ito, S., D. Yamagami, M. Umehara, A. Hanada, S. Yoshida, Y. Sasaki, S. Yajima, J. Kyozuka, M. Ueguchi-Tanaka, M. Matsuoka, K. Shirasu, S. Yamaguchi, and T. Asami. 2017. Regulation of strigolactone biosynthesis by gibberellin signaling. *Plant Physiol* 174 (2):1250-1259.

Jia, K., L. Baz, and S. Al-Babili. 2017. From carotenoids to strigolactones. *J Exp Bot* 69 (9):2189-2204.

Jiang, L., X. Liu, G. Xiong, H. Liu, F. Chen, L. Wang, X. Meng, G. Liu, H. Yu, Y. Yuan, W. Yi, L. Zhao, H. Ma, Y. He, Z. Wu, K. Melcher, Q. Qian, H. E. Xu, Y. Wang, and J. Li. 2013. DWARF 53 acts as a repressor of strigolactone signalling in rice. *Nature* 504 (7480):401-405.

Jiang, L., C. Matthys, B. Marquez-Garcia, C. De Cuyper, L. Smet, A. De Keyser, F. D. Boyer, T. Beeckman, S. Depuydt, and S. Goormachtig. 2016. Strigolactones spatially influence lateral root development through the cytokinin signaling network. *J Exp Bot* 67 (1):379-389.

Jiang, Y., Q. Xie, W. Wang, J. Yang, X. Zhang, N. Yu, Y. Zhou, and E. Wang. 2018. Medicago AP2-domain transcription factor WRI5a Is a master regulator of lipid biosynthesis and transfer during mycorrhizal symbiosis. *Mol Plant* 11 (11):1344-1359.

Jung, J., M. K. Ried, M. Hothorn, and Y. Poirier. 2018. Control of plant phosphate homeostasis by inositol pyrophosphates and the SPX domain. *Curr Opi Biotech* 49:156-162.

Kagale, S., and K. Rozwadowski. 2014. EAR motif-mediated transcriptional repression in plants. *Epigenetics* 6 (2):141-146.

Kapulnik, Y., and H. Koltai. 2014. Strigolactone involvement in root development, response to abiotic stress, and interactions with the biotic soil environment. *Plant Physiol* 166 (2):560-569.

Kapulnik, Y., N. Resnick, E. Mayzlish-Gati, Y. Kaplan, S. Wininger, J. Hershenhorn, and H. Koltai. 2011. Strigolactones interact with ethylene and auxin in regulating root-hair elongation in Arabidopsis. *J Exp Bot* 62 (8):2915-2924.

Kawaguchi, M. 2014. Genes for autoregulation of nodulation. In *The Lotus japonicus Genome*, edited by S. Tabata and J. Stougaard. Berlin, Heidelberg: Springer Berlin Heidelberg, 73-78.

Kawaharada, Y., E. K. James, S. Kelly, N. Sandal, and J. Stougaard. 2017. The Ethylene Responsive Factor Required for Nodulation 1 (ERN1) transcription factor is required for infection-thread formation in *Lotus japonicus*. *Mol Plant Microbe Interact* 30 (3):194-204.

Kohlen, W., T. Charnikhova, R. Bours, J. A. Lopez-Raez, and H. Bouwmeester. 2013. Tomato strigolactones: a more detailed look. *Plant Signal Behav* 8 (1):e22785.

Koren, D., N. Resnick, E. M. Gati, E. Belausov, S. Weininger, Y. Kapulnik, and H. Koltai. 2013. Strigolactone signaling in the endodermis is sufficient to restore root responses and involves SHORT HYPOCOTYL 2 (SHY2) activity. *New Phytol* 198 (3):866-874.

Kretzschmar, T., W. Kohlen, J. Sasse, L. Borghi, M. Schlegel, J. B. Bachelier, D. Reinhardt, R. Bours, H. J. Bouwmeester, and E. Martinoia. 2012. A petunia ABC protein controls strigolactone-dependent symbiotic signalling and branching. *Nature* 483 (7389):341-344.

Kumar, S., G. Stecher, and K. Tamura. 2016. MEGA7: Molecular Evolutionary Genetics Analysis version 7.0 for bigger datasets. *Mol Biol Evol* 33 (7):1870-1874.

Kyozuka, J., N. Tsutsumi, Z. Hu, M. Nakazono, T. Yamauchi, J. Yang, Y. Jikumaru, S. Yamaguchi, H. Ichikawa, T. Tsuchida-Mayama, Y. Nagamura, and I. Takamure. 2013. Strigolactone and cytokinin act antagonistically in regulating rice mesocotyl elongation in darkness. *Plant Cell Physiol* 55 (1):30-41.

Lantzouni, O., C. Klermund, and C. Schwechheimer. 2017. Largely additive effects of gibberellin and strigolactone on gene expression in *Arabidopsis thaliana* seedlings. *Plant J* 92 (5):924-938.

Li, W., K. H. Nguyen, H. D. Chu, C. V. Ha, Y. Watanabe, Y. Osakabe, M. A. Leyva-Gonzalez, M. Sato, K. Toyooka, L. Voges, M. Tanaka, M. G. Mostofa, M. Seki, M. Seo, S. Yamaguchi, D. C. Nelson, C. Tian, L. Herrera-Estrella, and L. P. Tran. 2017. The karrikin receptor KAI2 promotes drought resistance in *Arabidopsis thaliana*. *PLoS Genet* 13 (11):e1007076.

Li, W., K. H. Nguyen, C. V. Ha, Y. Watanabe, and L. P. Tran. 2019. Crosstalk between the cytokinin and MAX2 signaling pathways in growth and callus formation of *Arabidopsis thaliana*. *Biochemical Biophysical Research Comm* 511 (2):300-306.

Liang, Y., S. Ward, P. Li, T. Bennett, and O. Leyser. 2016. SMAX1-LIKE7 signals from the nucleus to regulate shoot development in arabidopsis via partially EAR motif-independent mechanisms. *Plant Cell* 28 (7):1581-1601.

Lin, H., R. Wang, Q. Qian, M. Yan, X. Meng, Z. Fu, C. Yan, B. Jiang, Z. Su, J. Li, and Y. Wang. 2009. DWARF27, an iron-containing protein required for the biosynthesis of strigolactones, regulates rice tiller bud outgrowth. *Plant Cell* 21 (5):1512-1525.

Liu, G., M. Stirnemann, C. Gubeli, S. Egloff, P. E. Courty, S. Aubry, M. Vandenbussche, P. Morel, D. Reinhardt, E. Martinoia, and L. Borghi. 2019. Strigolactones play an important role in shaping exodermal morphology via a KAI2-dependent pathway. *iScience* 17:144-154.

Liu, X., S. Yang, M. Zhao, M. Luo, C. Yu, C. Chen, R. Tai, and K. Wu. 2014. Transcriptional repression by histone deacetylases in plants. *Mol Plant* 7 (5):764-772.

Lopez-Raez, J. A., T. Charnikhova, V. Gomez-Roldan, R. Matusova, W. Kohlen, R. De Vos, F. Verstappen, V. Puech-Pages, G. Becard, P. Mulder, and H. Bouwmeester. 2008. Tomato strigolactones are derived from carotenoids and their biosynthesis is promoted by phosphate starvation. *New Phytol* 178 (4):863-874.

Luginbuehl, L. H., G. N. Menard, S. Kurup, H. Van Erp, G. V. Radhakrishnan, A. Breakspear, G. E. D. Oldroyd, and P. J. Eastmond. 2017. Fatty acids in arbuscular mycorrhizal fungi are synthesized by the host plant. *Science* 356 (6343):1175-1178.

Luo, J., J. Zhou, and J. Zhang. 2018. Aux/IAA gene family in plants: molecular structure, regulation, and function. *Int J Mol Sci* 19 (1):259.

Ma, H., J. Duan, J. Ke, Y. He, X. Gu, T. Xu, H. Yu, Y. Wang, J. S. Brunzelle, Y. Jiang, S. B. Rothbart, H. E. Xu, J. Li, and K. Melcher. 2017. A D53 repression motif induces oligomerization of TOPLESS corepressors and promotes assembly of a corepressor-nucleosome complex. *Sci Adv* 3 (6):e1601217.

MacLean, A. M., A. Bravo, and M. J. Harrison. 2017. Plant signaling and metabolic pathways enabling arbuscular mycorrhizal symbiosis. *Plant Cell* 29 (10):2319-2335.

Malolepszy, A., T. Mun, N. Sandal, V. Gupta, M. Dubin, D. Urbanski, N. Shah, A. Bachmann, E. Fukai, H. Hirakawa, S. Tabata, M. Nadzieja, K. Markmann, J. Su, Y. Umehara, T. Soyano, A. Miyahara, S. Sato, M. Hayashi, J. Stougaard, and S. U. Andersen. 2016. The *LORE1* insertion mutant resource. *Plant J* 88 (2):306-317.

Martín-Rodríguez, J. Á., R. León-Morcillo, H. Vierheilig, J. A. Ocampo, J. Ludwig-Müller, and J. M. García-Garrido. 2011. Ethylene-dependent/ethylene-independent ABA regulation of tomato plants colonized by arbuscular mycorrhiza fungi. *New Phytol* 190 (1):193-205.

Marzec, M., D. Gruszka, P. Tylec, and I. Szarejko. 2016. Identification and functional analysis of the *HvD14* gene involved in strigolactone signaling in *Hordeum vulgare*. *Physiologia Plantarum* 158 (3):341-355.

Mayzlish-Gati, E., C. De-Cuyper, S. Goormachtig, T. Beeckman, M. Vuylsteke, P. B. Brewer, C. A. Beveridge, U. Yermiyahu, Y. Kaplan, Y. Enzer, S. Wininger, N. Resnick, M. Cohen, Y. Kapulnik, and H. Koltai. 2012. Strigolactones are involved in root response to low phosphate conditions in Arabidopsis. *Plant Physiol* 160 (3):1329-1341.

McDaniel, B. K., and B. M. Binder. 2012. *Ethylene Receptor 1* (*ETR1*) is sufficient and has the predominant role in mediating inhibition of ethylene responses by silver in *Arabidopsis thaliana*. *J Biol Chem* 287 (31):26094-26103.

McGonigle, T. P., M. H. Miller, D. G. Evans, G. L. Fairchild, and J. A. Swan. 1990. A new method which gives an objective measure of colonization of roots by vesicular—arbuscular mycorrhizal fungi. *New Phytol* 115 (3):495-501.

Mockaitis, K., and M. Estelle. 2008. Auxin receptors and plant development: a new signaling paradigm. *Annu Rev Cell Dev Biol* 24:55-80.

Muday, G. K., A. Rahman, and B. M. Binder. 2012. Auxin and ethylene: collaborators or competitors? *Trends Plant Sci* 17 (4):181-195.

Mukherjee, A., and J. Ané. 2011. Germinating spore exudates from arbuscular mycorrhizal fungi: molecular and developmental responses in plants and their regulation by ethylene. *Mol Plant Microbe Interact* 24 (2):260-270.

Mun, T., A. Bachmann, V. Gupta, J. Stougaard, and S. U. Andersen. 2016. Lotus Base: An integrated information portal for the model legume *Lotus japonicus*. *Sci Rep* 6:39447.

Nakajima, M., A. Shimada, Y. Takashi, Y. Kim, S. Park, M. Ueguchi-Tanaka, H. Suzuki, E. Katoh, S. Iuchi, M. Kobayashi, T. Maeda, M. Matsuoka, and I. Yamaguchi. 2006.

Identification and characterization of Arabidopsis gibberellin receptors. *Plant J* 46 (5):880-889.
Nakamura, H., Y. Xue, T. Miyakawa, F. Hou, H. Qin, K. Fukui, X. Shi, E. Ito, S. Ito, S. Park, Y. Miyauchi, A. Asano, N. Totsuka, T. Ueda, M. Tanokura, and T. Asami. 2013. Molecular mechanism of strigolactone perception by DWARF14. *Nature Communications* 4:2613.
Nelson, D. C., G. R. Flematti, J. A. Riseborough, E. L. Ghisalberti, K. W. Dixon, and S. M. Smith. 2010. Karrikins enhance light responses during germination and seedling development in *Arabidopsis thaliana*. *Proc. Natl. Acad. Sci. U.S.A.* 107 (15):7095-7100.
Nelson, D. C., J. A. Riseborough, G. R. Flematti, J. Stevens, E. L. Ghisalberti, K. W. Dixon, and S. M. Smith. 2009. Karrikins discovered in smoke trigger Arabidopsis seed germination by a mechanism requiring gibberellic acid synthesis and light. *Plant Physiol* 149 (2):863-873.
Nelson, D. C., A. Scaffidi, E. A. Dun, M. T. Waters, G. R. Flematti, K. W. Dixon, C. A. Beveridge, E. L. Ghisalberti, and S. M. Smith. 2011. F-box protein MAX2 has dual roles in karrikin and strigolactone signaling in *Arabidopsis thaliana*. *Proc. Natl. Acad. Sci. U.S.A.* 108 (21):8897-8902.
Oh, E., J. Zhu, H. Ryu, I. Hwang, and Z. Wang. 2014. TOPLESS mediates brassinosteroid-induced transcriptional repression through interaction with BZR1. *Nature Communications* 5:4140.
Overvoorde, P., H. Fukaki, and T. Beeckman. 2010. Auxin control of root development. *Perspectives biol* 2 (6):a001537-a001537.
Pandya-Kumar, N., R. Shema, M. Kumar, E. Mayzlish-Gati, D. Levy, H. Zemach, E. Belausov, S. Wininger, M. Abu-Abied, Y. Kapulnik, and H. Koltai. 2014. Strigolactone analog GR24 triggers changes in PIN2 polarity, vesicle trafficking and actin filament architecture. *New Phytol* 202 (4):1184-1196.
Parniske, M. 2008. Arbuscular mycorrhiza: the mother of plant root endosymbioses. *Nat Rev Microbiol* 6 (10):763-775.
Patro, R., G. Duggal, M. I. Love, R. A. Irizarry, and C. Kingsford. 2017. Salmon provides fast and bias-aware quantification of transcript expression. *Nature Methods* 14 (4):417-419.
Pauwels, L., G. F. Barbero, J. Geerinck, S. Tilleman, W. Grunewald, A. C. Pérez, J. M. Chico, R. V. Bossche, J. Sewell, E. Gil, G. García-Casado, E. Witters, D. Inzé, J. A. Long, G. De Jaeger, R. Solano, and A. Goossens. 2010. NINJA connects the co-repressor TOPLESS to jasmonate signalling. *Nature* 464:788-791.
Péret, B., M. Clément, L. Nussaume, and T. Desnos. 2011. Root developmental adaptation to phosphate starvation: better safe than sorry. *Trends Plant Sci* 16 (8):442-450.
Perry, J. A., T. L. Wang, T. J. Welham, S. Gardner, J. M. Pike, S. Yoshida, and M. Parniske. 2003. A TILLING reverse genetics tool and a web-accessible collection of mutants of the legume *Lotus japonicus*. *Plant Physiol* 131 (3):866-871.
Pimprikar, P., S. Carbonnel, M. Paries, K. Katzer, V. Klingl, M. J. Bohmer, L. Karl, D. S. Floss, M. J. Harrison, M. Parniske, and C. Gutjahr. 2016. A CCaMK-CYCLOPS-DELLA complex activates transcription of *RAM1* to regulate arbuscule branching. *Curr Biol* 26 (8):987-998.
Pimprikar, P., and C. Gutjahr. 2018. Transcriptional regulation of arbuscular mycorrhiza development. *Plant Cell Physiol* 59 (4):678-695.
Qin, G., H. Gu, Y. Zhao, Z. Ma, G. Shi, Y. Yang, E. Pichersky, H. Chen, M. Liu, Z. Chen, and L. Qu. 2005. An indole-3-acetic acid carboxyl methyltransferase regulates an Abidopsis leaf development. *Plant Cell* 17 (10):2693-2704.
Qin, H., and R. Huang. 2018. Auxin controlled by ethylene steers root development. *Int J Mol Sci* 19 (11).

Rasmussen, A., M. G. Mason, C. De Cuyper, P. B. Brewer, S. Herold, J. Agusti, D. Geelen, T. Greb, S. Goormachtig, T. Beeckman, and C. A. Beveridge. 2012. Strigolactones suppress adventitious rooting in Arabidopsis and pea. *Plant Physiol* 158 (4):1976-1987.

Reid, D., H. Liu, S. Kelly, Y. Kawaharada, T. Mun, S. U. Andersen, G. Desbrosses, and J. Stougaard. 2018. Dynamics of ethylene production in response to compatible nod factor. *Plant Physiol* 176 (2):1764-1772.

Ruyter-Spira, C., W. Kohlen, T. Charnikhova, A. van Zeijl, L. van Bezouwen, N. de Ruijter, C. Cardoso, J. A. Lopez-Raez, R. Matusova, R. Bours, F. Verstappen, and H. Bouwmeester. 2011. Physiological effects of the synthetic strigolactone analog GR24 on root system architecture in Arabidopsis: another belowground role for strigolactones? *Plant Physiol* 155 (2):721-734.

Ruzicka, K., K. Ljung, S. Vanneste, R. Podhorska, T. Beeckman, J. Friml, and E. Benkova. 2007. Ethylene regulates root growth through effects on auxin biosynthesis and transport-dependent auxin distribution. *Plant Cell* 19 (7):2197-2212.

Scaffidi, A., M. T. Waters, Y. K. Sun, B. W. Skelton, K. W. Dixon, E. L. Ghisalberti, G. R. Flematti, and S. M. Smith. 2014. Strigolactone hormones and their stereoisomers signal through two related receptor proteins to induce different physiological responses in Arabidopsis. *Plant Physiol.* 165 (3):1221-1232.

Schaller, G. E., and B. M. Binder. 2017. Inhibitors of ethylene biosynthesis and signaling. *Methods Mol Biol* 1573:223-235.

Shinjiro, Y. 2008. Gibberellin metabolism and its regulation. *Annu Rev Plant Biol* 59 (1):225-251.

Shinohara, N., C. Taylor, and O. Leyser. 2013. Strigolactone can promote or inhibit shoot branching by triggering rapid depletion of the auxin efflux protein PIN1 from the plasma membrane. *PLoS Biol* 11 (1):e1001474.

Shyu, C., P. Figueroa, C. L. DePew, T. F. Cooke, L. B. Sheard, J. E. Moreno, L. Katsir, N. Zheng, J. Browse, and G. A. Howe. 2012. JAZ8 lacks a canonical degron and has an EAR motif that mediates transcriptional repression of jasmonate responses in Arabidopsis. *Plant Cell* 24 (2):536-550.

Simon, S., and J. Petrášek. 2011. Why plants need more than one type of auxin. *Plant Sci* 180 (3):454-460.

Soneson, C., M. I. Love, and M. D. Robinson. 2015. Differential analyses for RNA-seq: transcript-level estimates improve gene-level inferences. *F1000Res* 4:1521.

Soundappan, I., T. Bennett, N. Morffy, Y. Liang, J. P. Stanga, A. Abbas, O. Leyser, and D. C. Nelson. 2015. SMAX1-LIKE/D53 family members enable distinct MAX2-dependent responses to strigolactones and karrikins in Arabidopsis. *Plant Cell* 27 (11):3143-3159.

Spatafora, J. W., Y. Chang, G. L. Benny, K. Lazarus, M. E. Smith, M. L. Berbee, G. Bonito, N. Corradi, I. Grigoriev, A. Gryganskyi, T. Y. James, K. O'Donnell, R. W. Roberson, T. N. Taylor, J. Uehling, R. Vilgalys, M. M. White, and J. E. Stajich. 2016. A phylum-level phylogenetic classification of zygomycete fungi based on genome-scale data. *Mycologia* 108 (5):1028-1046.

Stanga, J. P., N. Morffy, and D. C. Nelson. 2016. Functional redundancy in the control of seedling growth by the karrikin signaling pathway. *Planta* 243 (6):1397-1406.

Stanga, J. P., S. M. Smith, W. R. Briggs, and D. C. Nelson. 2013. *SUPPRESSOR OF MORE AXILLARY GROWTH2 1* controls seed germination and seedling development in Arabidopsis. *Plant Physiol* 163 (1):318-330.

Stirnberg, P., I. J. Furner, and H. M. Ottoline Leyser. 2007. MAX2 participates in an SCF complex which acts locally at the node to suppress shoot branching. *Plant J* 50 (1):80-94.

Stirnberg, P., J. Liu, S. Ward, S. L. Kendall, and O. Leyser. 2012a. Mutation of the cytosolic ribosomal protein-encoding *RPS10B* gene affects shoot meristematic function in Arabidopsis. *BMC Plant Biol* 12 (1):160.

Stirnberg, P., S. Zhao, L. Williamson, S. Ward, and O. Leyser. 2012b. FHY3 promotes shoot branching and stress tolerance in Arabidopsis in an AXR1-dependent manner. *Plant J* 71 (6):907-920.

Strader, L. C., G. L. Chen, and B. Bartel. 2010. Ethylene directs auxin to control root cell expansion. *Plant J* 64 (5):874-884.

Sun, T. 2011. The molecular mechanism and evolution of the GA–GID1–DELLA signaling module in plants. *Curr Biol* 21 (9):R338-R345.

Sun, Y. K., A. Scaffidi, J. Yao, K. Melville, S. M. Smith, G. R. Flematti, and M. T. Waters. 2019. Divergent receptor proteins confer responses to different karrikins in two ephemeral weeds: BioRxiv 376939.

Swarbreck, S. M., Y. Guerringue, E. Matthus, F. J. C. Jamieson, and J. M. Davies. 2019. Impairment in karrikin but not strigolactone sensing enhances root skewing in *Arabidopsis thaliana*. *Plant J* (98):607-621.

Tiwari, S. B., G. Hagen, and T. J. Guilfoyle. 2004. Aux/IAA proteins contain a potent transcriptional repression domain. *Plant Cell* 16 (2):533-543.

Toh, S., D. Holbrook-Smith, M. E. Stokes, Y. Tsuchiya, and P. McCourt. 2014. Detection of parasitic plant suicide germination compounds using a high-Throughput Arabidopsis HTL/KAI2 strigolactone perception system. *Chem. & Biol.* 21 (9):1253.

Torrey, J. G. 1950. The induction of lateral roots by indoleacetic acid and root decapitation. *American J Bot* 37 (4):257-264.

Tsuchisaka, A., and A. Theologis. 2004. Unique and overlapping expression patterns among the Arabidopsis *1-Amino-Cyclopropane-1-Carboxylate Synthase* gene family members. *Plant Physiol* 136 (2):2982-3000.

Ueda, H., and M. Kusaba. 2015. Strigolactone regulates leaf senescence in concert with ethylene in Arabidopsis. *Plant Physiol* 169 (1):138-147.

Umehara, M., A. Hanada, S. Yoshida, K. Akiyama, T. Arite, N. Takeda-Kamiya, H. Magome, Y. Kamiya, K. Shirasu, K. Yoneyama, J. Kyozuka, and S. Yamaguchi. 2008. Inhibition of shoot branching by new terpenoid plant hormones. *Nature* 455 (7210):195-200.

Urbanski, D. F., A. Malolepszy, J. Stougaard, and S. U. Andersen. 2012. Genome-wide LORE1 retrotransposon mutagenesis and high-throughput insertion detection in Lotus japonicus. *Plant J* 69 (4):731-741.

Van de Poel, B., and D. Van Der Straeten. 2014. 1-aminocyclopropane-1-carboxylic acid (ACC) in plants: more than just the precursor of ethylene! *Front Plant Sci* 5.

Van Rongen, M., T. Bennett, F. Ticchiarelli, and O. Leyser. 2019. Connective auxin transport contributes to strigolactone-mediated shoot branching control independent of the transcription factor BRC1. *PLoS Genet* 15 (3):e1008023.

Vandenbussche, F., and D. Van Der Straeten. 2012. The role of ethylene in plant growth and development. In *Annu Plant Rev*.

Végh, A., N. Incze, A. Fábián, H. Huo, K. J. Bradford, E. Balázs, and V. Soós. 2017. Comprehensive analysis of *DWARF14-LIKE2* (*DLK2*) reveals its functional divergence from strigolactone-related paralogs. *Front Plant Sci* 8 (1641):1-14.

Vierheilig, H., A. P. Coughlan, U. Wyss, and Y. Piché. 1998. Ink and vinegar, a simple staining technique for arbuscular-mycorrhizal fungi. *Appl Environ Microbiol* 64 (12):5004-5007.

Villaecija Aguilar, J. A., M. Hamon-Josse, S. Carbonnel, A. Kretschmar, K. Ljung, T. Bennett, and C. Gutjahr. 2019. KAI2 regulates root and root hair development by modulating auxin distribution.

Walker, C., and T. Bennett. 2017. Reassessing the evolution of strigolactone synthesis and signalling, 228320.

Wallner, E. S., V. Lopez-Salmeron, I. Belevich, G. Poschet, I. Jung, K. Grunwald, I. Sevilem, E. Jokitalo, R. Hell, Y. Helariutta, J. Agusti, I. Lebovka, and T. Greb. 2017. Strigolactone- and karrikin-independent SMXL proteins are central regulators of phloem formation. *Curr Biol* 27 (8):1241-1247.

Wang, L., B. Wang, L. Jiang, X. Liu, X. Li, Z. Lu, X. Meng, Y. Wang, S. M. Smith, and J. Li. 2015. Strigolactone signaling in Arabidopsis regulates shoot development by targeting D53-Like SMXL repressor proteins for ubiquitination and degradation. *Plant Cell* 27 (11):3128-3142.

Wang, W., J. Shi, Q. Xie, Y. Jiang, N. Yu, and E. Wang. 2017. Nutrient exchange and regulation in arbuscular mycorrhizal symbiosis. *Mol Plant* 10 (9):1147-1158.

Wang, Y., and H. J. Bouwmeester. 2018. Structural diversity in the strigolactones. *J Exp Bot* 69 (9):2219-2230.

Waters, M. T., C. Gutjahr, T. Bennett, and D. C. Nelson. 2017. Strigolactone signaling and evolution. *Annu Re. Plant Biol* (68):291-322.

Waters, M. T., D. C. Nelson, A. Scaffidi, G. R. Flematti, Y. K. Sun, K. W. Dixon, and S. M. Smith. 2012. Specialisation within the DWARF14 protein family confers distinct responses to karrikins and strigolactones in Arabidopsis. *Development* 139 (7):1285-1295.

Waters, M. T., A. Scaffidi, G. R. Flematti, and S. M. Smith. 2015a. Substrate-induced degradation of the alpha/beta-fold hydrolase KARRIKIN INSENSITIVE2 requires a functional catalytic triad but is independent of MAX2. *Mol Plant* 8 (5):814-817.

Waters, M. T., A. Scaffidi, S. L. Moulin, Y. K. Sun, G. R. Flematti, and S. M. Smith. 2015b. A *Selaginella moellendorffii* ortholog of KARRIKIN INSENSITIVE2 functions in Arabidopsis development but cannot mediate responses to karrikins or strigolactones. *Plant Cell* 27 (7):1925-1944.

Wojciechowski, M. F., M. Lavin, and M. J. Sanderson. 2004. A phylogeny of legumes (Leguminosae) based on analysis of the plastid *matK* gene resolves many well-supported subclades within the family. *American J Bot* 91 (11):1846-1862.

Wu, Y., B. Hou, W. Lee, S. Lu, C. Yang, H. Vaucheret, and H. Chen. 2017. DCL2- and RDR6-dependent transitive silencing of *SMXL4* and *SMXL5* in Arabidopsis *dcl4* mutants causes defective phloem transport and carbohydrate over-accumulation. *Plant J* 90 (6):1064-1078.

Yao, R., Z. Ming, L. Yan, S. Li, F. Wang, S. Ma, C. Yu, M. Yang, L. Chen, L. Chen, Y. Li, C. Yan, D. Miao, Z. Sun, J. Yan, Y. Sun, L. Wang, J. Chu, S. Fan, W. He, H. Deng, F. Nan, J. Li, Z. Rao, Z. Lou, and D. Xie. 2016. DWARF14 is a non-canonical hormone receptor for strigolactone. *Nature* 536 (7617):469-473.

Yoneyama, K., R. Arakawa, K. Ishimoto, H. I. Kim, T. Kisugi, X. Xie, T. Nomura, F. Kanampiu, T. Yokota, T. Ezawa, and K. Yoneyama. 2015. Difference in Striga-susceptibility is reflected in strigolactone secretion profile, but not in compatibility and host preference in arbuscular mycorrhizal symbiosis in two maize cultivars. *New Phytol* 206 (3):983-989.

Yoneyama, K., X. Xie, D. Kusumoto, H. Sekimoto, Y. Sugimoto, Y. Takeuchi, and K. Yoneyama. 2007. Nitrogen deficiency as well as phosphorus deficiency in sorghum promotes the production and exudation of 5-deoxystrigol, the host recognition signal for arbuscular mycorrhizal fungi and root parasites. *Planta* 227 (1):125-132.

Yoshida, H., E. Tanimoto, T. Hirai, Y. Miyanoiri, R. Mitani, M. Kawamura, M. Takeda, S. Takehara, K. Hirano, M. Kainosho, T. Akagi, M. Matsuoka, and M. Ueguchi-Tanaka.

2018. Evolution and diversification of the plant gibberellin receptor GID1. *Proc Natl Acad Sci U S A* 115 (33):E7844-E7853.

Yoshida, S., H. Kameoka, M. Tempo, K. Akiyama, M. Umehara, S. Yamaguchi, H. Hayashi, J. Kyozuka, and K. Shirasu. 2012. The D3 F-box protein is a key component in host strigolactone responses essential for arbuscular mycorrhizal symbiosis. *New Phytol* 196 (4):1208-1216.

Yu, Y., and S. F. Yang. 1979. Auxin-induced ethylene production and its inhibition by aminoethoxyvinylglycine and colbalt ion. *Plant Physiol* (64):1074-1077.

Zhou, F., Q. Lin, L. Zhu, Y. Ren, K. Zhou, N. Shabek, F. Wu, H. Mao, W. Dong, L. Gan, W. Ma, H. Gao, J. Chen, C. Yang, D. Wang, J. Tan, X. Zhang, X. Guo, J. Wang, L. Jiang, X. Liu, W. Chen, J. Chu, C. Yan, K. Ueno, S. Ito, T. Asami, Z. Cheng, J. Wang, C. Lei, H. Zhai, C. Wu, H. Wang, N. Zheng, and J. Wan. 2013. D14-SCF(D3)-dependent degradation of D53 regulates strigolactone signalling. *Nature* 504 (7480):406-410.

XI. List of figures

XII. List of tables

XIII. Acknowledgments

I would like to thank many people who supported and helped in many ways during those many years.

A Ph.D. is a long adventure, similar to a single-handed yacht race, in which you know when you start, but you are not sure when and where you will dock. Luckily, you have some assistance, in my case, it was Prof. Dr. Caroline Gutjahr. She has guided me during all those years, scientifically but also in many other aspects. I feel lucky but also grateful to have been able to learn on her side.

Also, I would like to thank all the members of this Ph.D. committee, Prof. Dr. Martin Parniske, PD. Dr. Cordelia Bolle, Prof. Dr. Angelika Böttger, Prof. Dr. Wofgang Frank and Prof. Dr. Andreas klingl, for giving their valuable time and efforts in evaluating this work.

The Genetic department is rich in talented people. I have learned a lot from them, and I have particularly enjoyed our many enthusiastic discussions at the traditional Journal Club. This hour was definitively the best moment of the week thanks to the entertaining and pedagogic talents of Prof. Martin Parniske.

I would like to express my sincere thanks to the people who actually make it easier to do science in the lab. Obviously, I mean the technicians: Karl-Heinz Braun, Gisela Brinkmann, Ute Bergmann, Jessica Folgman, Adriana Hörmann, and Klea Bendebende-Doulioglu. I would like to thank them for their comprehensive state of mind, constant support and exemplary professionalism.

I would like to thank the Graduate School Life Science Munich (LSM) and the SFB924 for financial support, creating an excellent networking environment and the organization of extremely beneficial courses. I would especially like to thank the LSM coordinator Francisca Rosa Mende for her help and guidance in administrative tasks.

My Ph.D. was a very long and not easy way, sometimes a burden but also with true moments of fun and happiness. Those moments will always be associated with amazing colleagues and friends. I truly want to thank them by distilling few anecdotes.

An enormous gracias to my first office mate, Carolina Senés, with who I spent hours discussing science and its politics, but also more light subjects that I won't detail here. She was my lifebuoy during the first years, always ready to cheer me up. Your "*Pfffff! Who cares?*" still gently echoes in my ears. After her departures, it has never been the same. *See you in Valhalla*.

Kindness and support were all around in the firsts years. It was particularly true with Gloria Torres, Macarena Marin, Kinga Sedzielewska and Marion Cerri. As very experienced postdocs, they have enriched me with really great pieces of advice. Also, I will not forget Marion's farewell speech, a powerful dose of motivation, and as usual with generosity.

I must write a small paragraph on Victor Gimenez. First, as an excellent biochemist, he gave me an uncountable number of meaningful advice for protein expression and purification. Second, as a person, he was incredibly funny. I was always hoping to meet him in the protein room, and when I could see him through the door's window, an uncontrolled smiled was rising on my face. I regret to not have work with proteins earlier.

Another Spanish should be in this list: José Antonio Villaécija Aguilar *de Villaécija la ciudad más caliente en España ¡* Again a funny guy, a nice person, and bright scientist. Close to perfection, but no: he is fanatic of real Madrid. More seriously, José was an admirable colleague and friend all along my Ph.D. Our proximity helped strongly my scientific progress as many ideas flourished after our discussions or the share of a result. Being fan for life of Charlton Athletics and HC Olomouc helped to forge strong bonds.

Working with Lotus strigolactones mutants was not an easy task for me, neither for our wonderful and kind greenhouse caretaker Anna Heuberger. Due to their highly

branched phenotypes, my mutants became the safe harbor and spreading point of diseases and pathogens in the greenhouse, generating more gardening work. Despite this, Anna always took great care of my plants. The ultimate proof is that in her holidays my plants had to suffer from massive increases of mortality rate…

Being at the very beginning of the construction of the Gutjahr group, I have seen its constant expansion. More than a numeric increase, a real enhancement was at work. Each member brought its own knowledge. I have learned from every single one of the Gutjahr members, and I would like to thank them all for this but also for the nice environment created, especially the people with who I was directly involved in my work, the Karrikin people: José Villaécija-Aguilar, Salar Torabi, and Kartikye Varshney. Not directly involved in the karrikin research at the beginning, Das Debatosh became quickly an indispensable player with his impressive bioinformatics skills and ethylene signaling knowledge. Also, he was a reliable ethylene inhibitors provider. Another important contributor to my work, was Verena Klingl, and I really want to thank her for her help. She is as good in extracting RNA and making cDNA than she is in hip-hop dancing, and god knows how good she is in the latest.

After 6 years in the lab, my most precious discovery is unequivocally a lovely and fascinating little woman, Priya Pimprikar. First, as a colleague, and much more after, she has made me a better scientist and a better person. Without her, I would have probably never finished this Ph.D. Her positive influence is on so many aspects, and if I have to cite one of them, I would like to mention her amazing capacity to buffer my frustration originated from this Ph.D. Also, I won't be able to say how many times she sat next to me at 2 a.m. at the plant-bench helping me sealing my plates… This thesis is definitely also her achievement. For all of this: धन्यवाद.

Last but not least, I would like to express my most profound gratitude to my family for their unconditional support. To my parents, *Carbo* and *la petite mère* who never surrendered and invariably did their maximum to make me reach my goals. I definitively don't deserve them, but what can they do, selfish genes are in action.